Radiation from Elementary Sources Located in Chiral Surrounded Dispersive Medium

Kiran Mujeeb

Department of Electronics

Quaid-i-Azam University, Islamabad, Pakistan.

A Thesis Submitted in Partial Fulfillment of the Requirements for the Degree of

Master of Philosophy

in

Electronics

February, 2015

Department of Electronics
Quaid-i-Azam University
Islamabad

A thesis entitled "Radiation from elementary sources located in chiral surrounded dispersive medium" by Kiran Mujeeb in partial fulfilment of the requirements for the degree of Master of Philosophy, has been approved and accepted by the following

---

Advisor
Dr. Aqeel A. Syed
Assistant Professor
Department of Electronics
Quaid-i-Azam University, Islamabad
Pakistan

Chairman
Dr. Farhan Saif
Associate Professor
Department of Electronics
Quaid-i-Azam University, Islamabad
Pakistan

Dedicated to my father who struggled all his life to make this dream a reality and my mother Diljan Khanum (Late).

May her soul rest in peace (Ameen)

Also my brothers and sisters who sacrificed for the completion of this dissertation.

Acknowledgements

First of all thousand thanks of Almighty Allah who created everything from spinning electrons to spiraling galaxies with astonishing beauty and symmetry, also Hazrat Muhammad (peace be upon) His last Prophet who taught us to reveal the truth behind the natural phenomena which gives us motivation for research.
Firstly, it is my pleasure to acknowledge my advisor, Dr. Aqeel A. Syed for being encouraging, informative and galvanizing during discussion sessions. This acknowledgement would not be conclusive without remembering the impleding times of research when an advisor is really needed to get through these tough patches and help and support of my adviser was inimitable during that time.
It is my pleasure to acknowledge Dr. Qaisar Abass Naqvi for being polite and helpful. His help and support was inimitable during every tough time of my research. I am very grateful for his encouragement toward productivity in research. His consistency, hard work and routine work always inspired me and motivated me. He is very sincere with his profession and his teaching style and methodology is inspiration for every teacher.
I am grateful to Dr. Azhar Abass Rizvi, the role model for hard workers. I can never forget his thought provoking lectures. I am indebted to Dr. Aqueel Ashraf who helped me to improve my programming skills. Dr. Hassan Mahmood, Miss Qurat ul Ain Minhas, Miss Farhat Majeed, Mr. Musarrat Abbas, Dr. Zeshan Akbar, Dr. Arshad Fiaz and Dr. Farhan Saif are the name of some personalities who has great contribution in my studies. I am grateful to all of my teachers for their support.

I think these acknowledgements remain incomplete without mentioning my family because their prayers, efforts and moral and financial support enabled me to complete my M.Phil. My special gratitude to my loving father whose love and affection has been with me throughout my life. He is a role model for me. I am grateful to my brothers, Ahmad Nadeem and Muhammad Naeem for their moral and financial support. I am indebted to them for everything they have done for me. I must thank my brother Muhammad Wasim who always encouraged me and help me to continue my study.

At this time i can not forget the love, care and affection of Nighat Mujeeb and Eshrat Mujeeb. These are the characters in my life who realized me that i can achieve any milestone in my life by hardwork. It is a matter of pleasure for me to pay my gratitude to Farah Mujeeb, Sonia Mujeeb, Sahar Mujeeb and Attia Mujeeb who encouraged me and always sacrificed for me.

I want to mention a special personality in my life Noor-Ul-Huda Mujeeb (Shahzadi Mujeeb) who always refreshed me at home. I want to thank my brother in laws specially Zahoor Ahmad for his support and concern.

Now i would like to appreciate all my friends and lab fellows specially Miss Iffat Sehar, Mr. Tayyab Malik, Mr. Abdul Salam, Mr. Faizan Raza and Mr. Zahir for their valuable discussion on subject matters and for their cooperation.

Finally, I want to acknowledge the staff and administration of the Department of Electronics at Quaid-i-Azam university for providing us a working environment.

Kiran Mujeeb
January, 2015

Abstract

Transmission of electromagnetic fields through an interface of bounded dispersive dielectric-magnetic and unbounded chiral metamaterial is studied in the present thesis. Planar interface and current sheet as a source of excitation placed in non-dispersive/dispersive dielectric magnetic medium surrounded by unbounded chiral/chiral nihility medium is considered. Transmission of electromagnetic fields from non-dispersive/dispersive/nihility interfaces placed in chiral medium is determined. Also a circular cylindrical interface of infinite length and a line source located within the dispersive dielectric-magnetic medium, as source of excitation, are considered. Lorentz -Drude model is used for dispersive dielectric-magnetic medium. The fields transmitted from the dispersive medium, occupied by the cylinder, into unbounded chiral/chiral nihility metamaterials are obtained. Characteristics of radiation in chiral nihility metamaterial from dispersive cylinder having very small radii is also explored. This limiting case may enable us to comment on radiation behavior of an elementary source located in an unbounded chiral nihility metamaterial. Case of nihility cylinder carrying line source and surrounded by unbounded chiral metamaterial is also taken into account. Coated dielectric cylinder is also considered. Behavior of transmitted field for these cases is analyzed with respect to different parameters of the geometry.

Contents

Chapter 1

Introduction

1.1 Chiral and Chiral Nihility Metamaterials

In recent years materials are artificially fabricated which have new physically realizable response not otherwise observed in nature. These artificial materials are called metamaterials. These materials are fabricated by adding inhomogeneities in host medium or on host surface. Metramaterials are not new in electromagnetic applications. In 1898 Bose [1] constructed materials consisting of twisted structures having properties known as chiral characteristics. A chiral medium is a continuous medium and supports right circularly polarized (RCP) wave and left circularly polarized (LCP) wave because chiral metamaterial support two wave numbers. The word chiral express a body which has non superimposeable mirror image of itself. Chiral media exhibit interesting properties in optical range of frequencies such as circular dichroism. Chiral media are used in antennas and arrays, antenna radomes, microstrips and waveguides. A chiral medium is a reciprocal medium and can be described using Maxwell electromagnetic equations. A chiral medium is composed of uniformly distributed and randomly oriented chiral objects which can not be superimposed on their mirror images either by a translation or rotation. This property of medium is known as handedness and a chiral object is either right handed or left handed. Unlike the dielectric media chiral media gives rise to co- polarized and cross-polarized fields. When a linearly polarized wave is

made incident on a chiral interface the incident wave splits in two waves and after passing through the chiral medium these two waves combines to give a linearly polarized wave whose plane of polarization is rotated with respect to plane of polarization of the incident wave. Therefore, chirality of a medium causes rotation of plane of polarization. DNA, amino acid, sugar solution and proteins are some natural chiral objects while wire helix, irregular tetrahedron, hand gloves and stringed instruments are some examples of man made chiral objects. Different media are classified on the basis of their permittivity and

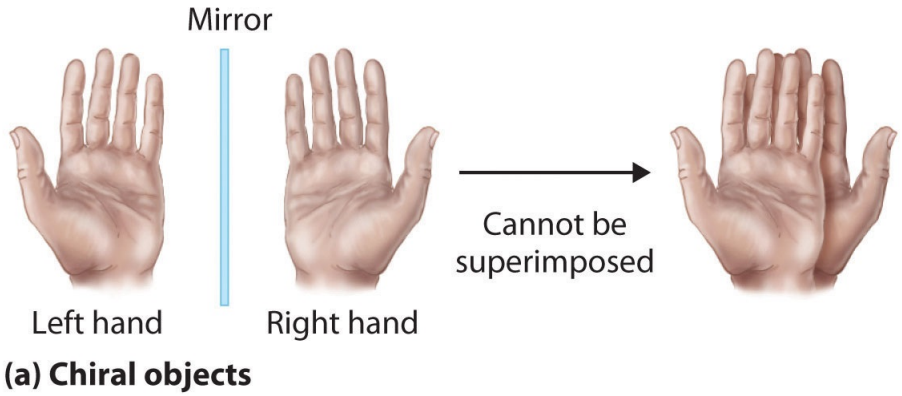

Figure 1.1: Chiral object.

Figure 1.2: Helix an example of chiral object.

permeability, medium with both permittivity and permeability greater than zero ($\epsilon > 0, \mu > 0$) are characterized as double positive (DPS) meterials and all naturally occuring media exhibit this characteristic. A medium with permittivity less than zero and permeability greater than zero ($\epsilon < 0, \mu > 0$) will be characterized as epsilon-negative (ENG) medium and many plasmas exhibit

this property in the visible and infrared range of frequency. A medium with permittivity greater than zero and permeability less than zero $(\epsilon > 0, \mu < 0)$ will be characterize as mu-negative (MNG) medium and gyrotropis materials exhibit this characteristic in certain range of frequency. And a medium with both permittivity and permeability less than zero $(\epsilon < 0, \mu < 0)$ will be characterized as double negative (DNG) medium and these materials have only been constructed artificially. These materials are not found in nature but are physically realizable.

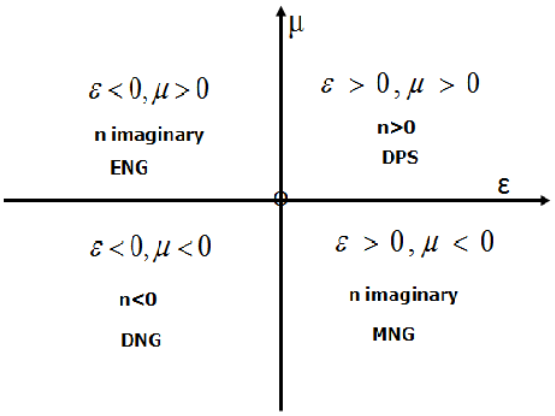

Figure 1.3: Classification of electromagnetic materials.

In 1811 Arago observed the presence of optical activity in quartz crystal and observed that plane of polarization of linearly polarized light rotates by quartz crystal. In 1812 Biot proved that optical activity depends on thickness of crystal plate and on the wavelength of light. Later, in 1821 Fresnel showed that light rays of a crystal quartz separates into two circularly polarized rays. He said that the difference of velocities causes the optical activity. In 1914 Lindman looked for optical activity in radio waves and he discussed the wave interaction with small helices to create artificial chiral media where he proved the existence of polarization rotation. Confirmatory experiment of existence of chirality, performed by Tinoco and Freedman, provided further results on dependence of rotation on frequency. In 1968 Vaselago [2] introduced the Left Handed Materials (LHM's) which possess negative permittivity and permeability and these LHM exhibit negative refraction and negative group velocity.

In these materials direction of Poynting vector is antiparallel to the direction of phase velocity. Due to these interesting properties chiral media is center of interest for researchers in the field of electromagnetics for last few decades [2–10]. Several names have been suggested for this type of media such as left handed media [2, 3, 5, 11–14], backward wave media [7], negative refractive index media and DNG metamaterials [8]. Lindman [15] worked on chiral media in 1914. Behavior of electromagnetic waves in chiral media was discussed by Juggard et al.[16]. Engheta and Juggard [17] discussed the electromagnetic chirality and its applications. Engheta and Bissiri [18] discussed one and two dimensional dydic Greens function in chiral media. Radiation of electromagnetic waves from canonical arrays is examined by Jaggard and Sun [19]. Radiation characteristics of chiral coated slotted cylindrical antenna has been studied by Mahmoud [20]. The constitutive relations for chiral metamaterial are given by [21] and written as

$$\mathbf{D} = \epsilon_0 \epsilon_c \mathbf{E} + j\kappa \sqrt{\epsilon_0 \mu_0} \mathbf{H} \tag{1.1}$$

$$\mathbf{B} = \mu_0 \mu_c \mathbf{H} - j\kappa \sqrt{\epsilon_0 \mu_0} \mathbf{E} \tag{1.2}$$

The concept of nihility was given by Lakhtakia [22, 23] in electromagnetics. For nihility medium both relative permittivity and permeability are null valued. The idea of nihility is very usefull for those researchers interested in solving different problems of electromagnetics [24–29]. The nihility medium does not allow the electromagnetic energy to propagate in it. For nihility medium Maxwell equations reduce to form

$$\nabla \times \mathbf{E} = 0 \tag{1.3}$$

$$\nabla \times \mathbf{H} = 0 \tag{1.4}$$

For nihility metamaterial constitutive relations are

$$\mathbf{D} = 0 \tag{1.5}$$

$$\mathbf{B} = 0 \tag{1.6}$$

For nihility medium both relative permittivity and permeability are zero at certain frequency so the wave number for nihility medium is also null valued and no wave propagates in nihility medium. Nihility cylinder and perfect lenses are discussed by Lakhtakia et al. [28, 30, 31] and Ziolkowski discussed the propagation in and scattering from a matched zero index medium [32] for which both ralative permittivity and permeability of the medium approaches to zero. Ahmed and Naqvi [24] discussed directive EM radiation of line source in the presence of coated nihility cylinder.
Chiral nihility is a special kind of chiral medium for which value of both relative permittivity and permeability are zero at certain frequency but chirality of medium is non zero. In chiral nihility medium two circular waves exist but one of them is backward wave. When a plane wave enters in chiral nihility medium from vacuum then phenomena of negative refraction occurs. The idea of electromagnetic waves and energy in chiral nihility medium is first given by Tretyakov [27]. The transmission and reflection [33–35] and scattering [24, 36] properties of chiral nihility metamaterial have been studied. Cheng et al. discussed waves in planar waveguide containing chiral nihility metamaterials [26]. Naqvi [37] presented the characteristics of electromagnetic waves at planer slab of chiral nihility metamaterial backed by fractional dual/PEMC interface. The constitutive relations for chiral nihility metamaterial are

$$\mathbf{D} = j\kappa\sqrt{\epsilon_0\mu_0}\mathbf{H} \tag{1.7}$$

$$\mathbf{B} = -j\kappa\sqrt{\epsilon_0\mu_0}\mathbf{E} \tag{1.8}$$

Ziolkwoski [32] simulated the line source radiation in Zero Index Medium (ZIM). Naqvi et al.[24] investigated the electromagnetic scattering of a line source from a perfect electromagnetic conductor circular cylinder coated with double positive material and double negative material. Qamar et al. [38] studied the radiation of elementary source placed in an unbounded chiral nihility metamaterial. They argued that there is no radiation in this case. It means, source is unable to radiate when located in unbounded chiral nihility metamaterial.

1.2 Dispersive Media

Dispersion is a phenomena in which the phase velocity of wave dependents on frequency. The most well known example of dispersion observed in daily life is rainbow, in which separation of white light into components of different wavelengths is observed due to dispersion. Effect of dispersion on properties of wave traveling are described by dispersion relations. In these dispersion relations wavelength and wave number of medium are related with frequency of the wave. From dispersion relation phase velocity and group velocity have an expression for refractive index. If the speed of EM wave depends only on physical properties of the medium then the speed of EM waves remain constant and is independent of frequency of the medium and behavior of the wave traveling in this medium remains same, this type of medium is called non-dispersive medium. EM waves in unbounded free space are non-dispersive. But if speed of EM waves depends on frequency of the wave then this type of medium is said to be the dispersive medium.

All naturally occurring materials have positive index of refraction, but some materials with negative indices of refraction have also been explored, vaselago [2] observed that such materials did not violate any fundamental laws. These materials were termed as Left Handed Materials (LHM) and further it was also investigated that some properties of a LHM would be opposite to that of a Right Handed Material (RHM). When the value of permittivity and permeability become negative then the negative root of index of refraction must be chosen by

$$n = \mp\sqrt{\frac{\mu\epsilon}{\mu_0\epsilon_0}} \tag{1.9}$$

For dispersive medium permittivity and permeability of medium is frequency dependent, various frequency dependent permittivity and permeability expressions are used by various researchers [4–6, 11, 39–43] and Lorentz-Drude model one of most popular. Wave propagation through the DNG Lorentz/Drude slab embedded between two different dielectric is studied in [8, 39, 44].

In the Lorentz Drude model[41]

$$\epsilon(\omega) = \epsilon_0 \left(1 - \frac{\omega_{ep}^2 - \omega_{eo}^2}{\omega^2 - \omega_{eo}^2 + j\omega\delta_e}\right) \tag{1.10}$$

$$\mu(\omega) = \mu_0 \left(1 - \frac{\omega_{mp}^2 - \omega_{mo}^2}{\omega^2 - \omega_{mo}^2 + j\omega\delta_m}\right) \tag{1.11}$$

where, ω_{eo} is electronic resonance frequency, ω_{ep} is electronic plasma frequency, δ_e is electronic damping frequency, ω_{mo} is magnetic resonance frequency, ω_{mp} is magnetic plasma frequency and δ_m is magnetic damping frequency.

1.3 Overview

The present dissertation is composed of four chapters

Chapter-1 gives a brief overview of the history. Some interesting properties and characteristics of chiral metamaterials are also presented in this chapter. The second section of this chapter explains the dispersive medium. For dispersive medium frequency dependent ralations for permittivity and permeability of medium are described. Drude/Lorentz model is used for dispersive medium.

Chapter-2 presents the analysis of radiations of electromagnetic waves from a current sheet placed at the center of dispersive dielectric magnetic material surrounded by unbounded chiral metamaterial. For this purpose a slab of non-dispersive/dispersive dielectric medium, placed in unbounded chiral medium is considered. Lorentz-Drude model is used inside the slab whereas outside the slab unbounded chiral is considered. Several results are given for RCP and LCP component of transmitted field. Some special cases are also considered for this problem.

Chapter-3 presents the analysis of radiation of electromagnetic waves from a line source placed at the center of dispersive dielectric-magnetic material surrounded by unbounded chiral metamaterial. Lorentz-Drude model is used inside the cylinder and outside the cylinder unbounded chiral is considered. Nihility is taken as limiting case of a dielectric magnetic medium with both

permittivity and permeability approaching to zero. Two cases for unbounded host medium are considered, i.e., chiral and chiral nihility metamaterials. Chiral nihility is taken as limiting case of chiral with both permittivity and permeability approaching to zero, whereas chirality is nonzero. It is explored, how different combinations of mediums forming the interface effect transmission. Several results are give for transmitted field.

The purpose of this thesis is to study the transmission characteristics from different interfaces. A purpose of present work is also to study the radiation due to elementary source in unbounded chiral nihility metamaterial when source is placed in dispersive medium of very small radius. This may be considered as a limiting case of work present in [38].

Chapter-4 presents the analysis of radiation of electromagnetic waves from a line source placed at the center of dispersive dielectric magnetic coated dielectric cylinder placed in unbounded chiral medium. All the cases that are discussed for cylindrical problem in chapter are also discussed for coated cylinder in this chapter.

The thesis is concluded in **Chapter-5** .

Chapter 2

Radiation through a Slab of Dispersive Dielectric-Magnetic Placed in Chiral Metamaterial

Transmission of electromagnetic waves from different interfaces is an important topic. In this chapter transmitted field through a dispersive slab placed in chiral metamaterial is studied. Chiral nihility medium has also been studied here and assumed as a special case of chiral medium.

2.1 Problem Formulation

A dispersive dielectric magnetic slab of width $-d < z < +d$ is assumed to be placed in an unbounded chiral metamaterial. As a source of excitation, a time harmonic current sheet is assumed at $z = 0$. The constitutive parameters for dispersive dielectric-magnetic medium are represented by $(\epsilon_1(\omega), \mu_1(\omega))$, whereas chiral metamaterial is described by parameters $(\epsilon_2, \mu_2, \kappa)$

The geometry consists of three regions, Region-1 $(-d < z < +d)$ is dispersive dielectric-magnetic medium, Region-2 $(z > +d)$ is unbounded chiral metamaterial and Region-3 $(z > -d)$ is also an unbounded chiral metamate-

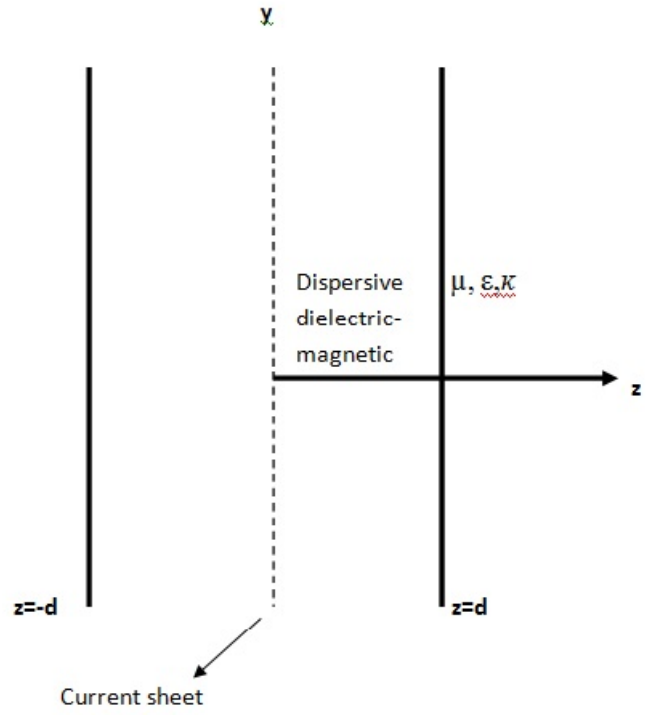

Figure 2.1: Dispersive dielectric-magnetic slab placed in an unbounded chiral metamaterial.

rial. The time harmonic electric current sheet source is expressed as

$$J_\omega(r) = -A\delta(z)\hat{x} \tag{2.1}$$

The plane waves generated by current sheet propagates in z direction. Electromagnetic fields inside the slab can be written as

$$\mathbf{E}_1(x,y,z) = A\exp(ik_1|z|)\hat{x} + R_1 e^{ik_1 z}\hat{x} + R_2 e^{-ik_1 z}\hat{x} \tag{2.2}$$

$$\mathbf{H}_1(x,y,z) = \frac{1}{\eta_1}\left(R_1 e^{ik_1 z}\hat{y} + R_2 e^{-ik_1 z}\hat{y}\right) \tag{2.3}$$

where for DPS slab

$$\eta_1 = \sqrt{\frac{\mu_1(\omega)}{\epsilon_1(\omega)}} \tag{2.4}$$

$$k_1 = \omega\sqrt{\epsilon_1(\omega)\mu_1(\omega)} \tag{2.5}$$

For DNG slab

$$\eta_1 = \sqrt{\frac{\mu_1(\omega)}{\epsilon_1(\omega)}} \tag{2.6}$$

$$k_1 = -\omega\sqrt{\epsilon_1(\omega)\mu_1(\omega)} \tag{2.7}$$

For MNG slab

$$\eta_1 = i\sqrt{\frac{|\mu_1(\omega)|}{|\epsilon_1(\omega)|}} \tag{2.8}$$

$$k_1 = i\omega\sqrt{|\epsilon_1(\omega)|\mu_1(\omega)|} \tag{2.9}$$

while for ENG slab

$$\eta_1 = -i\sqrt{\frac{|\mu_1(\omega)|}{|\epsilon_1(\omega)|}} \tag{2.10}$$

$$k_1 = i\omega\sqrt{|\epsilon_1(\omega)||\mu_1(\omega)|} \tag{2.11}$$

Transmitted field from dispersive slab in chiral metamaterial can be written as a linear combination of two circularly polarized plane waves as

$$\mathbf{E}_2(x,y,z) = \tau_1(\hat{x}+i\hat{y})e^{ik^+z} + \tau_2(\hat{x}-i\hat{y})e^{ik^-z} \tag{2.12}$$

$$\mathbf{H}_2(x,y,z) = \frac{i}{\eta_2}\left(\tau_1(\hat{x}+i\hat{y})e^{ik^+z} - \tau_2(\hat{x}-i\hat{y})e^{ik^-z}\right) \tag{2.13}$$

Fields in Region-3 can be written as

$$\mathbf{E}_3(x,y,z) = \tau_1(\hat{x}+i\hat{y})e^{-ik^+z} + \tau_2(\hat{x}-i\hat{y})e^{-ik^-z} \tag{2.14}$$

$$\mathbf{H}_2(x,y,z) = \frac{i}{\eta_2}\left(\tau_1(\hat{x}+i\hat{y})e^{-ik^+z} - \tau_2(\hat{x}-i\hat{y})e^{-ik^-z}\right) \tag{2.15}$$

where

$$k^{\pm} = \omega\sqrt{\epsilon_2\mu_2} \pm \kappa\sqrt{\epsilon_0\mu_0} \tag{2.16}$$

Applying the boundary conditions that tangential component of electric and magnetic field are continuous at the interface

$$n \times \mathbf{E}_1 = n \times \mathbf{E}_2, \quad \mathrm{z} = +\mathrm{d} \tag{2.17}$$

$$n \times \mathbf{H}_1 = n \times \mathbf{H}_2, \quad \mathrm{z} = +\mathrm{d} \tag{2.18}$$

$$n \times \mathbf{E}_1 = n \times \mathbf{E}_3, \quad \mathrm{z} = -\mathrm{d} \tag{2.19}$$

$$n \times \mathbf{H}_1 = n \times \mathbf{H}_3, \quad \mathrm{z} = -\mathrm{d} \tag{2.20}$$

By applying these boundry conditions we get a matrix equation which can be solved to find the unknown coefficient R_1, R_2, τ_1, τ_2, τ_3, τ_4.

$$AX = B \tag{2.21}$$

where

$$A = \begin{pmatrix} e^{-ik_1 d} & e^{ik_1 d} & -e^{ik^+ d} & -e^{ik^- d} & 0 & 0 \\ 0 & 0 & e^{ik^+ d} & e^{ik^- d} & 0 & 0 \\ e^{-ik_1 d} & e^{ik_{1z} d} & \frac{\eta_1}{\eta_2} e^{ik^+ d} & \frac{\eta_1}{\eta_2} e^{ik^- d} & 0 & 0 \\ e^{ik_1 d} & e^{-ik_1 d} & 0 & 0 & -e^{ik^+ d} & -e^{ik^- d} \\ 0 & 0 & 0 & 0 & e^{ik^+ d} & e^{ik^- d} \\ e^{ik_1 d} & e^{ik_1 d} & 0 & 0 & \frac{\eta_1}{\eta_2} e^{ik^+ d} & \frac{\eta_1}{\eta_2} e^{ik^- d} \end{pmatrix} \tag{2.22}$$

$$B = \begin{pmatrix} -e^{ik_1^{|d|}} \\ 0 \\ 0 \\ -e^{ik_1^{|d|}} \\ 0 \\ 0 \end{pmatrix} \tag{2.23}$$

$$X = \begin{pmatrix} R_1 \\ R_2 \\ \tau_1 \\ \tau_2 \\ \tau_3 \\ \tau_4 \end{pmatrix} \tag{2.24}$$

2.2 Numerical Results

2.2.1 Non Dispersive Dielectric-Magnetic Slab

In this section we discuss the results for non dispersive slab placed in chiral metamaterial and excited with current sheet placed at the origin of the slab. It is observed that reflection coefficient R_1 and R_2 are same due to symmetry.

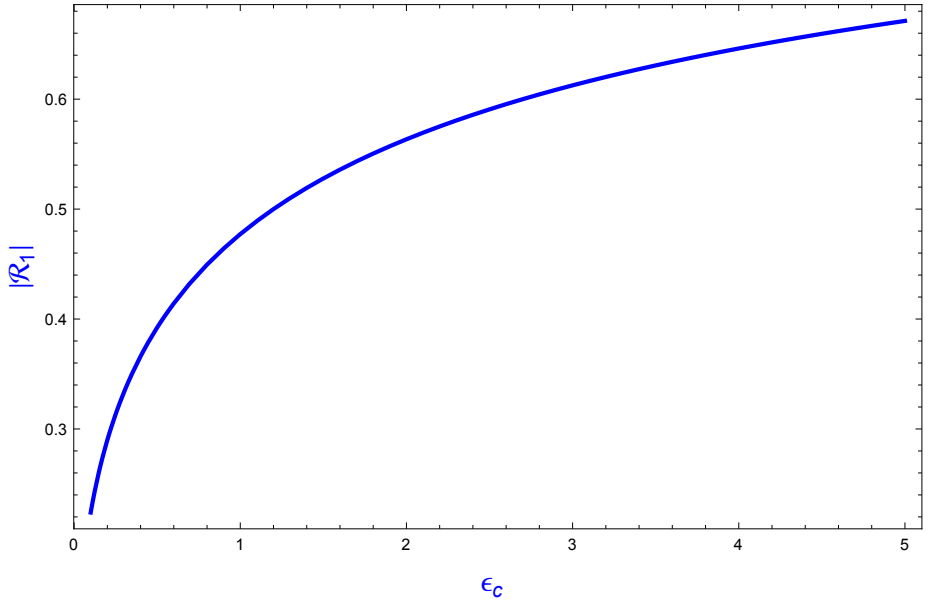

Figure 2.2: Absolute value of coefficient of RCP component of transmitted field through the interface of non dispersive dielectric slab and chiral metamaterial with respect to the relative permittivity of dielectric slab: $\epsilon_c = 0.9$, $\kappa = 0.01$, $\mu_r = \mu_c = 1$, $f = 1$GHz, $d = 0.01\lambda_1$.

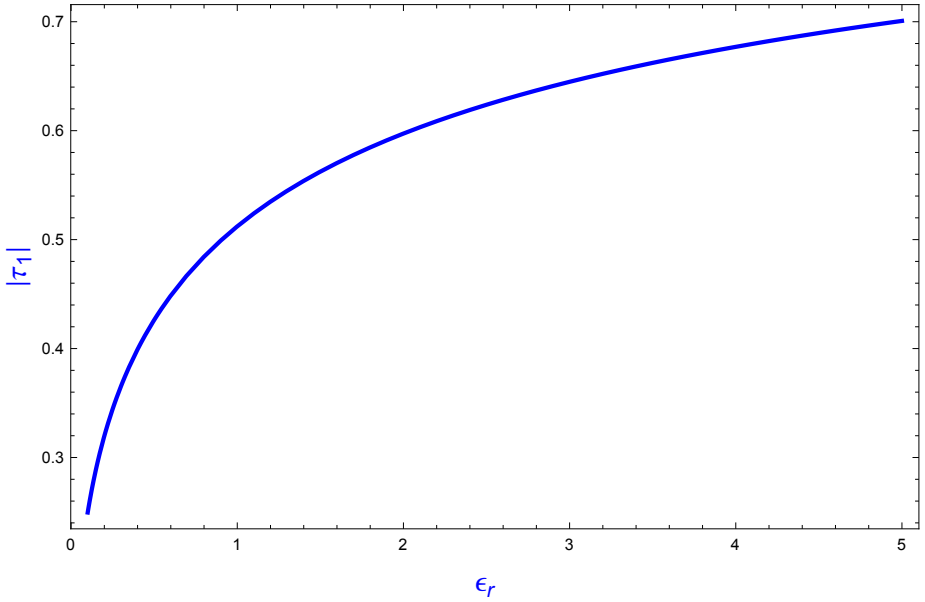

Figure 2.3: Absolute value of coefficient of RCP component of transmitted field through a non dispersive dielectric slab placed in chiral metamaterial with respect to the relative permittivity of dielectric slab: $\epsilon_c = 0.9$, $\kappa = 0.01$, $\mu_r = \mu_c = 1$, $f = 1$GHz, $d = 0.01\lambda_1$.

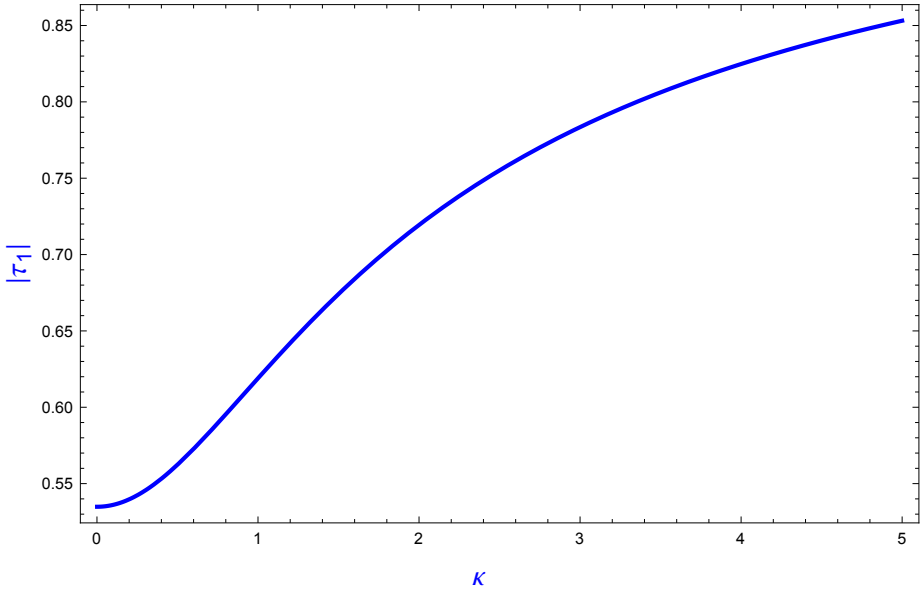

Figure 2.4: Absolute value of coefficient of RCP component of transmitted field through a non dispersive dielectric slab placed in chiral metamaterial with respect to chirality: $\epsilon_r = 1.2$, $\epsilon_c = 0.9$, $\kappa = 0.01$, $\mu_r = \mu_c = 1$, $f = 1GHz$, $d = 0.01\lambda_1$.

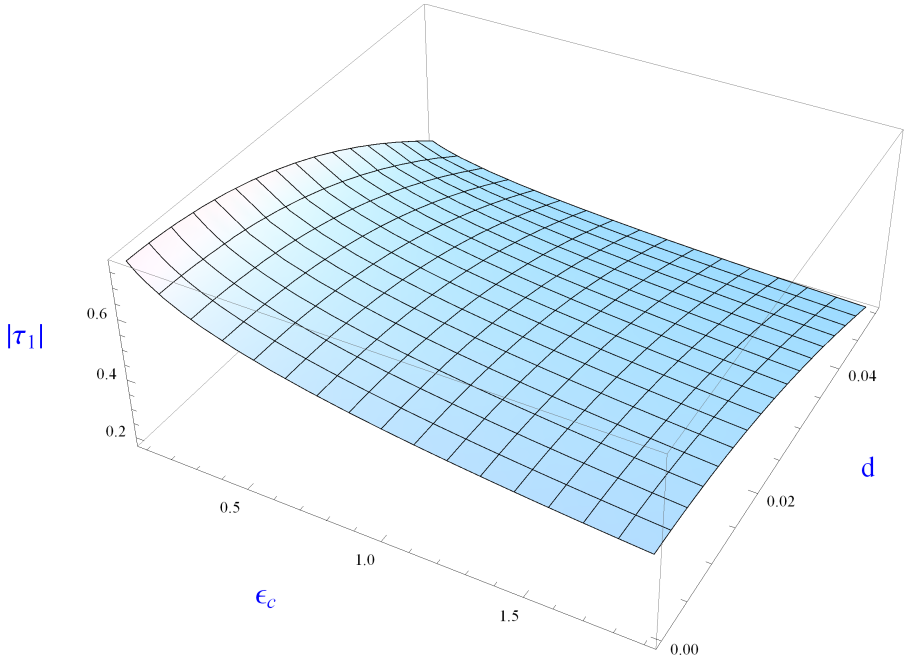

Figure 2.5: Absolute value of coefficient of RCP component of transmitted field of dielectric slab placed in chiral metamaterial with respect to distance and permittivity of chiral metamaterial: $\epsilon_r = 1.2$, $\kappa = 0.01$, $\mu_r = \mu_c = 1$, $f = 1$GHz .

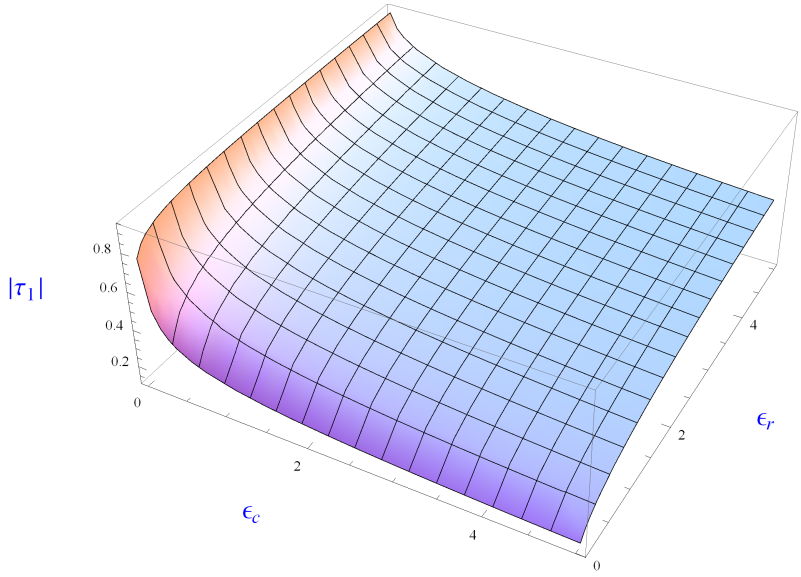

Figure 2.6: Absolute value of coefficient of RCP component of transmitted field of dielectric slab placed in chiral metamaterial with respect to distance and permittivity of chiral metamaterial: $\kappa = 0.01$, $\mu_r = \mu_c = 1$, $f = 1$GHz, $\epsilon_r = 1.2$.

Fig. 2.2 shows the effect of relative permittivity of dielectric slab on reflection coefficient. It is noted that absolute value of the coefficient of RCP component of transmitted field increases with increasing the relative permittivity of chiral metamaterial. Fig. 2.3 shows the effect of relative permittivity of dielectric slab on transmission. It is noticed that absolute value of the coefficient of RCP component of transmitted field increases with increasing the relative permittivity of dielectric slab. Fig. 2.4 shows the effect of chirality on coefficient of RCP-polarized component of transmitted field and it is observed that coefficient of RCP component of transmitted field increases with chirality of host chiral metamaterial. In Fig. 2.5 combined effect of permittivity and width of slab is observed. It shows that with increasing width coefficient of transmitted field decreases, i.e., away from source effect of field decreases. Fig. 2.6 shows the effect of relative permittivity of chiral metamaterial and relative permittivity of dielectric slab on absolute value of coefficient of RCP component of transmitted field.

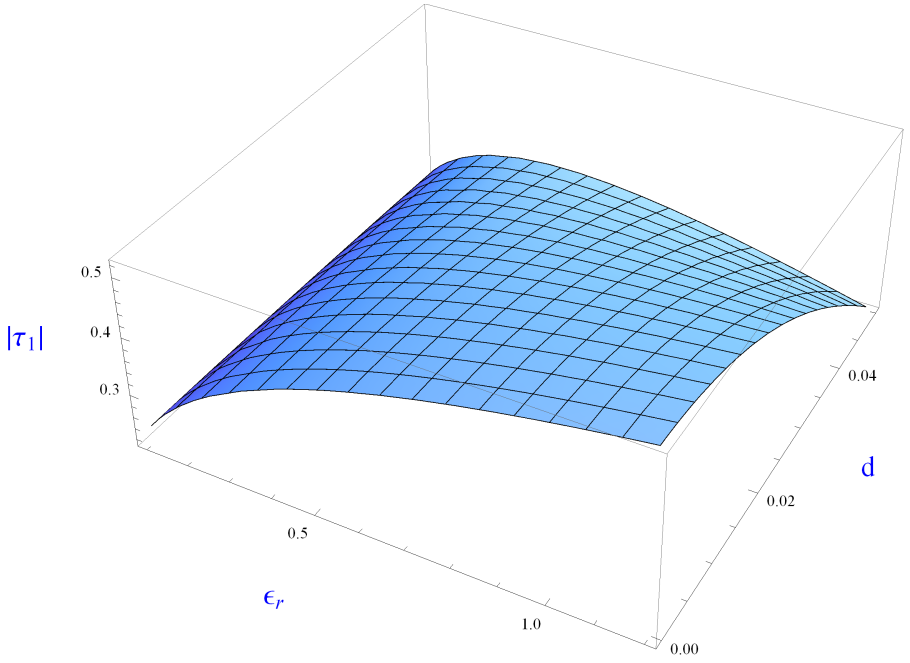

Figure 2.7: Absolute value of coefficient of RCP component of transmitted field of dielectric slab placed in chiral nihility metamaterial with respect to distance and permittivity of dielectric slab: $\kappa = 0.01$, $\mu_r = 1$, $f = 1$GHz .

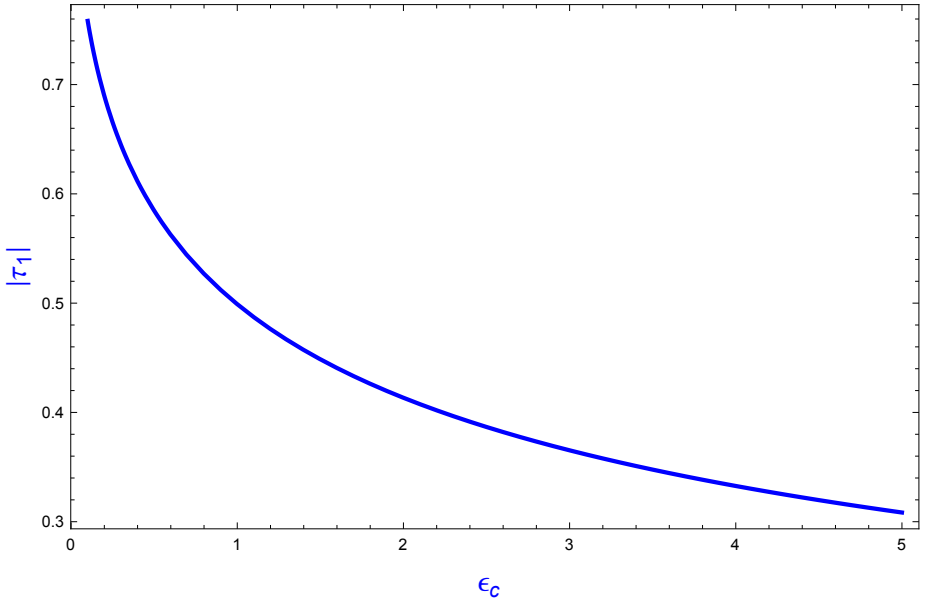

Figure 2.8: Absolute value of coefficient of RCP component of transmitted field of nihility slab placed in chiral metamaterial with respect to permittivity of chiral: $\kappa = 0.01$, $\mu_c = 1$, $f = 1$GHz .

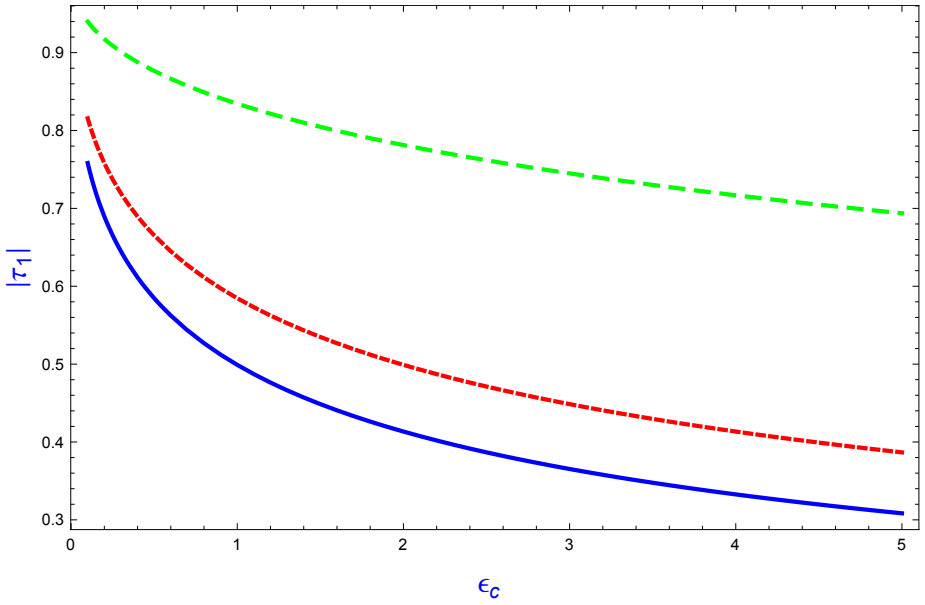

Figure 2.9: Absolute value of coefficient of RCP component of transmitted field of nihility slab placed in chiral metamaterial with respect to permittivity of chiral with $\mu_c = 1$, $f = 1$GHz: Solid line for $\kappa = 0.01$; small dashed line for $\kappa = 1$; dashed line for $\kappa = 5$.

Fig. 2.7 shows the effect of permittivity and width of slab when dielectric slab is placed in chiral nihility medium. In Fig. 2.8 effect of permittivity of chiral medium on absolute value of coefficient of RCP component of transmitted field is observed for nihility slab.
It can be noticed that effect of permittivity, chirality and distance is same for dielectric slab placed in chiral/chiral nihility medium. The only difference is that the transmission decreases in case of chiral nihility medium. In Fig. 2.9 absolute value of coefficient of RCP component of transmitted field is plotted against the permittivity of an unbounded chiral medium for different values of chirality.

2.2.2 Dependence of Dispersive Medium on Frequency

We first of all plot dispersion relations of Eq. (1.10) and Eq. (1.11) to show graphically the effect of frequency on permittivity and permeability. Following values of different parameters are considered for dispersive dielectric-magnetic medium: $f_{mp} = 10.95$GHz, $f_{mo} = 10.05$GHz,$f_{ep} = 12.8$GHz, $f_{eo} = 10.3$GHz and $\delta_m = \delta_e = 10$MHz.

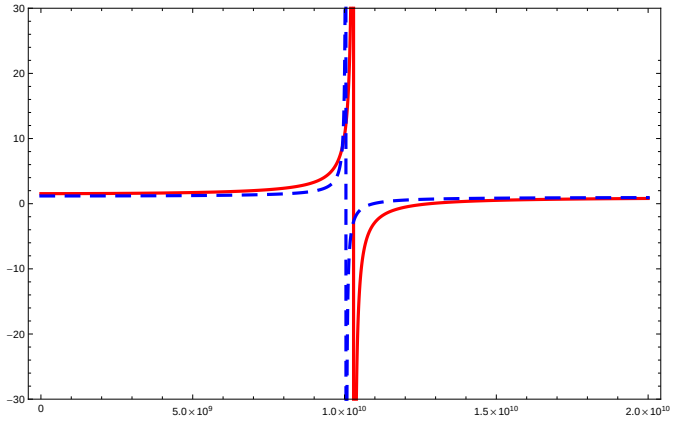

Figure 2.10: Behavior of the real part of permeability and permeability with respect to frequency for dispersive medium. Solid line for permittivity: Dashed line for permittivity.

Fig. 2.10 shows the variation of real part of permittivity and permeability with respect to the frequency. Permittivity shows resonance behavior at

10GHz, and permeability also shows resonance behavior but at 10.03GHz. From Fig. 2.10 effect of frequency on permittivity and permeability can be seen and it is noted that within frequency range of 10.1GHz − 10.3GHz permeability of medium is negative, within 10.4GHz − 10.9GHz both permittivity and permeability are negative and 11GHz − 12.7GHz permittivity is negative. And in frequency range below 10GHz and above 12.7GHz, both permittivity and permeability are positive.

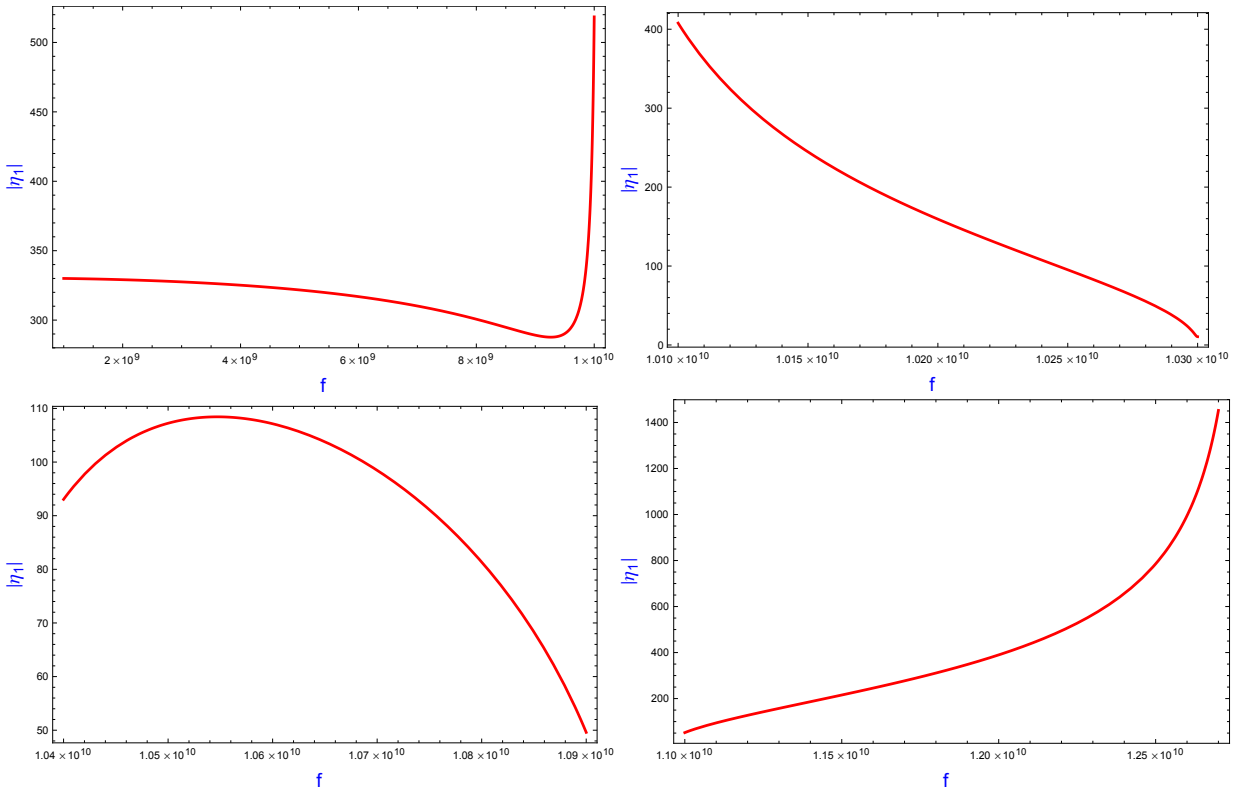

Figure 2.11: Behavior of intrinsic impedance of dispersive dielectric-magnetic medium with respect to frequency.

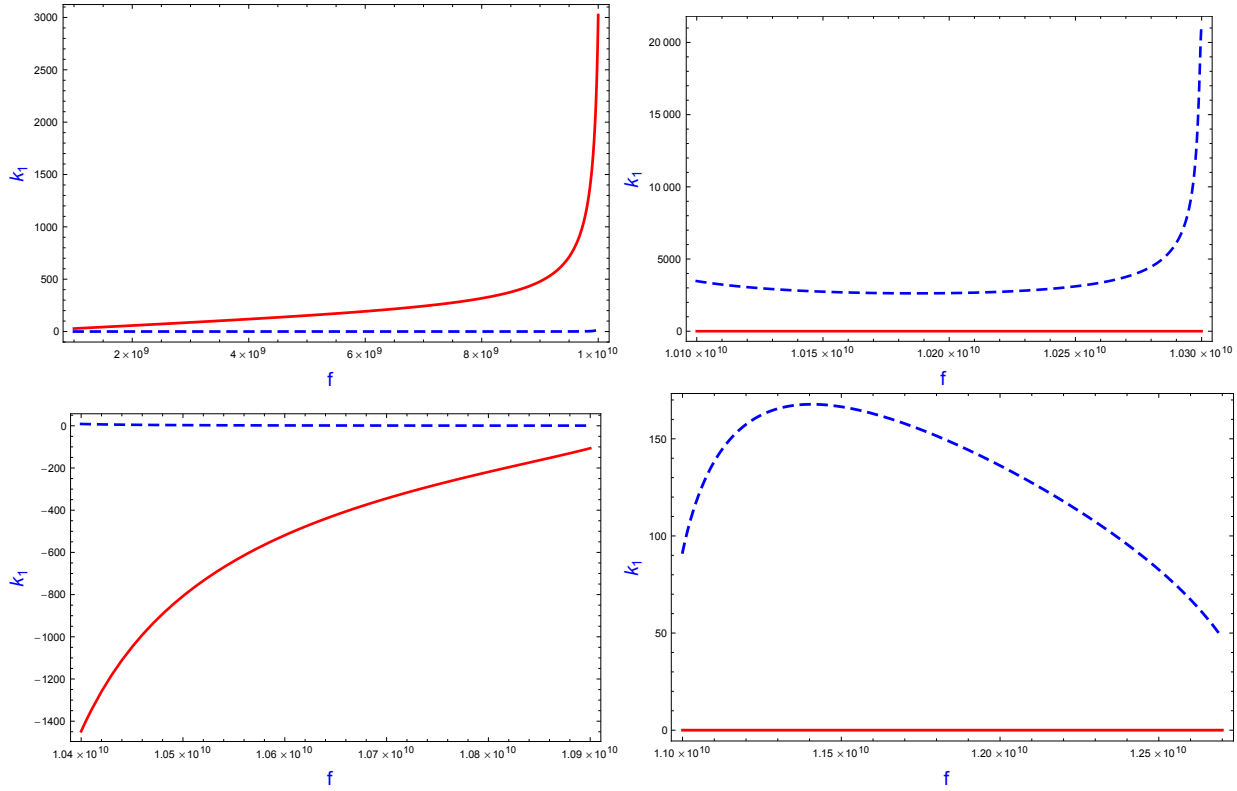

Figure 2.12: Behavior of wave number of dispersive dielectric-magnetic medium with respect to frequency: Dashed line for imaginary part of wave number; solid Line for real part of wave number.

Fig. 2.11 shows the effect of frequency on Absolute value of the intrinsic impedance of dispersive dielectric-magnetic medium. It is noticed that in frequency range for which dispersive dielectric-magnetic medium behaves as dispersive DNG medium, Absolute values of intrinsic impedance is small compared with those of DPS, MNG and ENG media. From Fig. 2.12 it can be seen that the frequency range for which medium behaves as DPS or DNG medium imaginary part of the wave number is zero and for MNG and ENG medium the real part of wave number is zero.

2.2.3 Dispersive Dielectric-Magnetic Slab

In this section dispersive dielectric-magnetic slab is considered to be placed in an unbounded chiral metamaterial. For above given values of dispersion parameters, transmitted field is determined by varying constitutive parameters. The effect of frequency on medium and on transmitted field is also analyzed.

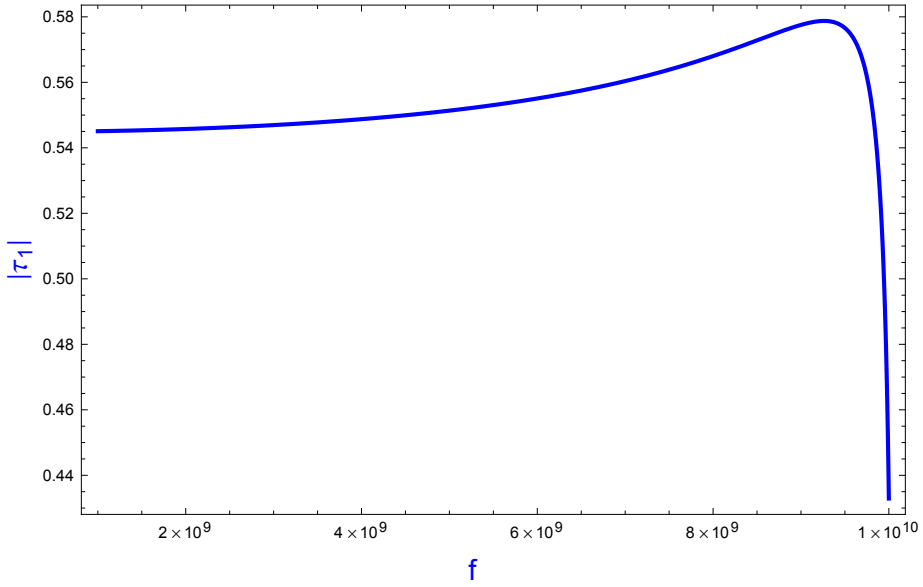

Figure 2.13: Absolute value of coefficient of RCP component of transmitted field through a dispersive DPS slab placed in chiral metamaterial: $\epsilon_c = 0.9$, $\mu_c = 1$, $d = 5$mm, $\kappa = 0.01$.

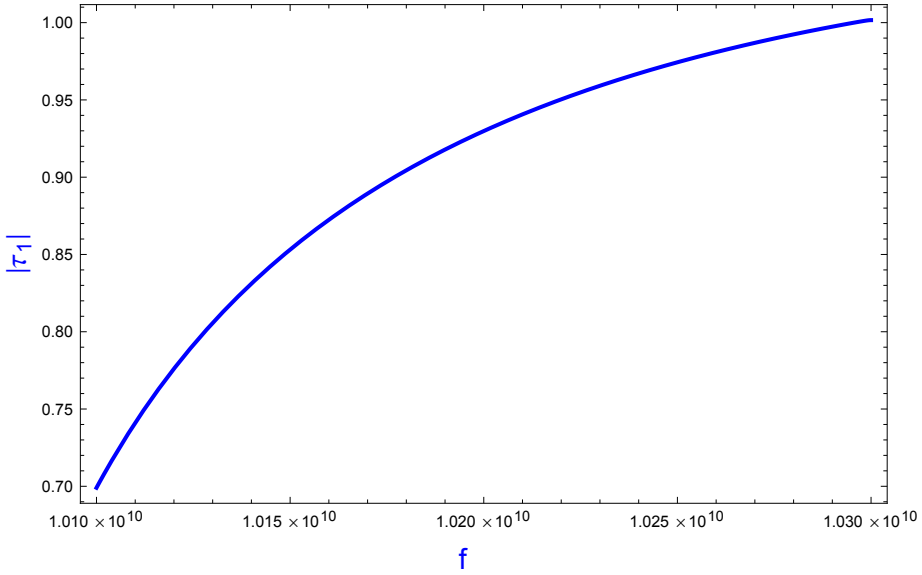

Figure 2.14: Absolute value of coefficient of RCP component of transmitted field through a dispersive MNG slab placed in chiral metamaterial: $\epsilon_c = 0.9$, $\mu_c = 1$, $d = 5$mm, $\kappa = 0.01$.

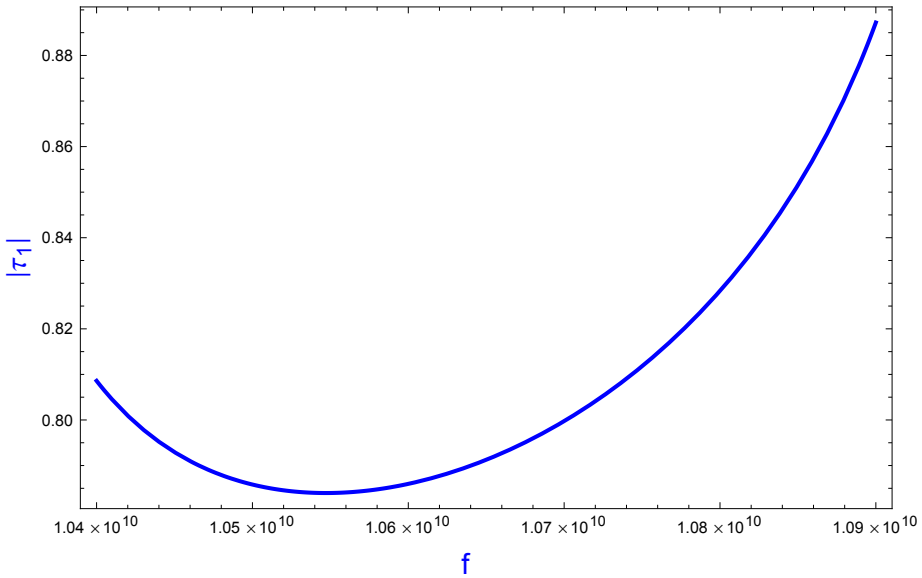

Figure 2.15: Absolute value of coefficient of RCP component of transmitted field through a dispersive DNG slab placed in chiral metamaterial: $\epsilon_c = 0.9$, $\mu_c = 1$, $d = 5$mm, $\kappa = 0.01$.

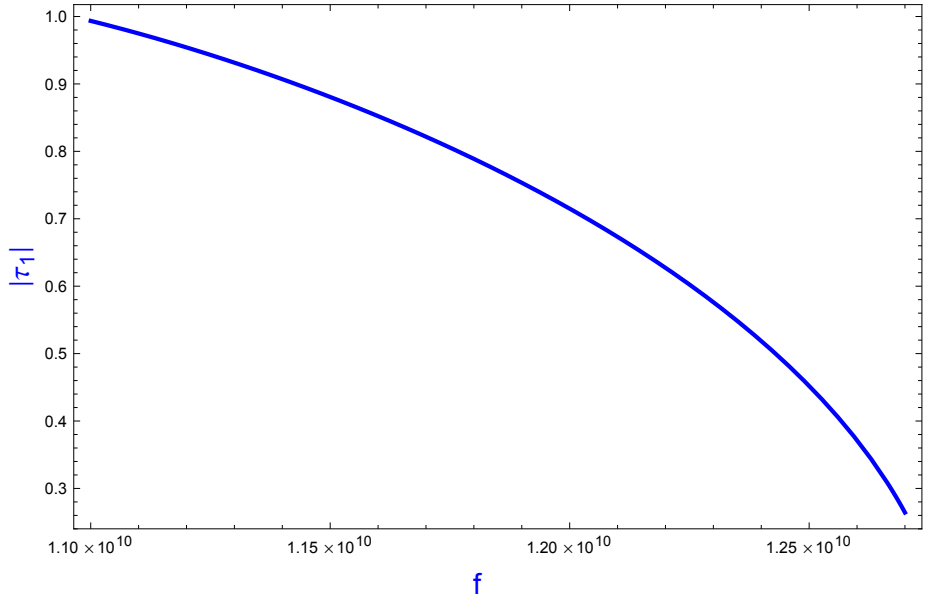

Figure 2.16: Absolute value of coefficient of RCP component of transmitted field through a dispersive ENG slab placed in chiral metamaterial: $\epsilon_c = 0.9$, $\mu_c = 1$, $d = 5$mm, $\kappa = 0.01$.

In Fig. 2.13, Fig. 2.14, Fig. 2.15 and in Fig. 2.16 coefficients of transmitted field through different interfaces is observed. Fig. 2.13 shows the behavior of absolute value of coefficient of RCP component of transmitted field when dispersive DPS slab is placed in an unbounded chiral metamaterial. In Fig. 2.14 behavior of absolute value of coefficient of RCP component of transmitted field is observed when dispersive MNG slab is located in chiral medium, Fig. 2.15 and Fig. 2.16 show the behavior of absolute value of coefficient of RCP component of transmitted field when the slab of DNG and ENG metamaterial is placed in an unbounded chiral metamaterial, respectively. It is noticed that at 10.3GHz and at 11GHz there is a complete transmission. In Fig. 2.17 effect of permittivity and frequency on absolute value of coefficient of RCP component of transmitted field can be seen. From Fig. 2.17, Fig. 2.18, Fig. 2.19 and Fig. 2.20 it can be seen that with increasing permittivity of chiral medium absolute value of coefficient of RCP component of transmitted field decreases.

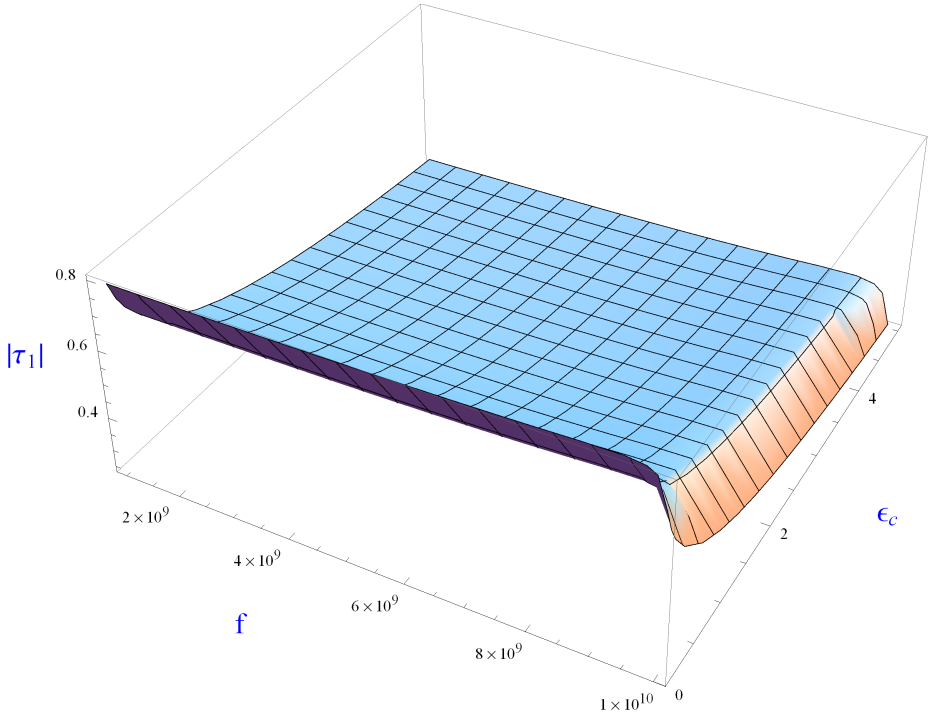

Figure 2.17: Absolute value of coefficient of RCP component of transmitted field through a dispersive DPS slab placed in chiral metamaterial: $\mu_c = 1$, $d = 5\text{mm}$, $\kappa = 0.01$.

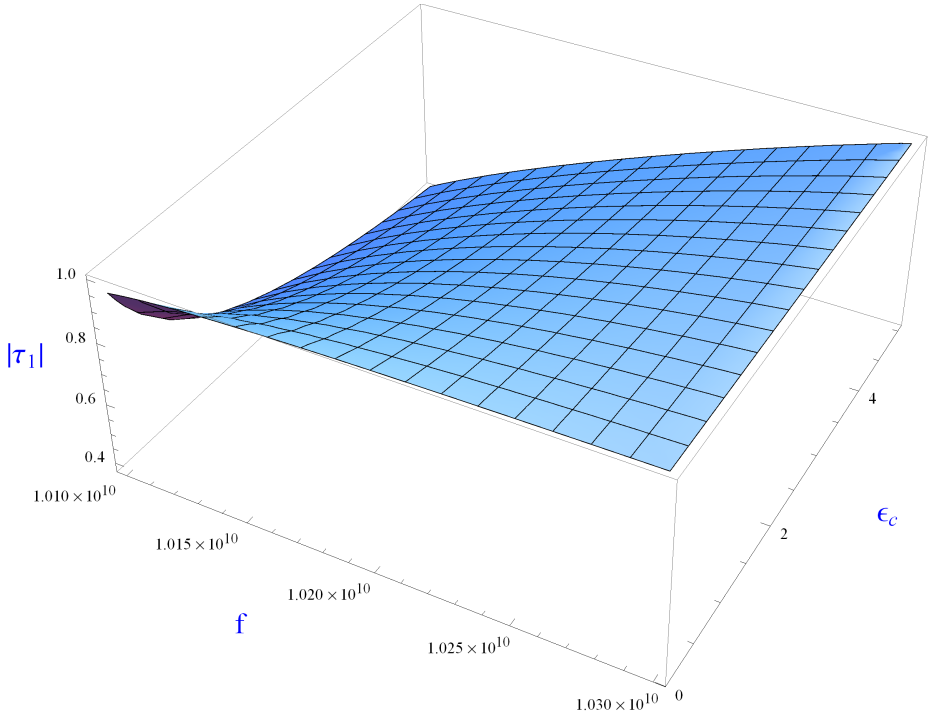

Figure 2.18: Absolute value of coefficient of RCP component of transmitted field through a dispersive MNG slab placed in chiral metamaterial: $\mu_c = 1$, $d = 5\text{mm}$, $\kappa = 0.01$.

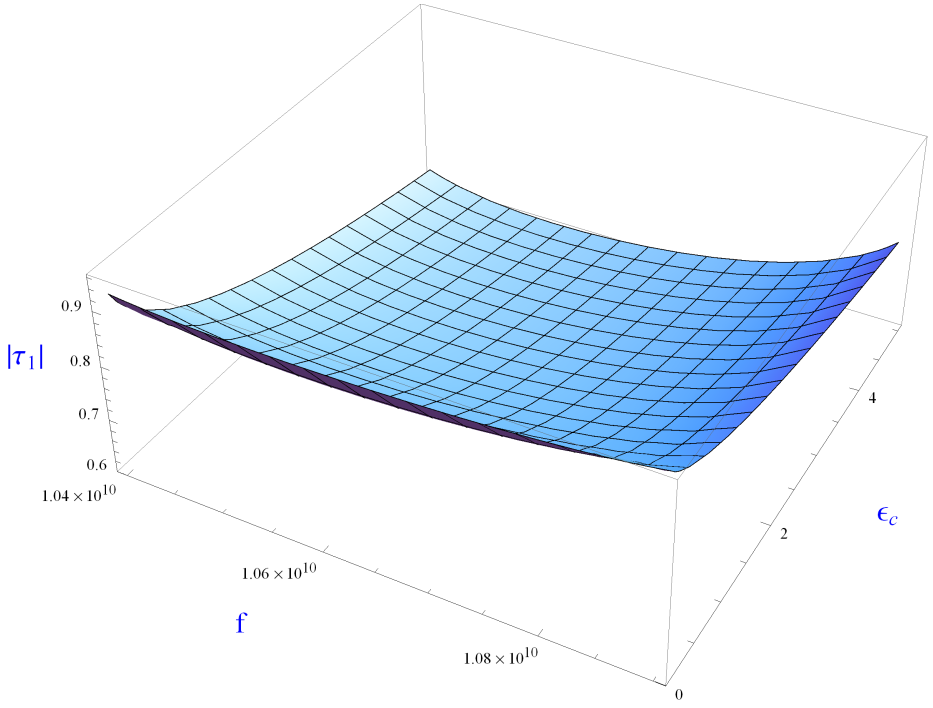

Figure 2.19: Absolute value of coefficient of RCP component of transmitted field through a dispersive DNG slab placed in chiral metamaterial: $\mu_c = 1$, $d = 5\text{mm}$, $\kappa = 0.01$.

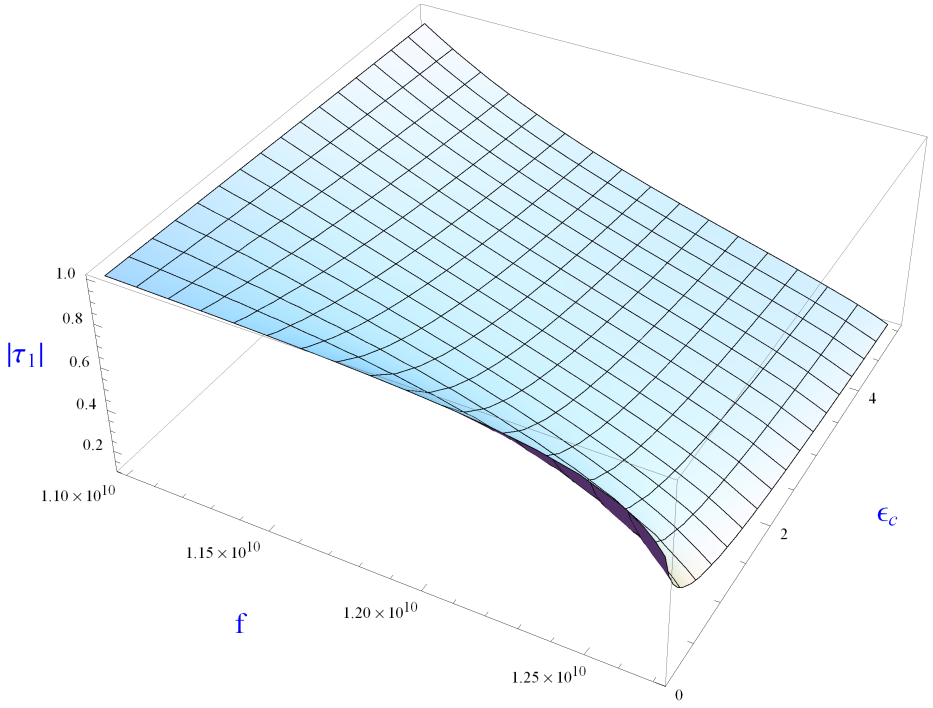

Figure 2.20: Absolute value of coefficient of RCP component of transmitted field through a dispersive ENG slab placed in chiral metamaterial: $\mu_c = 1$, $d = 5$mm, $\kappa = 0.01$.

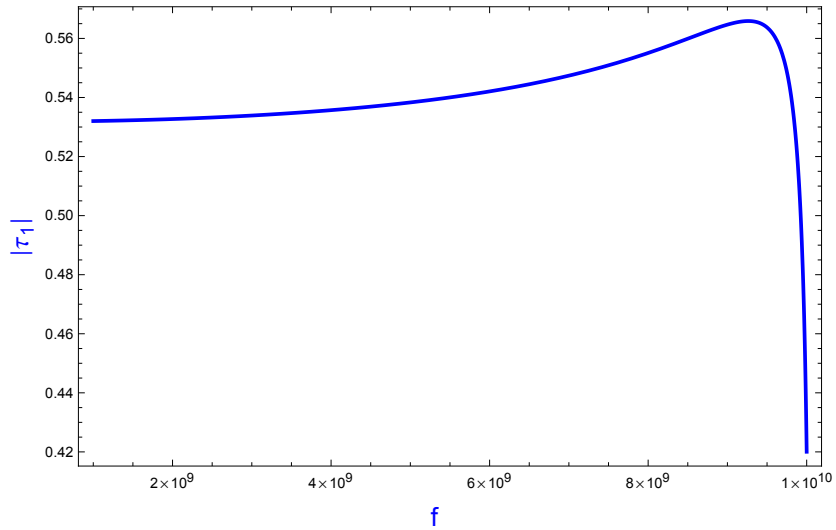

Figure 2.21: Absolute value of coefficient of RCP component of transmitted field through a dispersive DPS slab placed in chiral nihility metamaterial: $\mu_c = 1$, $d = 5$mm, $\kappa = 0.01$.

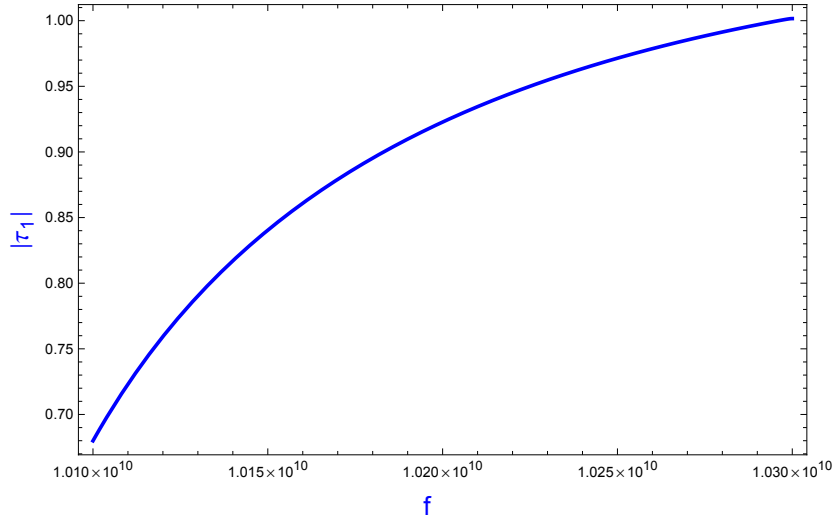

Figure 2.22: Absolute value of coefficient of RCP component of transmitted field through a dispersive MNG slab placed in chiral nihility metamaterial: $\mu_c = 1, d = 5\text{mm}, \kappa = 0.01$.

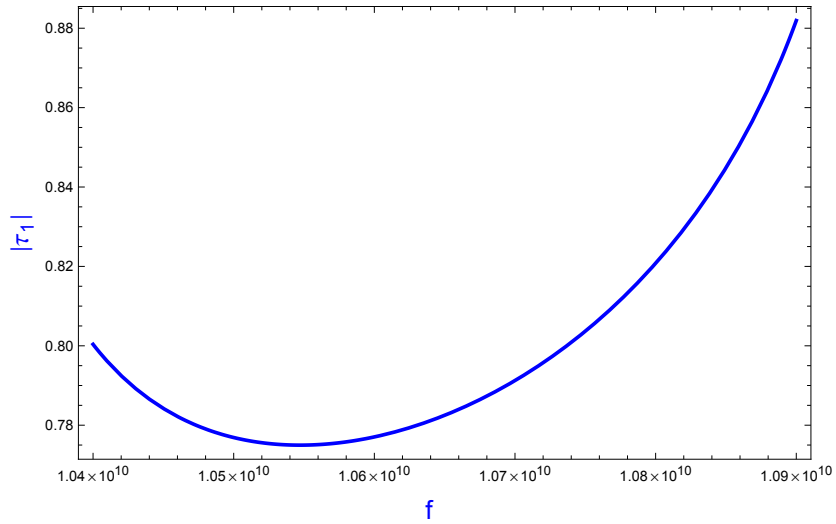

Figure 2.23: Absolute value of coefficient of RCP component of transmitted field through a dispersive DNG slab placed in chiral nihility metamaterial: $\mu_c = 1, d = 5\text{mm}, \kappa = 0.01$.

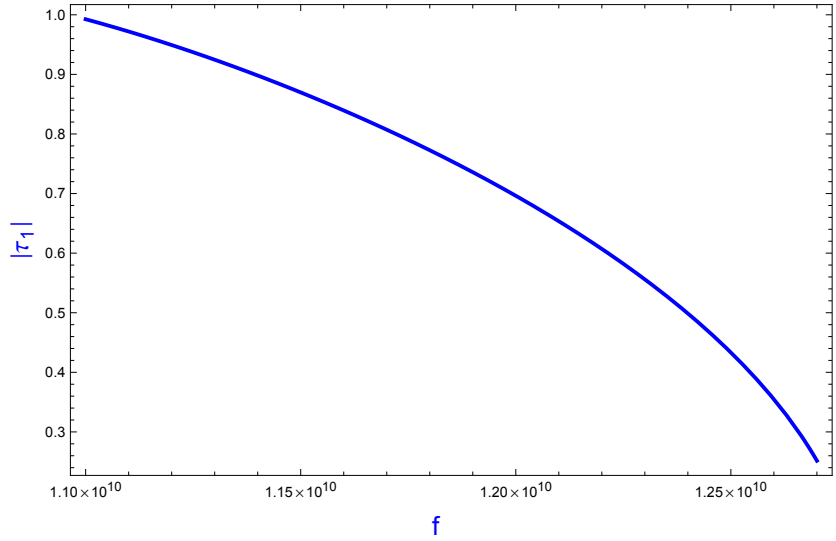

Figure 2.24: Absolute value of coefficient of RCP component of transmitted field through a dispersive ENG slab placed in chiral nihility metamaterial: $\mu_c = 1, d = 5\text{mm}, \kappa = 0.01$.

For Fig. 2.21 to Fig. 2.24 dispersive dielectric magnetic slab is considered to be placed in an unbounded chiral nihility metamaterial. It is noticed that the behavior of absolute value of coefficient of RCP component of transmitted field remains identical to that of chiral metamaterial except for a small decrease in amplitudes.

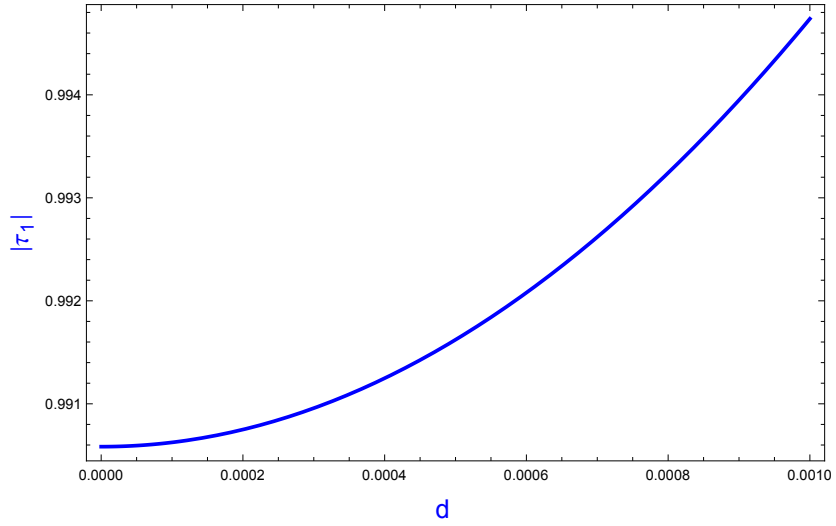

Figure 2.25: Absolute value of coefficient of RCP component of transmitted field through a dispersive ENG slab placed in chiral nihility metamaterial: $\mu_c = 1, d = 5\text{mm}, \kappa = 0.01$.

It is noticed in Fig. 2.25 that when a dispersive slab is placed in chiral metamaterial with increasing width of slab absolute value of coefficient of RCP component of transmitted field decreases but in case of chiral nihility host medium the behavior is different; that is, when the width of the slab is taken very small, amplitude of absolute value of coefficient of RCP component of transmitted field is also small and with increasing the width transmission coefficient also increases in this case. Note that for arbitrary small width, the present scenario becomes a special case of work present in [38].

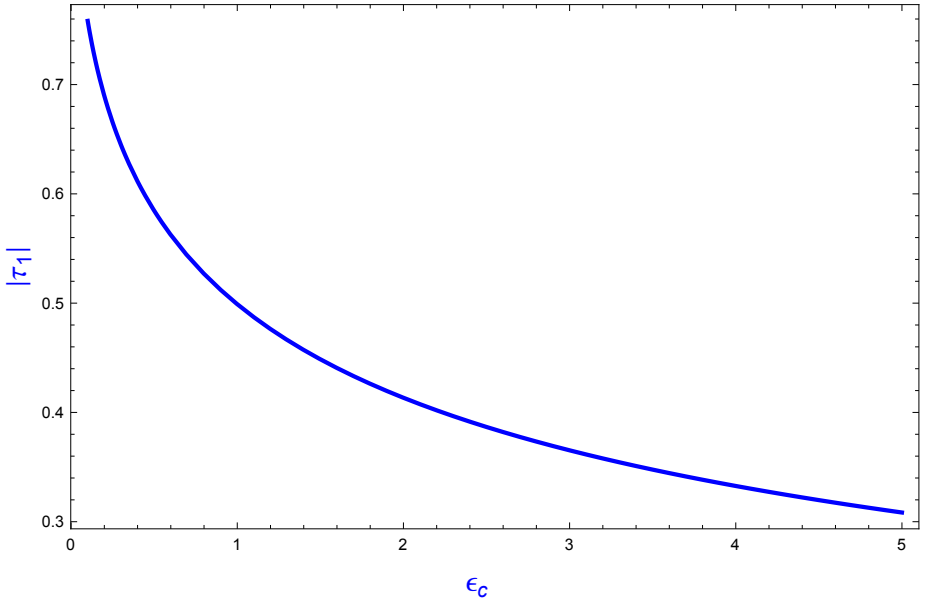

Figure 2.26: Absolute value of coefficient of RCP component of transmitted field from nihility slab placed in an unbounded chiral metamaterial with $\kappa = 0.01$.

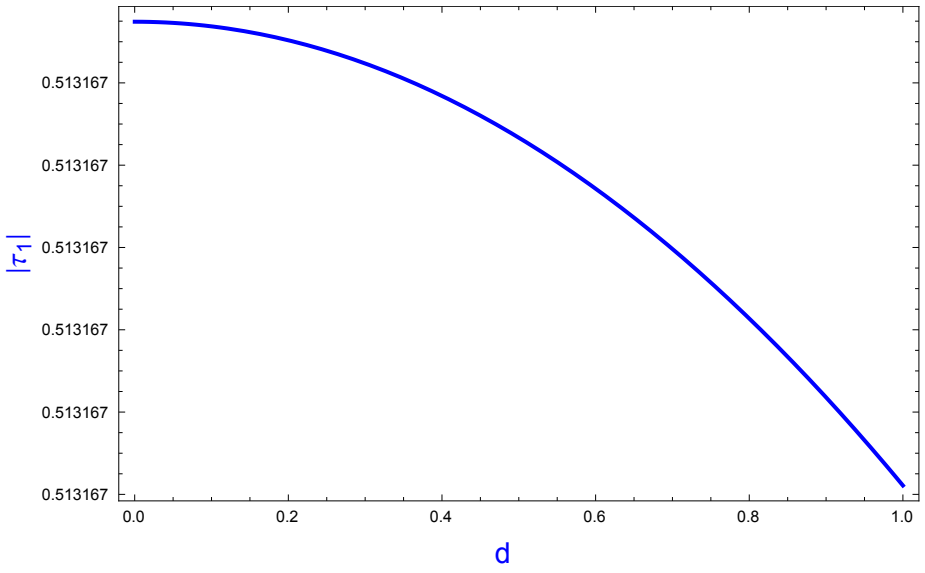

Figure 2.27: RCP coefficient of transmitted field from nihility slab with respect the width of slab .

When nihility slab is placed in chiral metamaterial then the effect of width

of the slab and permittivity of the host medium on coefficient of transmitted field can be seen in Fig. 2.26 and Fig. 2.27. It is noticed that with increasing the permittivity of host chiral metamaterial transmitted field decreases exponentially and also with the width of the slab transmitted field decreases.

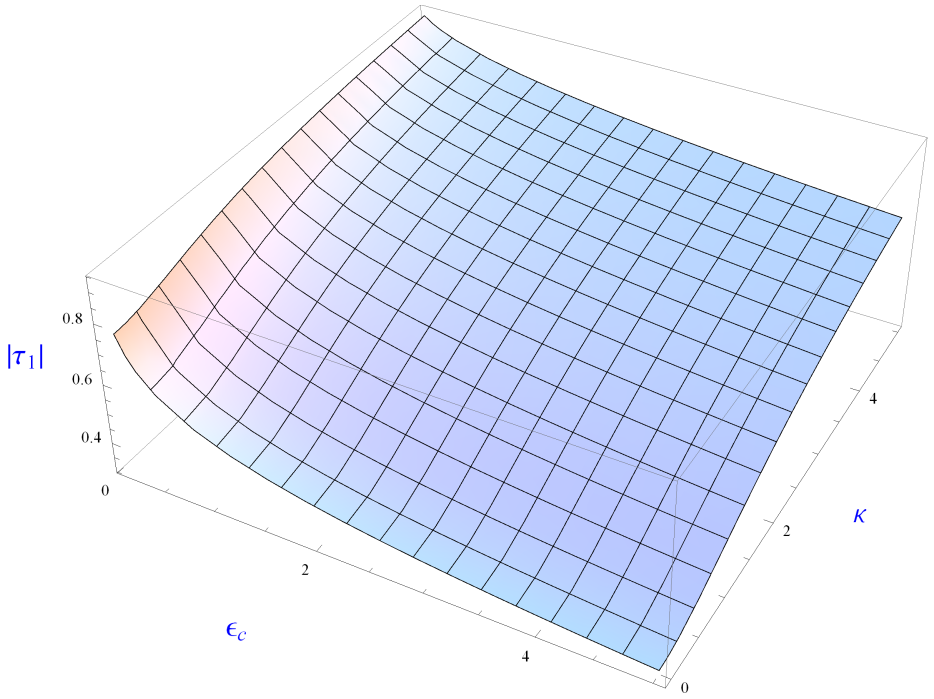

Figure 2.28: RCP coefficient of transmitted field from nihility slab with respect to permittivity and chirality of host chiral medium .

In Fig. 2.28 the effect of permittivity and chirality of host metamaterial on RCP coefficient of transmitted field is plotted. It can be seen from Fig. 2.28 that with permittivity of the chiral medium coefficient of RCP transmitted field decreases, whereas with chirality of the host medium coefficient of RCP transmitted field increases.

2.3 Summary

In this chapter radiation problem is discussed for which a current sheet is considered as a source of excitation. Current sheet is placed at the center of dispersive dielectric magnetic slab and field transmitted in an unbounded chiral

metamaterial is observed. Dielectric slab instead of dispersive dielectric magnetic slab is also considered and behavior of coefficients of transmitted field is noticed. We also discussed the dispersive dielectric slab surrounded by chiral nihility metamaterial, and nihility slab is also considered as a special case. For non-dispersive slab coefficient of transmitted field increases with increasing relative permittivity of dispersive slab and chirality of host chiral metamaterial, and decreases with relative permittivity of chiral medium. For dispersive slab transmission coefficient decreases with frequency for DPS and ENG slabs while increases for DNG and MNG slabs. At 10.3GHz and at 11GHz there is a complete transmission. Coefficient of RCP component of transmitted field decreases with permittivity of chiral medium and increases with increasing the chirality and relative permittivity of dispersive slab for DPS, MNG, DNG and ENG slabs. Coefficient of transmitted field decreases with increasing width of slab for host chiral metamaterial. For the case of host chiral nihility transmission coefficient approaches to zero for very small width of slab and increases with increasing the width of the slab.

Chapter 3

Radiation through a Cylindrical Interface of Dispersive Dielectric-Magnetic and Chiral Metamaterial

3.1 Formulation of the Problem

We consider a circular cylinder of radius a placed in a lossless, isotropic and reciprocal chiral metamaterial, in this chapter. An infinite line source carrying time harmonic current is assumed at the center of the cylinder. It is further assumed that the circular cylinder is composed of dispersive dielectric-magnetic medium whose parameters are described through Lorentz-Drude model. The constitutive parameters for dispersive dielectric-magnetic medium are represented as $(\epsilon_1(\omega), \mu_1(\omega))$, whereas chiral metamaterial is described by parameters $(\epsilon_2, \mu_2, \kappa)$. The region inside the cylinder is termed as Region- 1 and the region outside the cylinder is termed as Region 2. The constitutive relations for chiral metamaterial are given below[21]

$$\mathbf{D} = \epsilon_0 \epsilon_c \mathbf{E} - j\kappa\sqrt{\epsilon_0 \mu_0}\mathbf{H} \tag{3.1}$$

$$\mathbf{B} = \mu_0 \mu_c \mathbf{H} + j\kappa\sqrt{\epsilon_0 \mu_0}\mathbf{E} \tag{3.2}$$

where κ is parameter which describes chirality of the medium, ϵ_c and μ_c are relative permittivity and permeability of chiral medium, respectively. Field

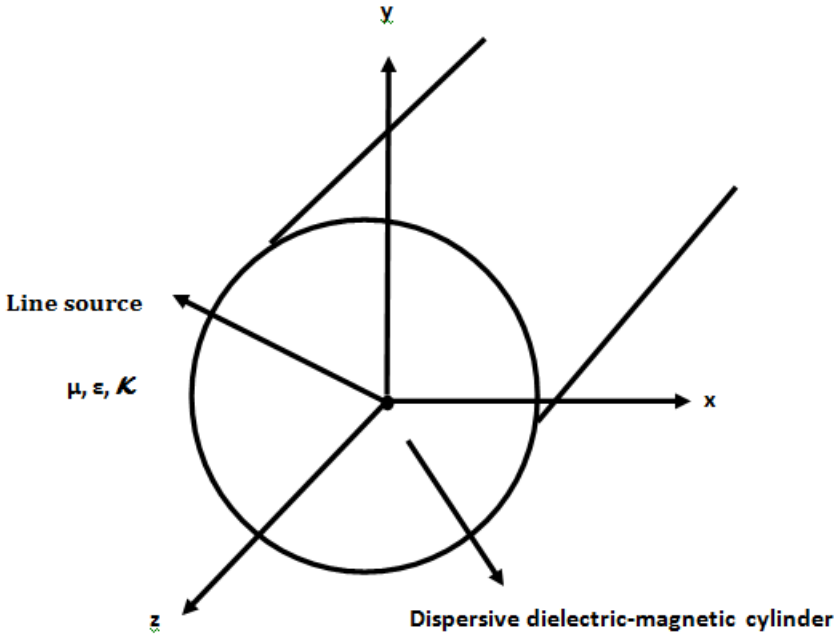

Figure 3.1: Dispersive dielectric-magnetic cylinder carrying line source and placed in an unbounded chiral metamaterial.

radiated due to a line source in an unbounded medium is given by[45]

$$\mathbf{E}_z = -\frac{k_1^2 I}{4\omega\epsilon_1} H_0^{(1)}(k_1\rho) \tag{3.3}$$

Here I is the current in the line source, ϵ_1 is permittivity of the dispersive-magnetic cylinder, $\epsilon_1(\omega) = \epsilon_0\epsilon_r(\omega)$ and $k_1(\omega)$ is wave number of dispersive

dielectric-magnetic cylinder and can be written as

$$k_1(\omega) = \omega\sqrt{\epsilon_1(\omega)\mu_1(\omega)}$$

Due to presence of line source, z-component of the total field in Region 1 can be written in terms of unknown component as

$$\mathbf{E}_{1z} = -\frac{k_1^2 I}{4\omega\epsilon_1} H_0^{(1)}(k_1\rho) - \frac{k_1^2 I}{4\omega\epsilon_1} \sum_{n=-\infty}^{n=+\infty} j^n a_n H_n^{(2)}(k_1\rho) e^{jn\phi} \tag{3.4}$$

$$\mathbf{H}_{1z} = \frac{k_1^2 I}{4j\omega\epsilon_1\eta_1} \sum_{n=-\infty}^{n=+\infty} j^n b_n H_n^{(2)}(k_1\rho) e^{jn\phi} \tag{3.5}$$

The corresponding ϕ component of electric and magnetic field may be obtained using Maxwell equations as

$$\mathbf{E}_\phi = -\frac{1}{j\omega\epsilon}\nabla \times \mathbf{E} \tag{3.6}$$

$$\mathbf{H}_\phi = \frac{1}{j\omega\mu}\nabla \times \mathbf{E} \tag{3.7}$$

And ϕ components can be written as

$$\mathbf{E}_{1\phi} = \frac{k_1^2 I}{4\omega\epsilon_1} \sum_{n=-\infty}^{n=+\infty} j^n b_n H_n^{(2)'}(k_1\rho) e^{jn\phi} \tag{3.8}$$

$$\mathbf{H}_{1\phi} = \frac{k_1^2 I}{4j\omega\epsilon_1\eta_1} H_0^{(1)'}(k_1\rho) + \frac{k_1^2 I}{4j\omega\epsilon_1\eta_1} \sum_{n=-\infty}^{n=+\infty} j^n a_n H_n^{(2)'}(k_1\rho) e^{jn\phi} \tag{3.9}$$

Here, $H_n^{(1)}(k_1\rho) = J_n(k_1\rho) + jY_n(k_1\rho)$ is the Hankel function of first kind and $H_n^{(2)}(k_1\rho) = J_n(k_1\rho) - jY_n(k_1\rho)$ is Hankel function of second kind and prime denote the derivative with respect to the argument. It is known that chiral medium supports two wave numbers so field in Region- 2 can be written in terms of two circularly polarized waves, i.e., linear combination of RCP and

LCP waves

$$\mathbf{E}_{2z} = -\frac{k_1^2 I}{4\omega\epsilon_1}\sum_{n=-\infty}^{n=+\infty} j^n\left[c_n H_n^{(1)}(k_+\rho) + d_n H_n^{(1)}(k_-\rho)\right]e^{jn\phi} \tag{3.10}$$

$$\mathbf{E}_{2\phi} = -\frac{k_1^2 I}{4\omega^2\epsilon_1\epsilon_2\eta_2}\sum_{n=-\infty}^{n=+\infty} j^n\left[c_n k_+ H_n^{(1)'}(k_+\rho) - d_n k_- H_n^{(1)'}(k_-\rho)\right]e^{jn\phi} \tag{3.11}$$

$$\mathbf{H}_{2z} = \frac{k_1^2 I}{4j\omega\epsilon_1\eta_2}\sum_{n=-\infty}^{n=+\infty} j^n\left[c_n H_n^{(1)}(k_+\rho) - d_n H_n^{(1)}(k_-\rho)\right]e^{jn\phi} \tag{3.12}$$

$$\mathbf{H}_{2\phi} = \frac{k_1^2 I}{4j\omega^2\epsilon_1\mu_2}\sum_{n=-\infty}^{n=+\infty} j^n\left[c_n k_+ H_n^{(1)'}(k_+\rho) + d_n k_- H_n^{(1)'}(k_-\rho)\right]e^{jn\phi} \tag{3.13}$$

where, a_n and b_n are coefficients for field within the cylinder. c_n is unknown coefficient for Right Circularly Polarized (RCP) coefficient field and d_n is the unknown coefficient for Left Circularly Polarized (LCP) coefficient of transmitted field in the Region- 2. Applying boundary conditions at $\rho = a$, the unknown coefficients can be obtained. The boundary conditions at interface $\rho = a$ are

$$\mathbf{E}_{1z} = \mathbf{E}_{2z}, \qquad \rho = a \tag{3.14}$$

$$\mathbf{H}_{1z} = \mathbf{H}_{2z}, \qquad \rho = a \tag{3.15}$$

$$\mathbf{E}_{1\phi} = \mathbf{E}_{2\phi}, \qquad \rho = b \tag{3.16}$$

$$\mathbf{H}_{1\phi} = \mathbf{H}_{2\phi}, \qquad \rho = b \tag{3.17}$$

Applying first boundary condition

$$\mathbf{E}_{1z} = \mathbf{E}_{2z}, \qquad \rho = b \tag{3.18}$$

$$\begin{aligned} &-\frac{k_1^2 I}{4\omega\epsilon_1}H_0^{(1)}(k_1 a) - \frac{k_1^2 I}{4\omega\epsilon_1}\sum_{n=-\infty}^{n=+\infty} a_n H_n^{(2)}(k_1 a)e^{jn\phi} \\ &= -\frac{k_1^2 I}{4\omega\epsilon_1}\sum_{n=-\infty}^{n=+\infty}\left[c_n H_n^{(1)}(k_+ a) + d_n H_n^{(1)}(k_- a)\right]e^{jn\phi} \end{aligned} \tag{3.19}$$

Multiplying both sides by $e^{-jm\phi}$ and integrating from 0 to 2π we get

$$\sum_{n=-\infty}^{n=+\infty} a_n H_n^{(2)}(k_1 a)\int_0^{2\pi} e^{j(n-m)\phi}d\phi - \sum_{n=-\infty}^{n=+\infty} c_n H_n^{(1)}(k_+ a)\int_0^{2\pi} e^{j(n-m)\phi}d\phi - \sum_{n=-\infty}^{n=+\infty} d_n H_n^{(1)}(k_- a)\int_0^{2\pi} e^{j(n-m)\phi}d\phi = H_0^{(1)}(k_1 a)\int_0^{2\pi} e^{jn\phi}d\phi \tag{3.20}$$

$$a_m H_m^{(2)}(k_1 a)\delta_{mn} - c_m H_m^{(1)}(k_+ a)\delta_{mn} - d_m H_m^{(1)}(k_- a)\delta_{mn} = H_0^{(1)}(k_1 a)\delta_{m0} \tag{3.21}$$

This equation can be written as

$$a_n H_n^{(2)}(k_1 a) - c_n H_n^{(1)}(k_+ a) - d_n H_n^{(1)}(k_- a) = H_0^{(1)}(k_1 a) \tag{3.22}$$

Applying boundary condition $\mathbf{H}_{1z} = \mathbf{H}_{2z}$ at $\rho = a$

$$b_n H_n^{(2)}(k_1 a) - \frac{\eta_1}{\eta_2} H_n^{(1)}(k_+ a) + \frac{\eta_1}{\eta_2} H_n^{(1)}(k_+ a) = 0 \tag{3.23}$$

Applying boundary conditions on ϕ component of electric and magnetic fields following two equations can be obtained

$$b_n H_n^{(2)'}(k_1 a) - \frac{k_+ \epsilon_1 \eta_1}{k_1 \epsilon_2 \eta_2} c_n H_n^{(1)'}(k_+ a) - \frac{k_- \epsilon_1 \eta_1}{k_1 \epsilon_2 \eta_2} d_n H_n^{(1)'}(k_- a) = 0 \tag{3.24}$$

$$\sum_{n=-\infty}^{n=+\infty} a_n H_n^{(2)'}(k_1 a)\int_0^{2\pi} e^{j(n-m)\phi}d\phi - \frac{k_+ \eta_1}{\omega\mu_2}\sum_{n=-\infty}^{n=+\infty} c_n H_n^{(1)'}(k_+ a)\int_0^{2\pi} e^{j(n-m)\phi}d\phi - \frac{k_- \eta_1}{\omega\mu_2}\sum_{n=-\infty}^{n=+\infty} d_n H_n^{(1)'}(k_- a)\int_0^{2\pi} e^{j(n-m)\phi}d\phi = -H_0^{(1)'}(k_1 a)\int_0^{2\pi} e^{j(m-0)\phi}d\phi \tag{3.25}$$

Eq. (25) can be written as

$$a_m H_m^{(2)'}(k_1 a)\delta_{mn} - \frac{k_+ \eta_1}{\omega\mu_2} c_m H_m^{(1)'}(k_+ a)\delta_{mn} - \frac{k_- \eta_1}{\omega\mu_2} d_n H_m^{(1)'}(k_- a)\delta_{mn} = -H_0^{(1)'}(k_1 a)\delta_{m0} \tag{3.26}$$

From Eq. (21) and Eq. (25) it can be noticed that $m = 0$ and also $n = m$. So the electric and magnetic field is independent of ϕ and field equations in Region- 1

and Region- 2 can be written as

$$\mathbf{E}_{1z} = -\frac{k_1^2 I}{4\omega\epsilon_1} H_0^{(1)}(k_1\rho) - \frac{k_1^2 I}{4\omega\epsilon_1} a_0 H_0^{(2)}(k_1\rho) \tag{3.27}$$

$$\mathbf{H}_{1z} = \frac{k_1^2 I}{4j\omega\epsilon_1\eta_1} b_0 H_0^{(2)}(k_1\rho) \tag{3.28}$$

$$\mathbf{E}_{1\phi} = \frac{k_1^2 I}{4\omega\epsilon_1} b_0 H_0^{(2)'}(k_1\rho) \tag{3.29}$$

$$\mathbf{H}_{1\phi} = \frac{k_1^2 I}{4j\omega\epsilon_1\eta_1} H_0^{(1)'}(k_1\rho) + \frac{k_1^2 I}{4j\omega\epsilon_1\eta_1} a_0 H_0^{(2)'}(k_1\rho) \tag{3.30}$$

$$\mathbf{E}_{2z} = -\frac{k_1^2 I}{4\omega\epsilon_1}\left[c_0 H_0^{(1)}(k_+\rho) + d_0 H_0^{(1)}(k_-\rho)\right] \tag{3.31}$$

$$\mathbf{E}_{2\phi} = -\frac{k_1^2 I}{4\omega^2\epsilon_1\epsilon_2\eta_2}\left[c_0 k_+ H_0^{(1)'}(k_+\rho) - d_0 k_- H_0^{(1)'}(k_-\rho)\right] \tag{3.32}$$

$$\mathbf{H}_{2z} = \frac{k_1^2 I}{4j\omega\epsilon_1\eta_2}\left[c_0 H_0^{(1)}(k_+\rho) - d_0 H_0^{(1)}(k_-\rho)\right] \tag{3.33}$$

$$\mathbf{H}_{2\phi} = \frac{k_1^2 I}{4j\omega^2\epsilon_1\mu_2}\left[c_0 k_+ H_0^{(1)'}(k_+\rho) + d_0 k_- H_0^{(1)'}(k_-\rho)\right] \tag{3.34}$$

Application of the boundary conditions yields following matrix equations. This matrix equation can be solved to find unknown coefficients a_0, b_0, c_0 and d_0.

$$AX = B \tag{3.35}$$

where

$$A = \begin{pmatrix} H_0^{(2)}(k_1 a) & 0 & -H_0^{(1)}(k_+ a) & -H_0^{(1)}(k_- a) \\ 0 & H_0^{(2)}(k_1 a) & -\frac{\eta_1}{\eta_2} H_0^{(1)}(k_+ a) & \frac{\eta_1}{\eta_2} H_0^{(1)}(k_+ a) \\ 0 & H_0^{(2)'}(k_1 a) & -\frac{k_+\epsilon_1\eta_1}{k_1\epsilon_2\eta_2} H_0^{(1)'}(k_+ a) & -\frac{k_-\epsilon_1\eta_1}{k_1\epsilon_2\eta_2} H_0^{(1)'}(k_- a) \\ H_0^{(2)'}(k_1 a) & 0 & -\frac{k_+\eta_1}{\omega\mu_2} H_0^{(1)'}(k_+ a) & -\frac{k_-\eta_1}{\omega\mu_2} H_0^{(1)'}(k_- a) \end{pmatrix}$$

$$B = \begin{pmatrix} -H_0^{(1)}(k_1 a) \\ 0 \\ 0 \\ -H_0^{(1)'}(k_1 a) \end{pmatrix}$$

$$X = \begin{pmatrix} a_0 \\ b_0 \\ c_0 \\ d_0 \end{pmatrix}$$

3.2 Fields for Different Parametric Values

This section presents some plots to study the behavior of coefficient of RCP and LCP transmitted field with variations of different parameters. It is noted that for values of parameters given above, medium occupied by the cylinder behaves as: within frequency range of 10.1GHz-10.3GHz as Mu Negative (MNG) medium, within 10.4GHz-10.9GHz as Double Negative (DNG) and 11GHz-12.7GHz as Epsilon Negative (ENG) metamaterial. In frequency range below 10GHz and above 12.7GHz, both permittivity and permeability are positive and medium behaves as Double Positive (DPS) metamaterial.

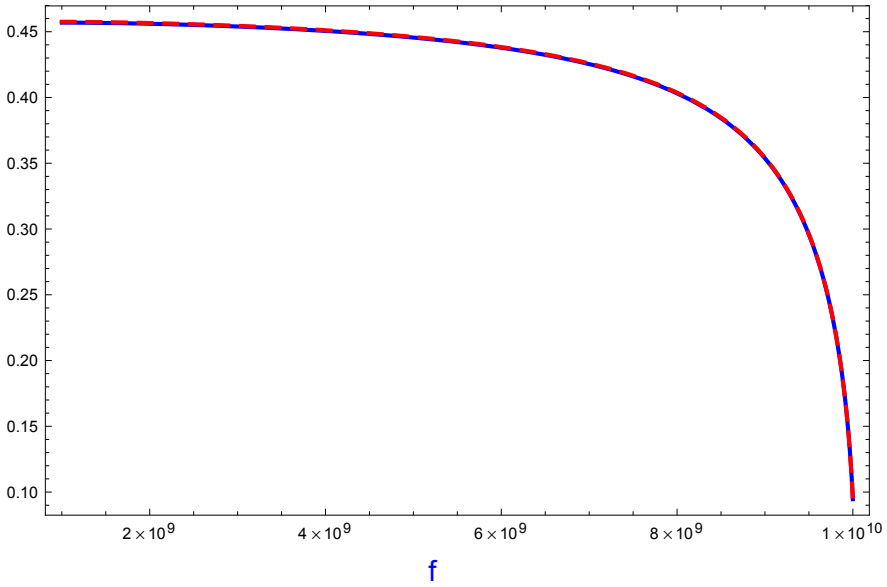

Figure 3.2: Behavior of transmitted coefficient of dispersive DPS cylinder placed in chiral metamaterial. Solid line for coefficient of RCP transmitted field; dashed line for coefficient of LCP transmitted field: $\epsilon_c = 0.9$, $\mu_c = 1$, $\kappa = 0.01$ and $a = 5$mm.

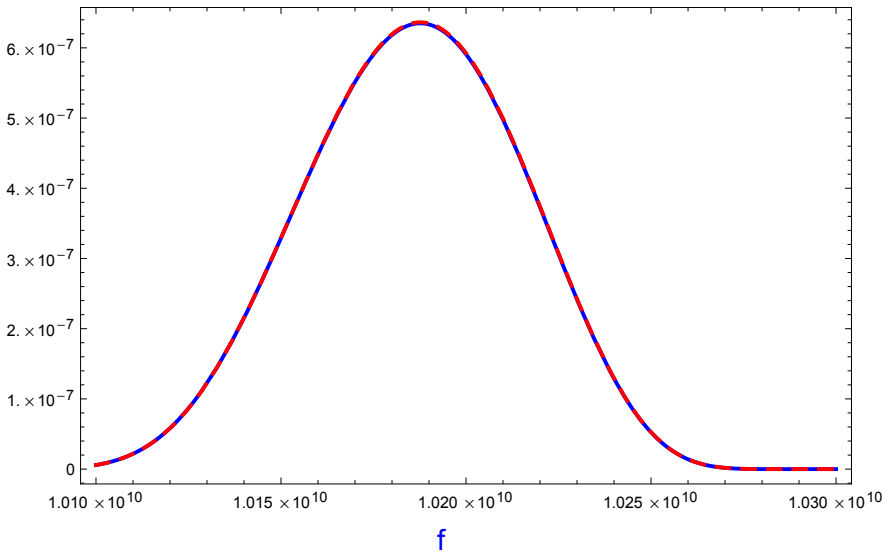

Figure 3.3: Behavior of coefficients of transmitted field from dispersive MNG cylinder placed in chiral metamaterial. Solid line for coefficient of RCP transmitted field; dashed line for coefficient of LCP transmitted field: $\epsilon_c = 0.9$, $\mu_c = 1$, $\kappa = 0.01$ and $a = 5$mm.

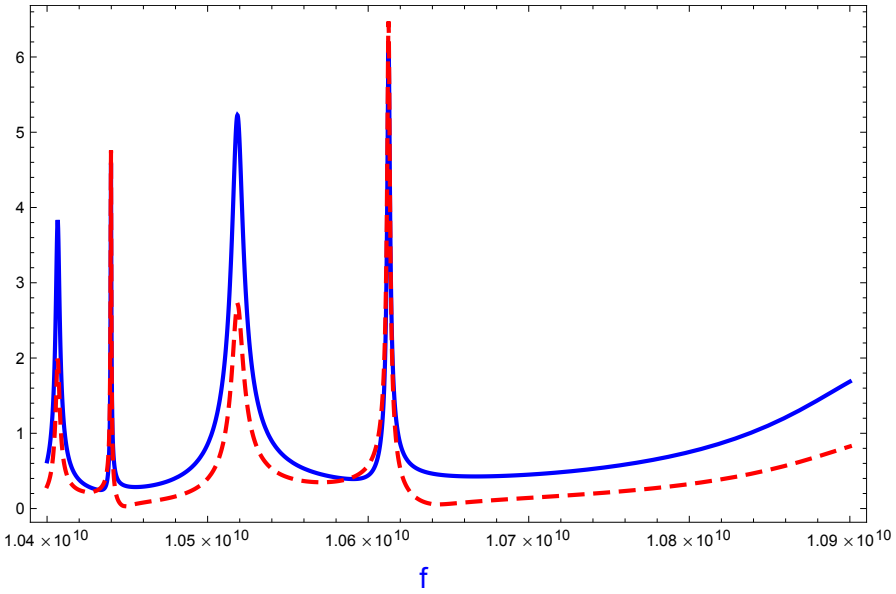

Figure 3.4: Behavior of coefficient of transmitted field from dispersive DNG cylinder placed in chiral metamaterial. Solid line for coefficient of RCP transmitted field; dashed line for coefficient of LCP transmitted field: $\epsilon_c = 0.9$, $\mu_c = 1$, $\kappa = 0.01$ and $a = 5$mm.

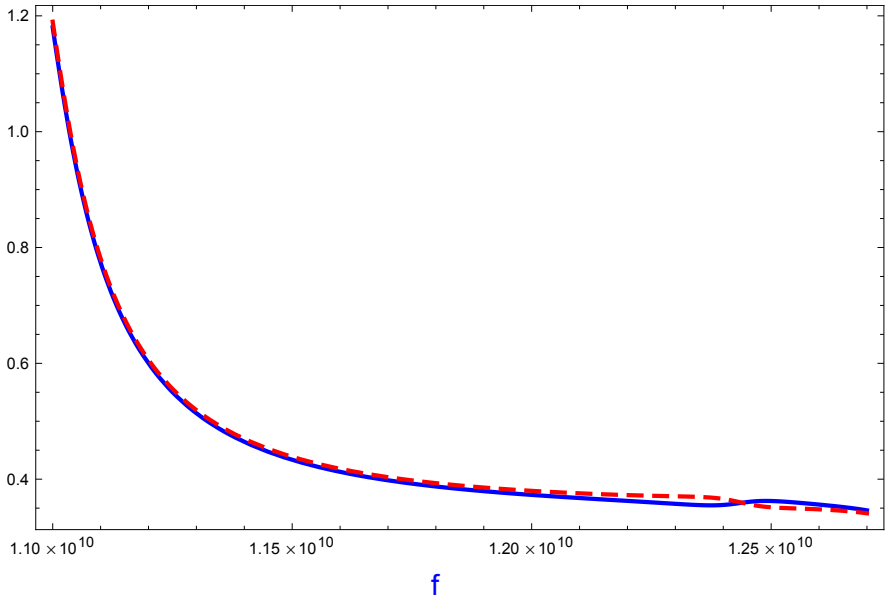

Figure 3.5: Behavior of coefficient of transmitted field from dispersive ENG cylinder placed in chiral metamaterial. Solid line for coefficient of RCP transmitted field; dashed line for coefficient of LCP transmitted field: $\epsilon_c = 0.9$, $\mu_c = 1$, $\kappa = 0.01$ and $a = 5$mm.

From Fig. 3.2 it is noticed that, for case of dispersive DPS cylinder, absolute value of coefficient of RCP transmitted field decreases with increasing frequency, behavior of absolute value of coefficient of LCP transmitted field is same. It is also noted that within 10.1GHz to 10.3GHz medium become MNG and behavior of absolute value of coefficient of RCP transmitted field and coefficient of LCP transmitted field can be seen in Fig. 3.3 and resonance appears in this case and this can be used as a band pass filter, within 10.4GHz to 10.9GHz medium behaves as DNG and within frequency range of 11GHz to 12.7GHz dispersive cylinder behaves as ENG and both for DNG/ENG cylinder placed in chiral metamaterial behavior of absolute values of coefficient of RCP and LCP transmitted field can be seen in Fig. 3.4 and Fig. 3.5. For dispersive DNG cylinder it is noticed that resonance contributions appears in absolute value of coefficient of RCP and coefficient of LCP when dispersion characteristics are incorporated. Absolute value of coefficients of RCP and LCP transmitted field decreases with frequency for dispersive ENG cylinder. It is noticed that absolute value of coefficient of RCP and coefficient of LCP transmitted field

are very weak for MNG cylinder placed in an unbounded chiral metamaterial because in this frequency range losses are maximum.

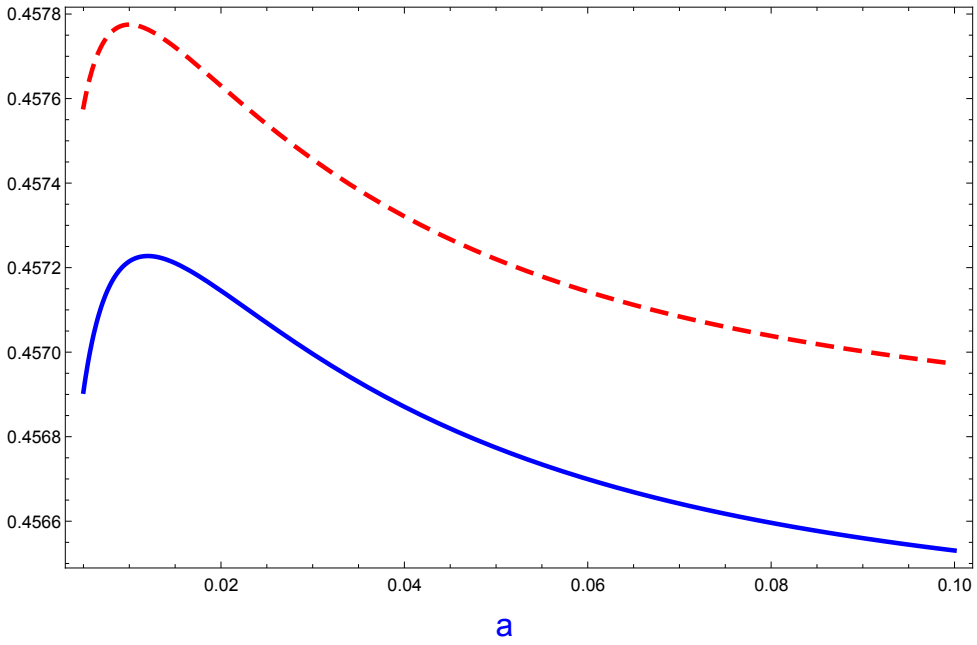

Figure 3.6: Behavior of coefficients of transmitted field from dispersive DPS cylinder placed in chiral metamaterial. Solid line for coefficient of RCP transmitted field; dashed line for coefficient of LCP transmitted field: $\epsilon_c = 0.9$, $\mu_c = 1$, $f = 1$GHz and $\kappa = 0.01$.

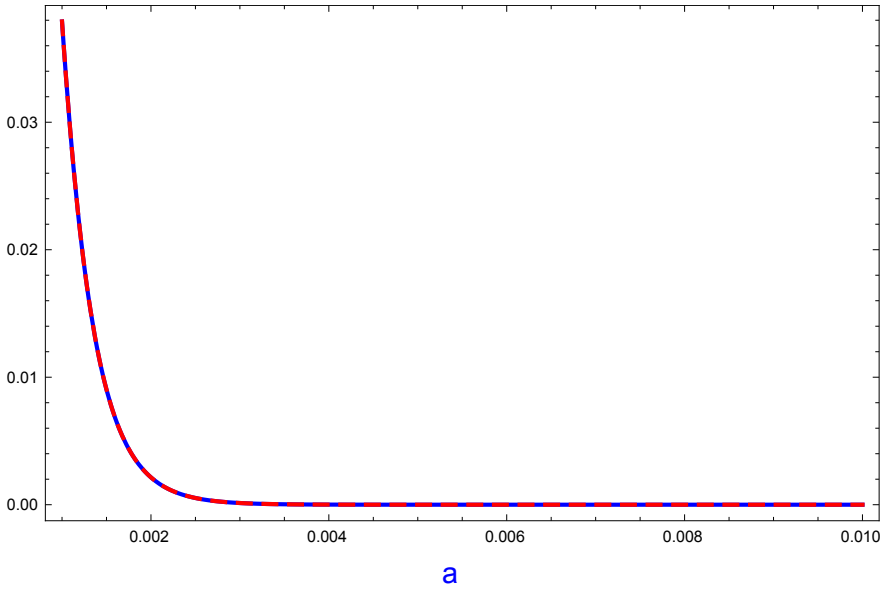

Figure 3.7: Behavior coefficient of transmitted field from dispersive MNG cylinder placed in chiral metamaterial. Solid line for coefficient of RCP transmitted field; dashed line for coefficient of LCP transmitted field: $\epsilon_c = 0.9$, $\mu_c = 1$, $f = 10.2$GHz and $\kappa = 0.01$.

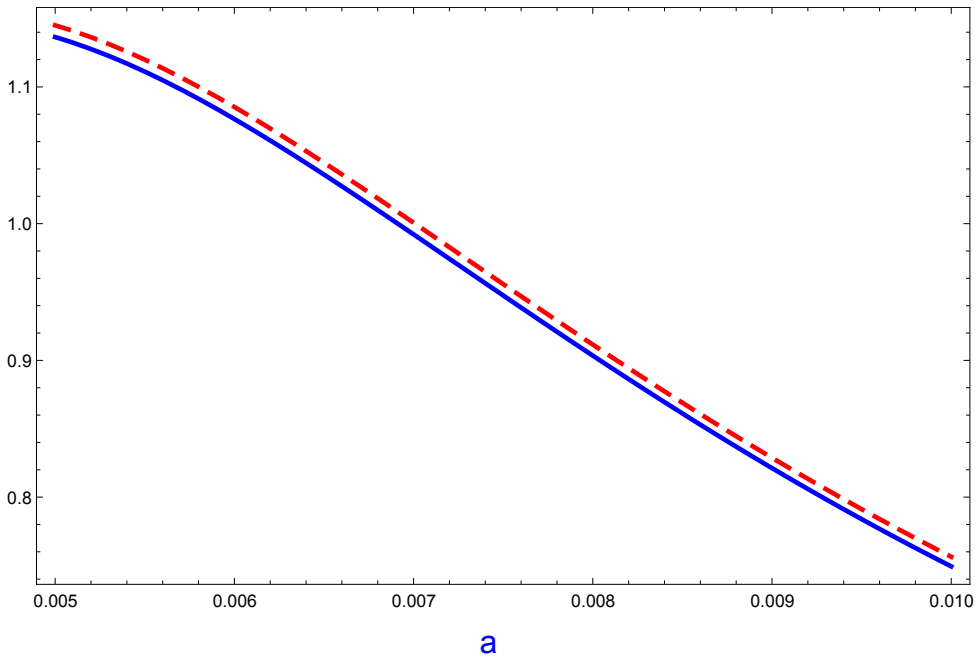

Figure 3.8: Behavior of coefficient of transmitted field from dispersive cylinder placed in chiral metamaterial. Solid line for coefficient of RCP transmitted field; dashed line for coefficient of LCP transmitted field: $f = 10.9$GHz, $\epsilon_c = 0.9$, $\mu_c = 1$ and $\kappa = 0.01$.

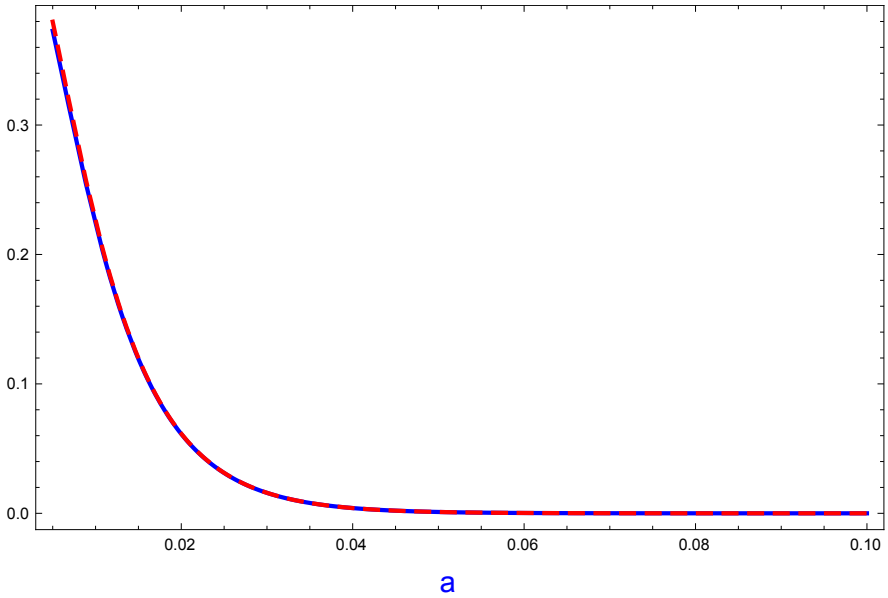

Figure 3.9: Behavior of coefficient of transmitted field for dispersive MNG cylinder with respect to radius of cylinder placed in chiral metamaterial. Solid line for coefficient of RCP transmitted field; dashed line for coefficient of LCP transmitted field: : $f = 12$GHz, $\epsilon_c = 0.9$, $\mu_c = 1$ and $\kappa = 0.01$.

From Fig. 3.6 and Fig. 3.7 effect of radius of the cylinder on absolute values of coefficient of RCP and LCP transmitted field can be seen. It is noticed that coefficient of RCP-polarized and LCP-polarized transmitted field decreases with increasing radius of the cylinder. It is noticed that for MNG cylinder at fixed frequency $f = 10.2$GHz if the radius of cylinder becomes very small then absolute value of coefficient of RCP and coefficient of LCP transmitted field of transmitted field are strong and with increasing radius of the cylinder the decay is very fast. In Fig. 3.8 and Fig. 3.9 effect of radius of the dispersive DNG and ENG cylinder on transmitted field is observed, it is noticed that both coefficient of RCP and LCP transmitted field decreases with increasing the radius of cylinder but for DNG cylinder coefficient of RCP and coefficient of LCP transmitted fields decreases slowly.

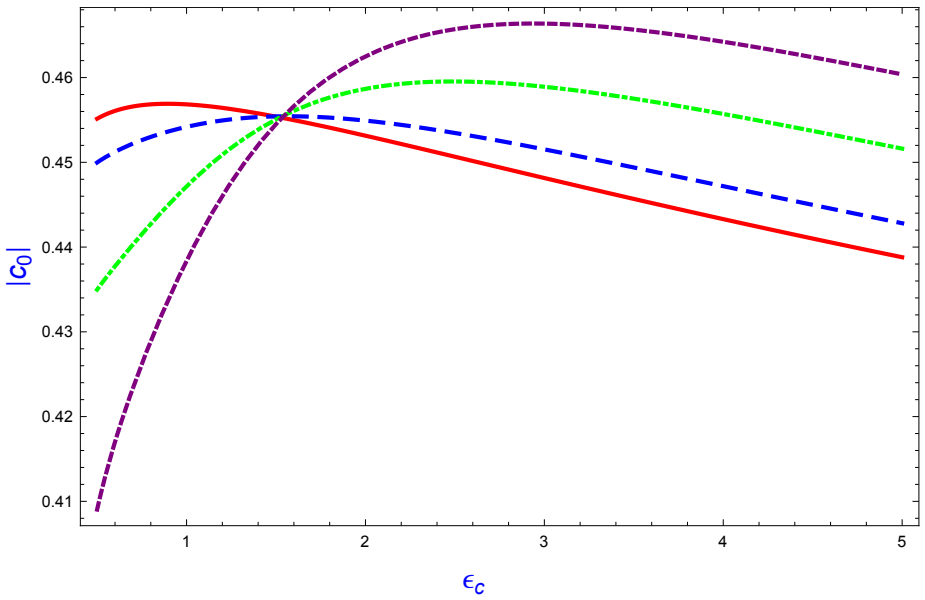

Figure 3.10: Behavior of absolute value of coefficient of RCP transmitted field from dispersive DPS cylinder placed in chiral metamaterial. Solid line for $\kappa = 0.01$; dashed line for $\kappa = 0.1$; dash dotted line for $\kappa = 0.3$; small dashed line for $\kappa = 0.5$: $\epsilon_c = 0.9$, $\mu_c = 1$, $\kappa = 0.01$ and $a = 5mm$.

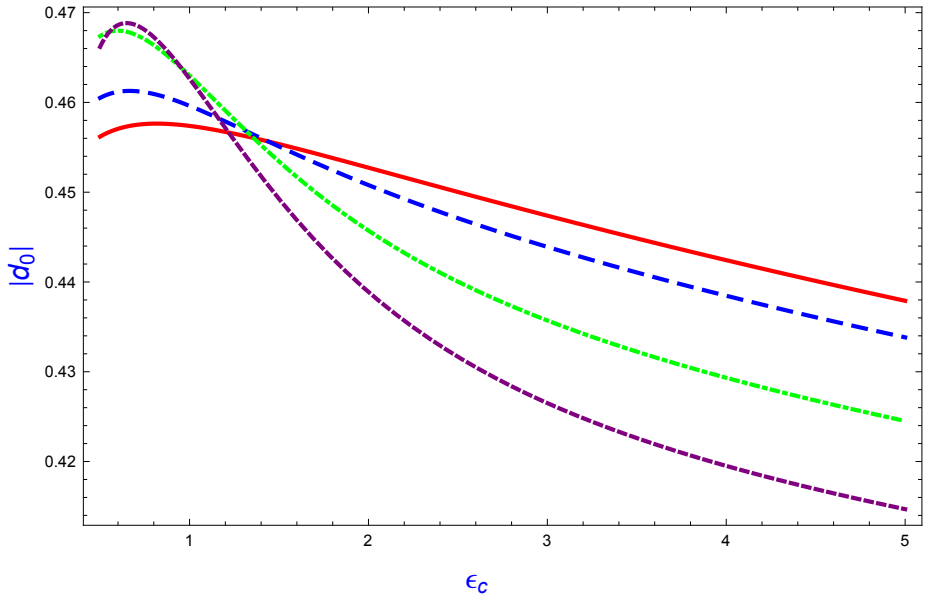

Figure 3.11: Behavior of absolute value of coefficient of LCP transmitted field from dispersive DPS cylinder placed in chiral metamaterial. Solid line for $\kappa = 0.01$; dashed line for $\kappa = 0.1$; dash dotted line for $\kappa = 0.3$; small dashed line for $\kappa = 0.5$: $\epsilon_c = 0.9$, $\mu_c = 1$, $\kappa = 0.01$ and $a = 5mm$.

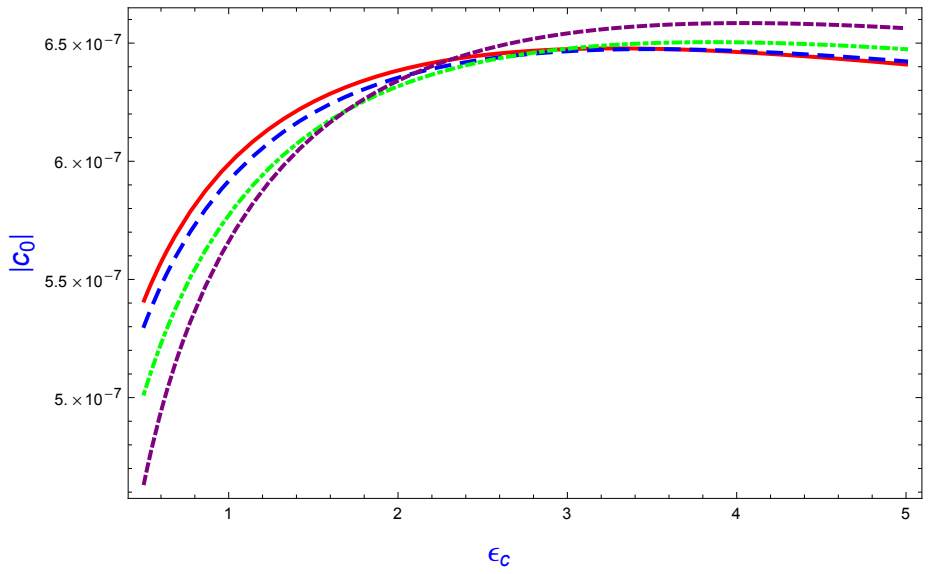

Figure 3.12: Behavior of absolute value of coefficient of RCP transmitted field from dispersive MNG cylinder placed in chiral metamaterial. Solid line for $\kappa = 0.01$; dashed line for $\kappa = 0.1$; dash dotted line for $\kappa = 0.3$; small dashed line for $\kappa = 0.5$: $\epsilon_c = 0.9$, $\mu_c = 1$, $\kappa = 0.01$ and $a = 5mm$.

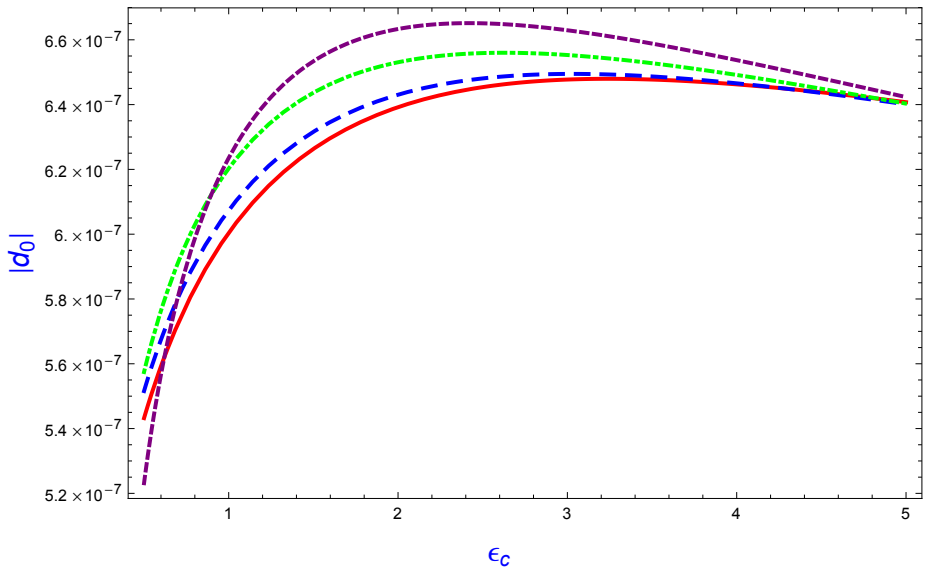

Figure 3.13: Behavior of absolute value of coefficient of LCP transmitted field from dispersive MNG cylinder placed in chiral metamaterial. Solid line for $\kappa = 0.01$; dashed line for $\kappa = 0.1$; dash dotted line for $\kappa = 0.3$; small dashed line for $\kappa = 0.5$: $\epsilon_c = 0.9$, $\mu_c = 1$, $\kappa = 0.01$ and $a = 5mm$.

Fig. 3.10 shows the behavior of absolute value of RCP coefficient of transmitted field of dispersive DPS cylinder with respect to permittivity of the host chiral medium for different values of chirality of the host chiral metamaterial, it is noticed that at $\epsilon_c = 1.5$ absolute value of coefficient of RCP transmitted is same for different values of chirality . And coefficient of LCP transmitted field increases with increasing the permittivity of the host medium and decreases with chirality and can be seen in Fig. 3.11. From Fig. 3.12 and Fig. 3.13 effect of permittivity and chirality of host chiral medium is observed for coefficient of RCP and coefficient of LCP transmitted field from dispersive MNG cylinder, and it is noticed that absolute value of coefficient of RCP and coefficient of LCP transmitted field increases with permittivity, absolute value of coefficient of RCP transmitted field decreases with chirality while coefficient of LCP transmitted field increases.

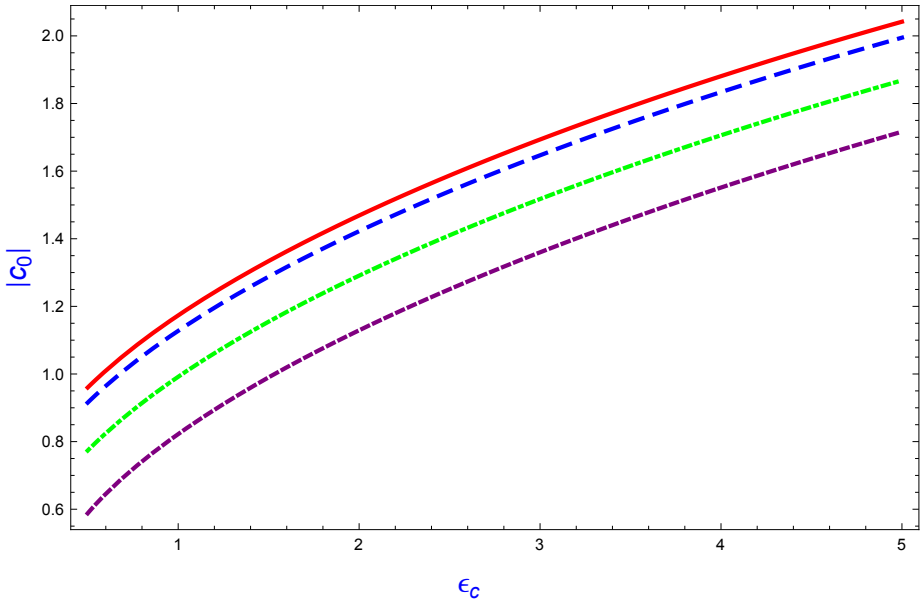

Figure 3.14: Behavior of absolute value of coefficient of transmitted field from dispersive DNG cylinder placed in an unbounded chiral metamaterial. Solid line for $\kappa = 0.01$; dashed line for $\kappa = 0.1$; dash dotted line for $\kappa = 0.3$; small dashed line for $\kappa = 0.5$: $\epsilon_c = 0.9$, $\mu_c = 1$ and $a = 5mm$.

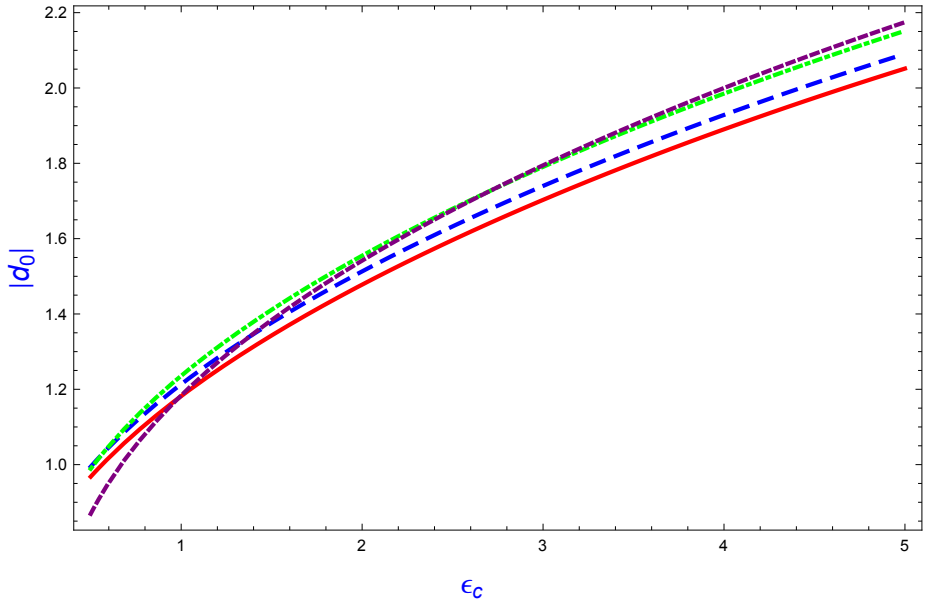

Figure 3.15: Behavior of absolute value of coefficient of LCP transmitted field of transmitted field from dispersive DNG cylinder placed in an unbounded chiral metamaterial. Solid line for $\kappa = 0.01$; dashed line for $\kappa = 0.1$; dash dotted line for $\kappa = 0.3$; small dashed line for $\kappa = 0.5$: $\epsilon_c = 0.9$, $\mu_c = 1$ and $a = 5mm$.

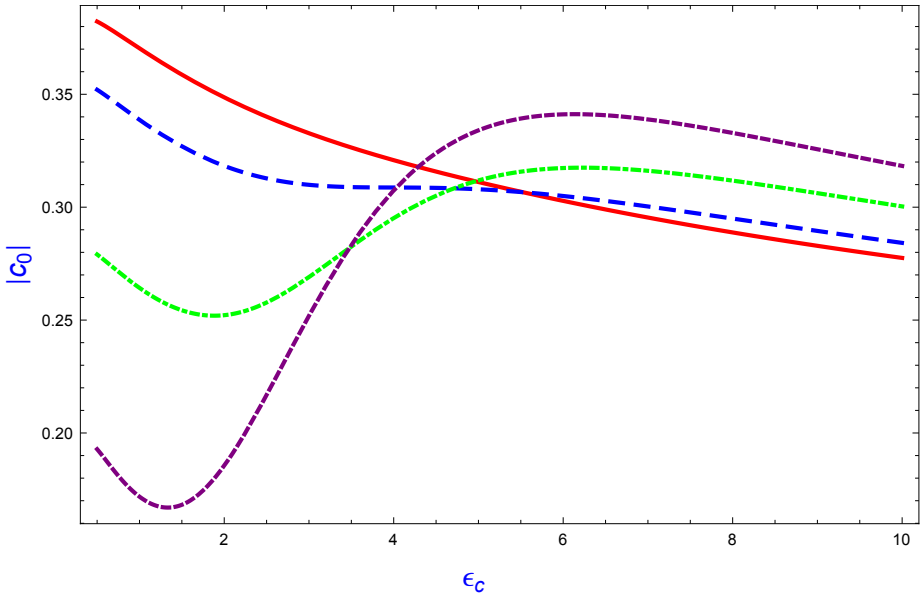

Figure 3.16: Behavior of absolute value of absolute value of coefficient of transmitted field from dispersive ENG cylinder placed in an unbounded chiral metamaterial. Solid line for $\kappa = 0.01$; dashed line for $\kappa = 0.1$; dash dotted line for $\kappa = 0.3$; small dashed line for $\kappa = 0.5$: $\epsilon_c = 0.9$, $\mu_c = 1$ and $a = 5mm$.

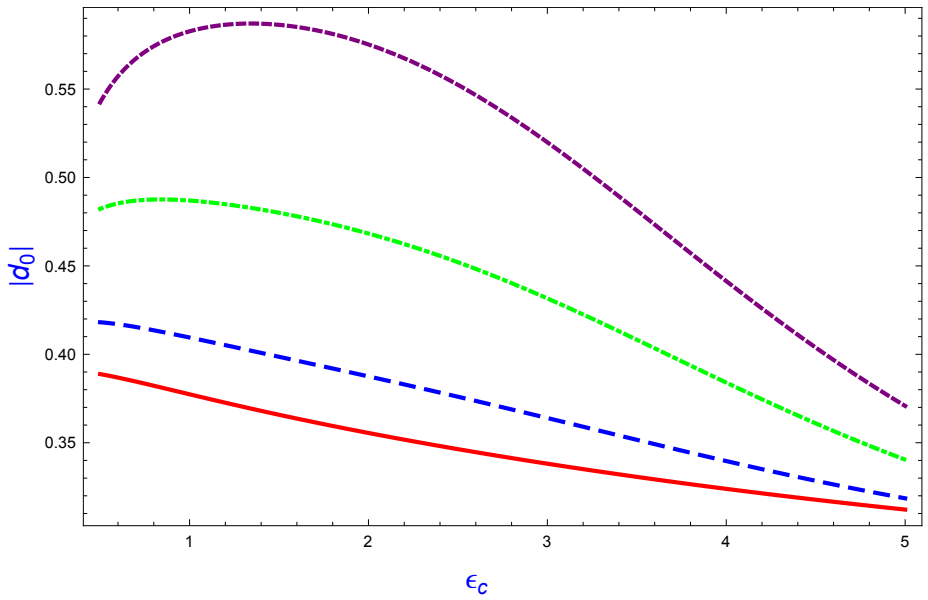

Figure 3.17: Behavior of absolute value of coefficient of transmitted field from dispersive ENG cylinder placed in an unbounded chiral metamaterial. Solid line for $\kappa = 0.01$; dashed line for $\kappa = 0.1$; dash dotted line for $\kappa = 0.3$; small dashed line for $\kappa = 0.5$: $\epsilon_c = 0.9$, $\mu_c = 1$ and $a = 5mm$.

Fig. 3.14 shows the behavior of absolute value of coefficient of transmitted field of dispersive DNG cylinder with respect to permittivity of the host chiral metamaterial and Fig. 3.15 shows the behavior of absolute value of coefficient of LCP transmitted field with respect to permittivity of host metamaterial, it is observed that absolute value of coefficient of RCP and coefficient of LCP transmitted field increases with increasing the permittivity of the host medium, also noticed that absolute value of coefficient of RCP transmitted field decreases with increasing the chirality whereas absolute value of coefficient of LCP transmitted field increases with increasing the chirality of the host chiral metamaterial. From Fig. 3.16 and Fig. 3.17 effect of permittivity and chirality of host chiral medium on absolute value coefficient of RCP and absolute value of coefficient of LCP transmitted field from dispersive ENG cylinder is observed.

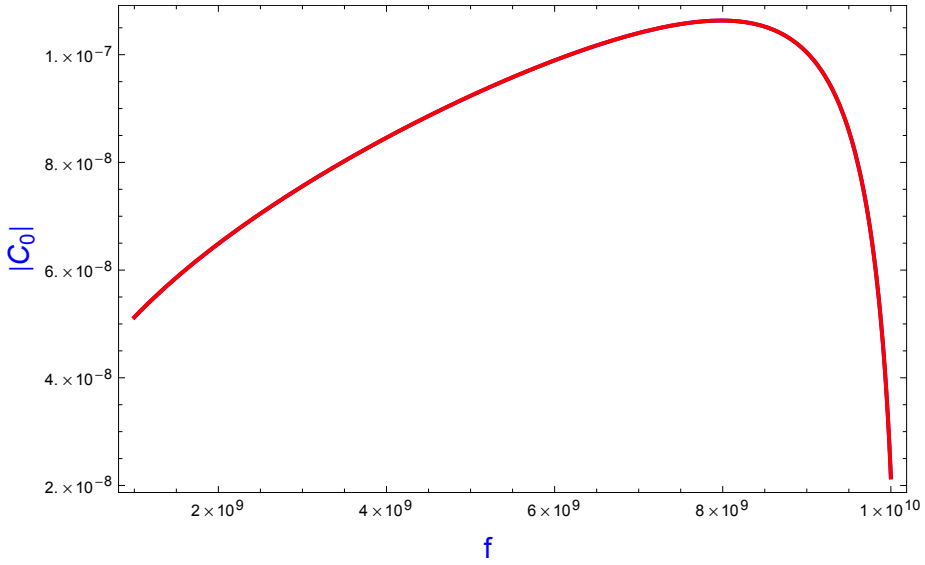

Figure 3.18: Behavior of absolute value of coefficient of transmitted field for dispersive DPS cylinder placed in chiral nihility metamaterial. Solid line for absolute value of coefficient of RCP transmitted field; dashed line for absolute value of coefficient of LCP transmitted field: $f = 1$GHz and $\kappa = 0.01$.

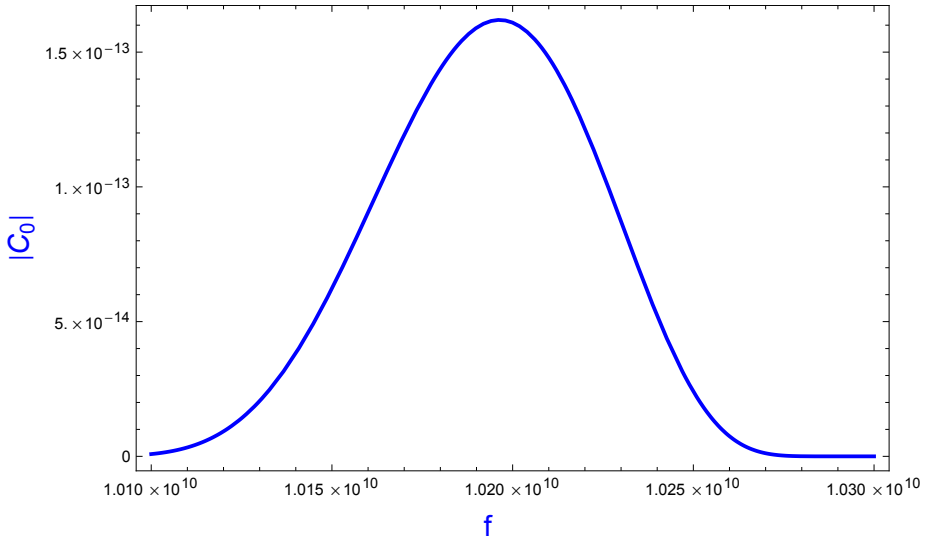

Figure 3.19: Behavior of absolute value of coefficient of transmitted field for dispersive MNG cylinder placed in chiral nihility metamaterial. Solid line for absolute value of coefficient of RCP transmitted field; dashed line for absolute value of coefficient of LCP transmitted field: $f = 10.2$GHz and $\kappa = 0.01$.

Fig. 3.18 and Fig. 3.19 shows the effect of frequency on absolute value of coefficient of transmitted field when dispersive DPS and dispersive MNG cylinders are assumed to be placed in chiral nihility metamaterial respectively.

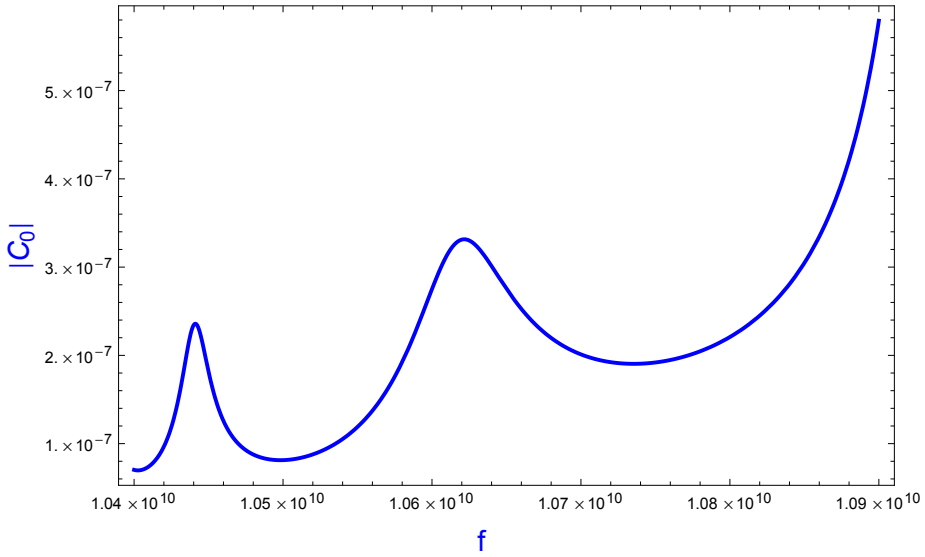

Figure 3.20: Behavior of absolute value of coefficient of transmitted field for dispersive DNG cylinder placed in chiral nihility metamaterial. Solid line for absolute value of coefficient of RCP transmitted field; dashed line for absolute value of coefficient of LCP transmitted field: $f = 10.9$GHz and $\kappa = 0.01$.

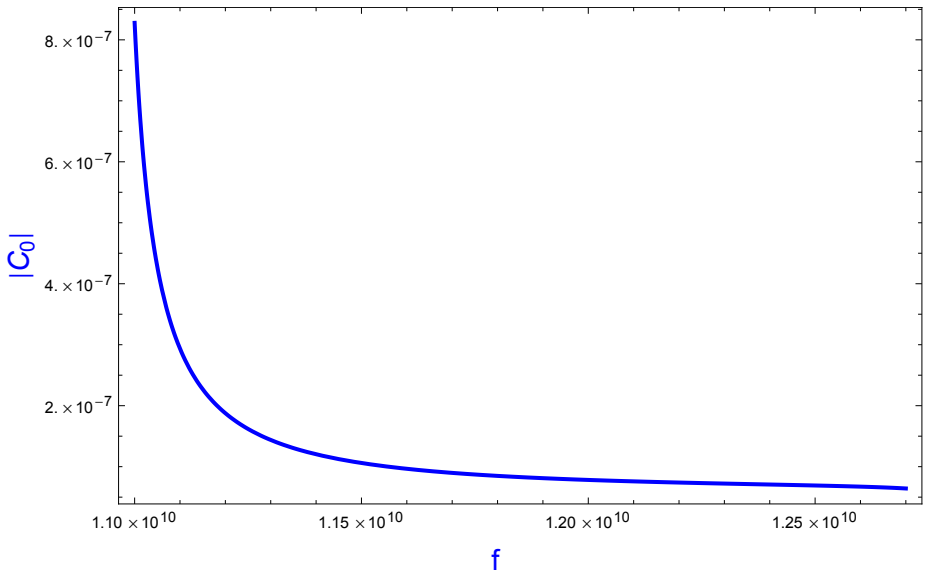

Figure 3.21: Behavior of absolute value of coefficient of transmitted field for dispersive ENG cylinder placed in chiral nihility metamaterial. Solid line for absolute value of coefficient of RCP transmitted field; dashed line for absolute value of coefficient of LCP transmitted field: $f = 12$GHz and $\kappa = 0.01$.

From Fig. 3.20 and Fig. 3.21 effect of frequency on absolute value of coefficient of transmitted field is observed for dispersive DNG and ENG cylinders respectively, it is noticed that behavior of absolute value of coefficient of transmitted field of dispersive DPS, MNG, DNG and ENG cylinders placed in host chiral nihility metamaterial is approximately same as that of host chiral medium except the amplitudes of absolute value of coefficients is very small.

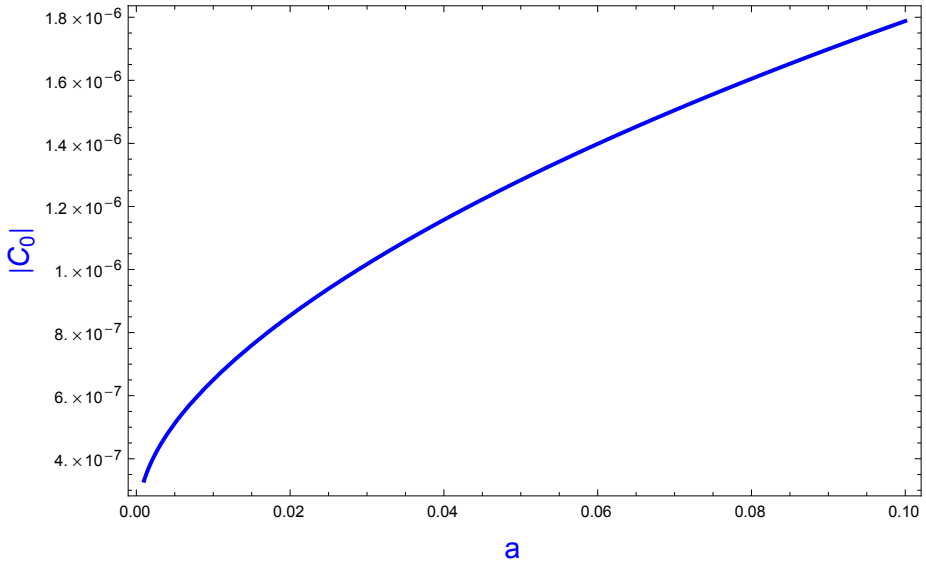

Figure 3.22: Behavior of absolute value of coefficient of RCP transmitted field of dispersive DPS cylinder with respect to radius of cylinder placed in chiral nihility metamaterial: $\kappa = 0.01$ and $f = 10.9$GHz.

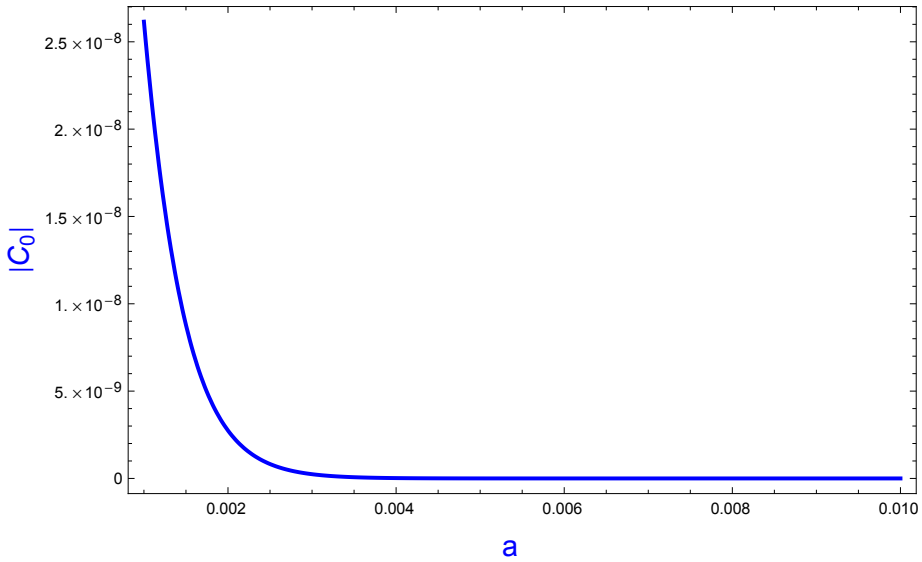

Figure 3.23: Behavior of absolute value of coefficient of RCP transmitted field of dispersive MNG cylinder with respect to radius of cylinder placed in chiral nihility metamaterial: $\kappa = 0.01$ and $f = 12$GHz.

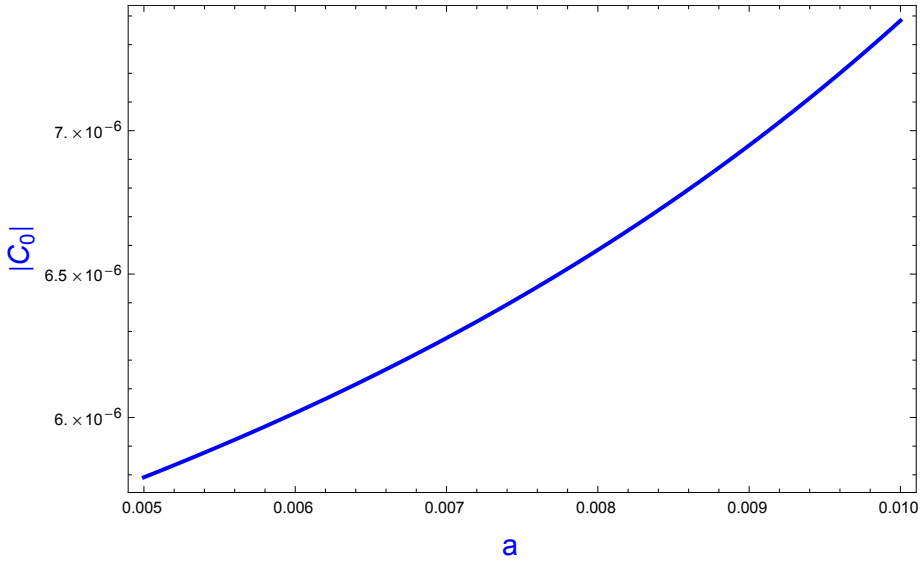

Figure 3.24: Behavior of absolute value of coefficient of RCP transmitted field for dispersive DNG cylinder: $\kappa = 0.01$ and $f = 10.9$GHz.

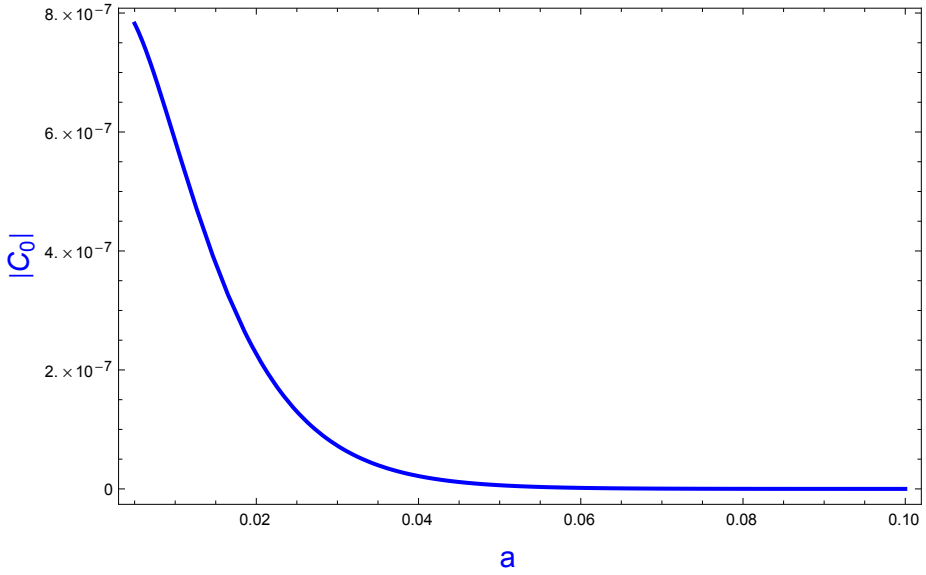

Figure 3.25: Behavior of absolute value of coefficient of RCP transmitted field for dispersive MNG cylinder: $\kappa = 0.01$ and $f = 12$GHz.

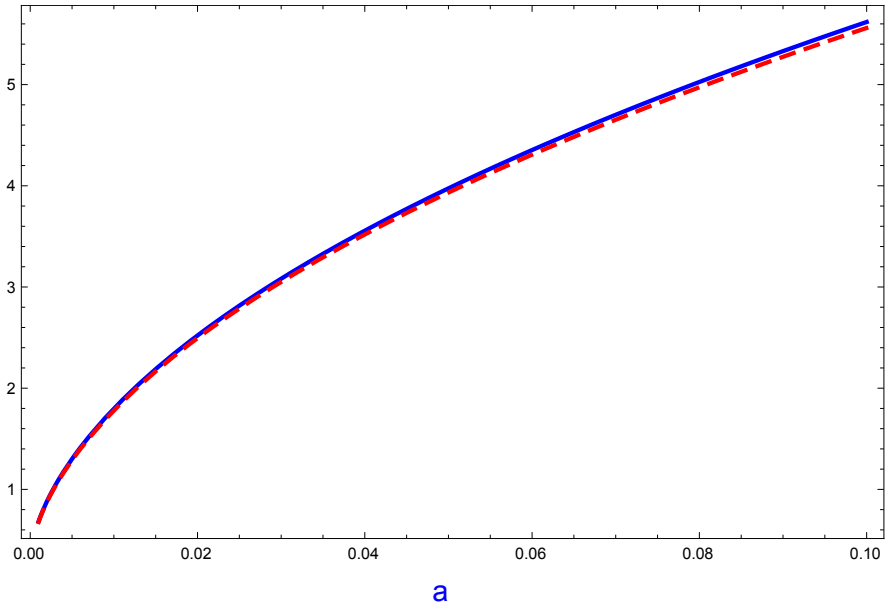

Figure 3.26: Transmitted field of nihility cylinder placed in an unbounded chiral metamaterial : $\epsilon_c = 0.9$, $\mu_c = 1$, $a = 5$mm, $\kappa = 0.01$.

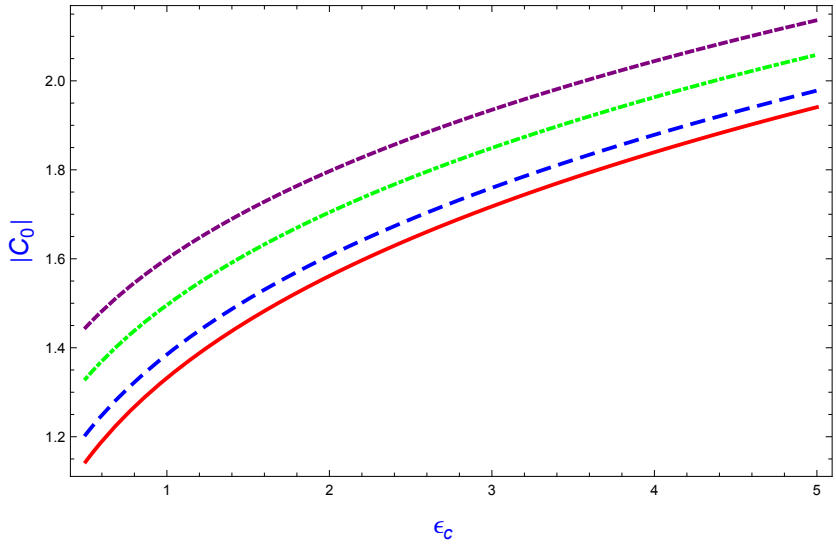

Figure 3.27: Behavior of transmitted field from nihility placed in chiral metamaterial. Solid line for $\kappa = 0.01$; dashed line for $\kappa = 0.1$; dash dotted line for $\kappa = 0.3$; small dashed line for $\kappa = 0.5$: $\epsilon_c = 0.9$, $\mu_c = 1$ and$a = 5mm$.

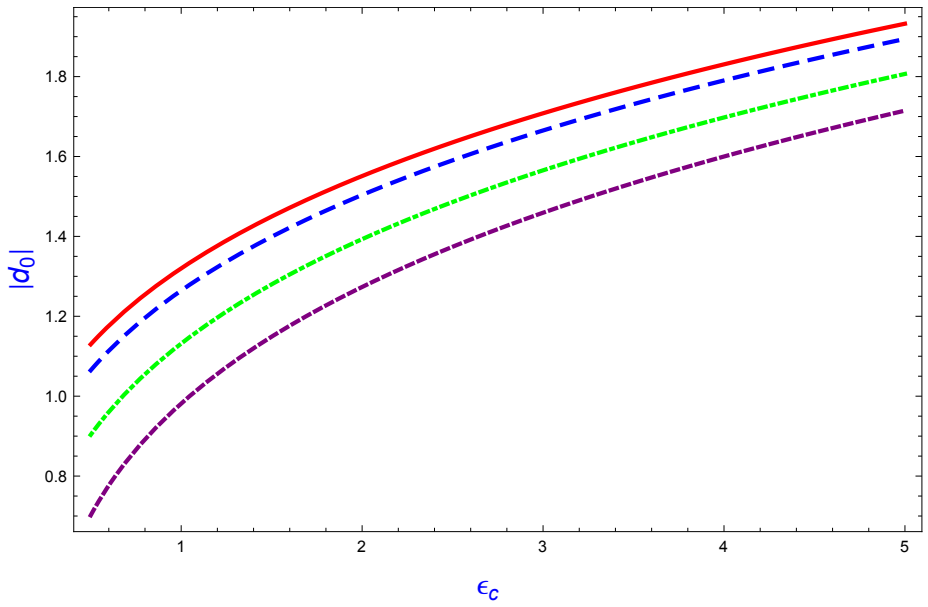

Figure 3.28: Behavior of transmitted field from nihility placed in chiral metamaterial. Solid line for $\kappa = 0.01$; dashed line for $\kappa = 0.1$; dash dotted line for $\kappa = 0.3$; small dashed line for $\kappa = 0.5$: $\epsilon_c = 0.9$, $\mu_c = 1$ and$a = 5mm$.

For Fig. 3.22-Fig. 3. 25 it is assumed that dispersive cylinder is placed in chiral nihility metamaterial. absolute value of coefficients of transmitted field are negligibly small and approaches to zero in contrast to that of chiral metamaterial. It is also noticed that for DPS, MNG, DNG and ENG cylinder transmitted field is very week and it is also noticed that absolute value of coefficient of RCP and absolute value of coefficient of LCP transmitted fields are same in case of host chiral nihility medium. For dispersive DPS and dispersive DNG cylinder placed in an unbounded chiral nihility metamaterial it is observed that with increasing the radius of the dispersive cylinder absolute value of coefficient of RCP transmitted field increases. It had been investigated by Qamar et al. [38] that source placed in an unbounded chiral nihility metamaterial unable to radiate and from Fig. 3.22 and Fig. 3.24 one may also conclude that when radius of dispersive dielectric magnetic cylinder is negligibly small the source does not radiate in chiral nihility metamaterial and with increasing the radius of the cylinder transmission increases. For Fig. 3.26, dispersive cylinder is assumed to be replaced with a nihility cylinder and an unbounded medium hosting the

cylinder is chiral. A growth in transmitted field is observed with the increase of permittivity of host chiral medium. It is also noted that a static field exists within the nihility cylinder. From Fig. 3.27 it can be seen that with increasing radius and permittivity of chiral medium absolute value of coefficient of RCP and absolute value of coefficient of LCP transmitted field increases.

3.3 Summary

In this chapter transmission through a dispersive dielectric-magnetic cylinder placed in chiral metamaterial is discussed. Effect of frequency on dispersive medium is analyzed and also effect of permittivity on radiated field is discussed. Field radiated from a line source placed in dispersive medium and surrounded by unbounded chiral nihility is also discussed here. Electric line source placed in nihility cylinder is also discussed in details. Absolute value of coefficient of transmitted field increases within the frequency range for which dispersive cylinder behaves as DPS cylinder and decreases within the frequency range for which dispersive cylinder behaves as ENG cylinder. Coefficient of RCP and coefficient of LCP transmitted field decreases with increasing the radius of the dispersive dielectric-magnetic cylinder placed in an unbounded chiral metamaterial. For MNG/DNG cylinder placed in an unbounded chiral metamaterial absolute of coefficient of RCP and absolute of coefficient of LCP transmitted field increases with permittivity whereas absolute value of coefficient of RCP transmitted field decreases and absolute value of coefficient of LCP transmitted field increases with increasing the chirality of the host chiral metamaterial.

In case of unbounded chiral nihility metamaterial, behavior of absolute of coefficient of RCP and absolute of coefficient of LCP transmitted is exactly same. And when the radius of the dispersive cylinder placed in chiral nihility metamaterial is small amplitude of absolute value of coefficient of RCP transmitted field is approximately zero.

In case of nihility cylinder placed in chiral metamaterial, coefficients of transmitted field increases when radius of the cylinder increases. It is also noticed that absolute of coefficient of RCP and absolute of coefficient of LCP transmit-

ted field increases with permittivity of the host chiral metamaterial and absolute value of coefficient of RCP transmitted field increases with chirality and absolute value of coefficient of LCP transmitted field decreases with increasing the chirality of the chiral medium.

Chapter 4

Radiation from Coated Dielectric Cylinder Placed in Unbounded Chiral Metamaterial

In this chapter RCP coefficient of transmitted field from a coated dielectric cylinder is discussed. The coating layer is of dispersive dielectric magnetic medium and cylinder is considered to be placed in an unbounded chiral metamaterial.

4.1 Problem Formulation

We consider a circular cylinder of radius a with constitutive parameters ϵ_1 and μ_1 while the outer cylinder is a coating layer of dispersive dielectric magnetic cylinder of uniform thickness with radius b and constitutive parameters ϵ_2 and μ_2. The coated cylinder is placed in chiral metamaterial with constitutive parameters ϵ_3, μ_3 and κ. An infinite electric line source is located at the center of the dielectric cylinder. The problem is divided in three regions. The region $0 \leqslant \rho \leqslant a$ is termed as Region 1 with wave number $k_1 = \omega\sqrt{\mu_1\epsilon_1}$, the coating layer $a \leqslant \rho \leqslant b$ is termed as region 2 with wave number $k_2 = \omega\sqrt{\epsilon_2(\omega)\mu_2(\omega)}$.

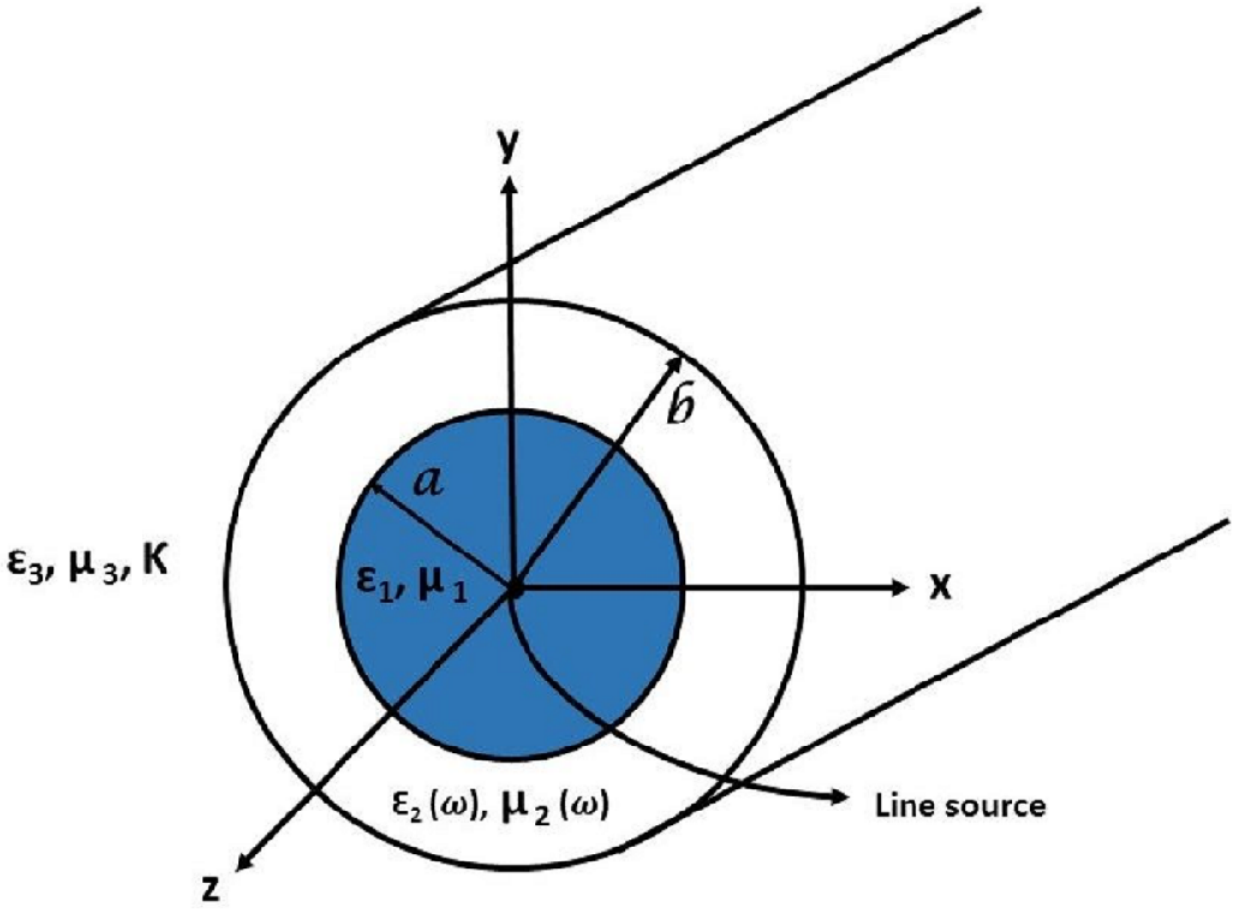

Figure 4.1: Dielectric cylinder coated with dispersive dielectric-magnetic .

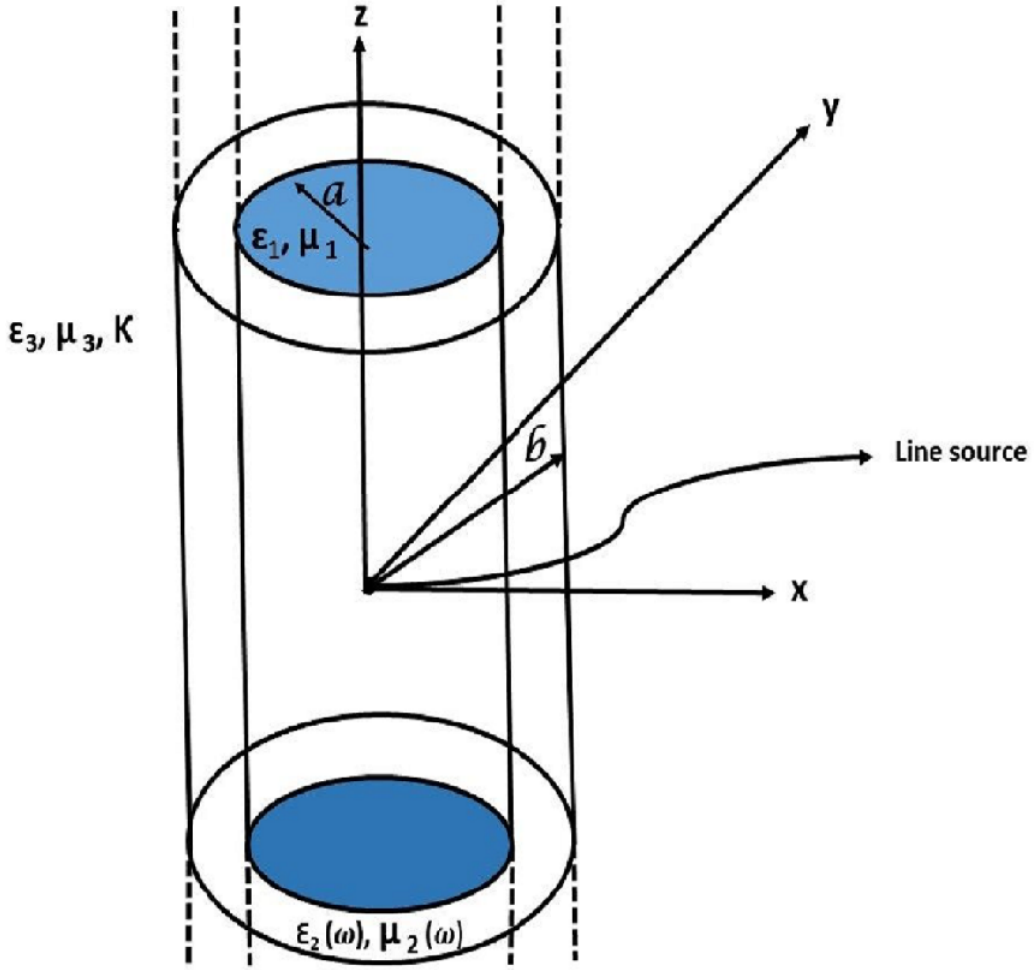

Figure 4.2: Dielectric cylinder coated with dispersive dielectric-magnetic .

The incident field is due to electric line source and the total field in region 1 can be written as sum of incident and reflected field

$$\mathbf{E}_{1z} = -\frac{k_1^2 I}{4\omega\epsilon_1} H_0^{(1)}(k_1\rho) - \frac{k_1^2 I}{4\omega\epsilon_1} \sum_{n=-\infty}^{n=+\infty} j^n a_n H_n^{(2)}(k_1\rho) e^{jn\phi} \tag{4.1}$$

$$\mathbf{H}_{1z} = \frac{k_1^2 I}{4j\omega\epsilon_1\eta_1} \sum_{n=-\infty}^{n=+\infty} j^n b_n H_n^{(2)}(k_1\rho) e^{jn\phi} \tag{4.2}$$

The corresponding ϕ component of electric and magnetic field may be ob-

tained using Maxwell equations as

$$\mathbf{E}_{1\phi} = \frac{k_1^3 I}{4\omega^2\epsilon_1^2\eta_1}\sum_{n=-\infty}^{n=+\infty} j^n b_n H_n^{(2)'}(k_1\rho)e^{jn\phi} \tag{4.3}$$

$$\mathbf{H}_{1\phi} = \frac{k_1^3 I}{4j\omega^2\epsilon_1\mu_1}H_0^{(1)'}(k_1\rho) + \frac{k_1^3 I}{4j\omega\epsilon_1\mu_1}\sum_{n=-\infty}^{n=+\infty} j^n a_n H_n^{(2)'}(k_1\rho)e^{jn\phi} \tag{4.4}$$

Region is bounded region and fields in region can be expressed as oppositely traveling cylindrical waves as

$$\mathbf{E}_{2z} = -\frac{k_1^2 I}{4\omega\epsilon_1}\sum_{n=-\infty}^{n=+\infty} j^n\left[c_n H_n^{(1)}(k_2\rho) + d_n H_n^{(2)}(k_2\rho)\right]e^{jn\phi} \tag{4.5}$$

$$\mathbf{E}_{2\phi} = -\frac{k_1^2 k_2 I}{4\omega^2\epsilon_1\epsilon_2\eta_2}\sum_{n=-\infty}^{n=+\infty} j^n\left[e_n H_n^{(1)'}(k_2\rho) + f_n H_n^{(2)'}(k_2\rho)\right]e^{jn\phi} \tag{4.6}$$

$$\mathbf{H}_{2z} = \frac{k_1^2 I}{4j\omega\epsilon_1\eta_2}\sum_{n=-\infty}^{n=+\infty} j^n\left[e_n H_n^{(1)}(k_2\rho) + f_n H_n^{(2)}(k_2\rho)\right]e^{jn\phi} \tag{4.7}$$

$$\mathbf{H}_{2\phi} = \frac{k_1^2 k_2 I}{4j\omega^2\epsilon_1\mu_2}\sum_{n=-\infty}^{n=+\infty} j^n\left[c_n H_n^{(1)'}(k_2\rho) + d_n H_n^{(2)'}(k_2\rho)\right]e^{jn\phi} \tag{4.8}$$

Region 3 is an unbounded chiral metamaterial and fields for chiral metamaterial can be written in form of unknown expansion coefficient as

$$\mathbf{E}_{3z} = -\frac{k_1^2 I}{4\omega\epsilon_1}\sum_{n=-\infty}^{n=+\infty} j^n\left[g_n H_n^{(1)}(k_+\rho) + h_n H_n^{(1)}(k_-\rho)\right]e^{jn\phi} \tag{4.9}$$

$$\mathbf{E}_{3\phi} = -\frac{k_1^2 I}{4\omega^2\epsilon_1\epsilon_3\eta_3}\sum_{n=-\infty}^{n=+\infty} j^n\left[g_n k_+ H_n^{(1)'}(k_+\rho) - h_n k_- H_n^{(1)'}(k_-\rho)\right]e^{jn\phi} \tag{4.10}$$

$$\mathbf{H}_{3z} = \frac{k_1^2 I}{4j\omega\epsilon_1\eta_3}\sum_{n=-\infty}^{n=+\infty} j^n\left[g_n H_n^{(1)}(k_+\rho) - h_n H_n^{(1)}(k_-\rho)\right]e^{jn\phi} \tag{4.11}$$

$$\mathbf{H}_{3\phi} = \frac{k_1^2 I}{4j\omega^2\epsilon_1\mu_3}\sum_{n=-\infty}^{n=+\infty} j^n\left[g_n k_+ H_n^{(1)'}(k_+\rho) + h_n k_- H_n^{(1)'}(k_-\rho)\right]e^{jn\phi} \tag{4.12}$$

In above equations a_n, b_n, c_n, d_n, e_n, f_n, g_n, h_n are unknown coefficients which has to be determined by applying boundary conditions that tangential components of electric field and magnetic field are continuous at the interfaces $\rho = a$

and $\rho = b$

$$\mathbf{E}_{1z} = \mathbf{E}_{2z}, \qquad \rho = a \tag{4.13}$$

$$\mathbf{H}_{1z} = \mathbf{H}_{2z}, \qquad \rho = a \tag{4.14}$$

$$\mathbf{E}_{1\phi} = \mathbf{E}_{2\phi}, \qquad \rho = a \tag{4.15}$$

$$\mathbf{H}_{1\phi} = \mathbf{H}_{2\phi}, \qquad \rho = a \tag{4.16}$$

While at $\rho = b$ boundary conditions are

$$\mathbf{E}_{2z} = \mathbf{E}_{3z}, \qquad \rho = b \tag{4.17}$$

$$\mathbf{H}_{2z} = \mathbf{H}_{3z}, \qquad \rho = b \tag{4.18}$$

$$\mathbf{E}_{2\phi} = \mathbf{E}_{3\phi}, \qquad \rho = b \tag{4.19}$$

$$\mathbf{H}_{2\phi} = \mathbf{H}_{3\phi}, \qquad \rho = b \tag{4.20}$$

Applying these boundary conditions a linear matrix equation is obtained which can be solved to find unknown coefficients.

4.2 Numerical Results and Discussion

In this section numerical results of the above discussion are presented. Plots show the behavior of absolute value of coefficient of RCP transmitted field of circular dispersive dielectric magnetic cylinder. Due to the dispersive medium type of the medium changes i.e., DPS, MNG, DNG and ENG, so different coating layers are considered.

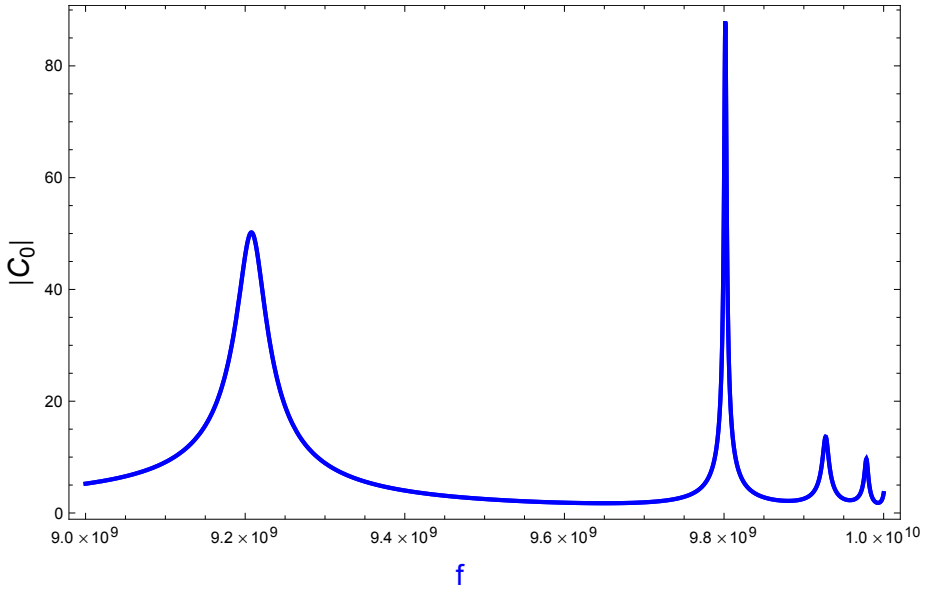

Figure 4.3: Absolute of coefficient of RCP transmitted field of dielectric cylinder with dispersive DPS coating cylinder: $\epsilon_c = 0.9$, $\kappa = 0.01$, $a = 5$mm, $b = 10$mm.

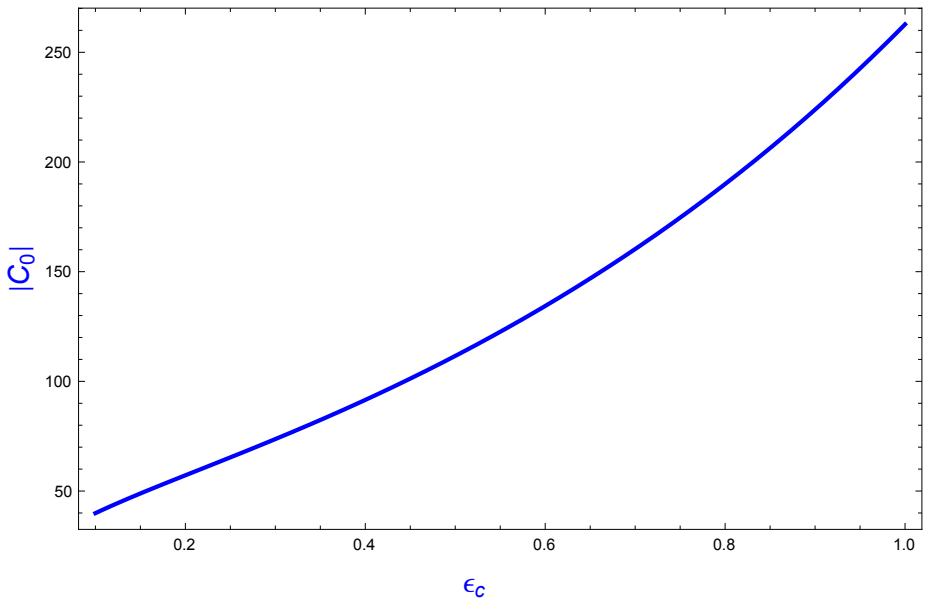

Figure 4.4: Absolute of coefficient of RCP transmitted field of dielectric cylinder with dispersive DPS coating cylinder with respect to permittivity of chiral metamaterial: $f == 1$GHz, $\kappa = 0.01$, $a = 5$mm, $b = 10$mm.

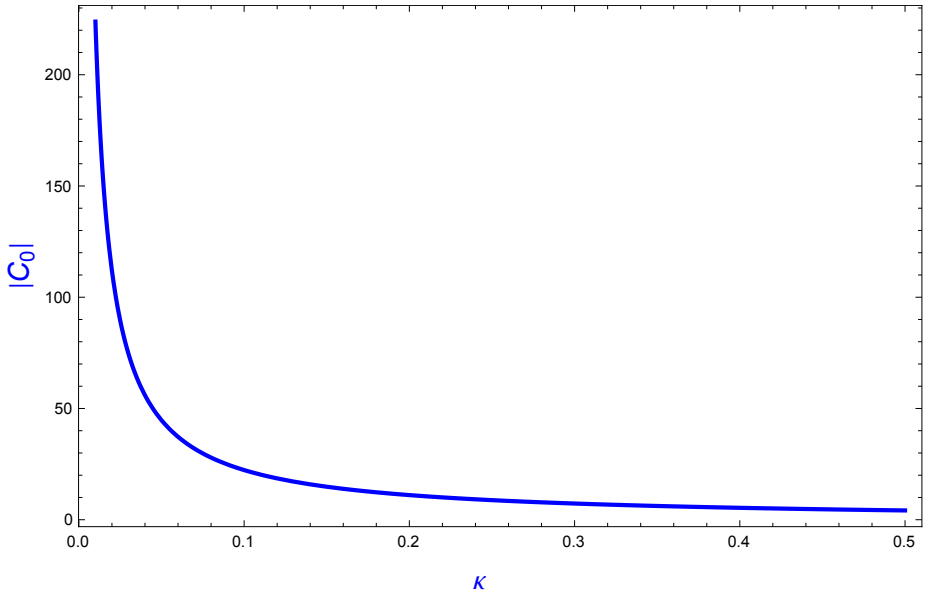

Figure 4.5: Absolute of coefficient of RCP transmitted field of dielectric cylinder with coating of dispersive DPS cylinder with respect to the chirality of chiral metamaterial: $f = 1$GHz, $\epsilon_c = 0.9$, $a = 5$mm, $b = 10$mm.

For Fig. 4.2 frequency range is selected for which coating layer is dispersive DPS, and behavior of coefficient of RCP transmitted field in chiral metamaterial is observed. It is noted that resonances appear when a dielectric cylinder is coated with dispersive DPS cylinder. In Fig. 4.3 effect of permittivity of chiral metamaterial is seen for a fixed frequency, the frequency is selected for which both permittivity and permeability are positive. It can be seen that with increasing permittivity of host chiral metamaterial coefficient of RCP transmitted field in chiral metamaterial increases. Fig. 4.4 shows the effect of chirality of host chiral metamaterial on field transmitted from dielectric cylinder coated with dispersive DPS metamaterial, placed in chiral metamaterial. The coefficient of RCP transmitted field in chiral metamaterial decreases with chirality of host chiral metamaterial.

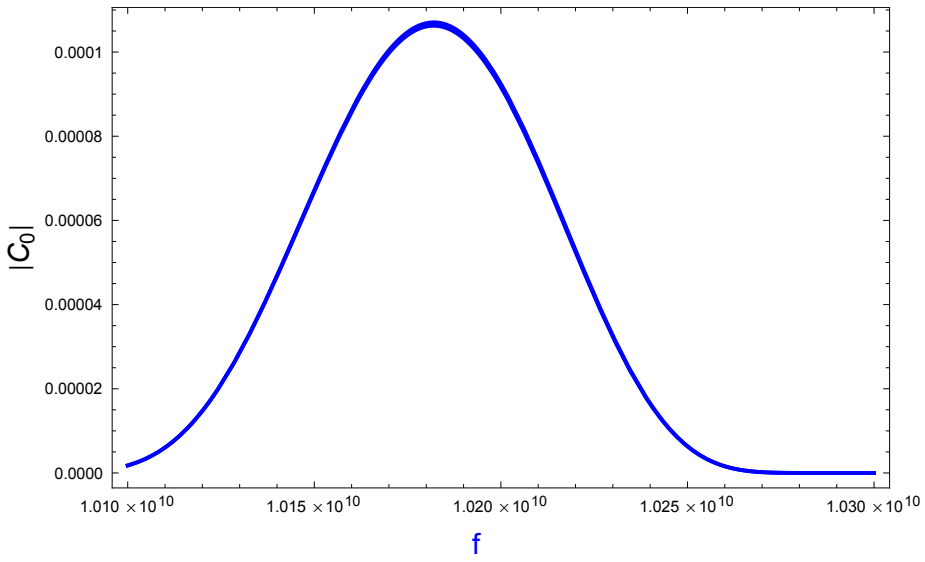

Figure 4.6: Absolute of coefficient of RCP transmitted field of dielectric cylinder with coating of dispersive MNG cylinder: $\epsilon_c = 0.9$, $\kappa = 0.01$, $a = 5$mm, $b = 10$mm.

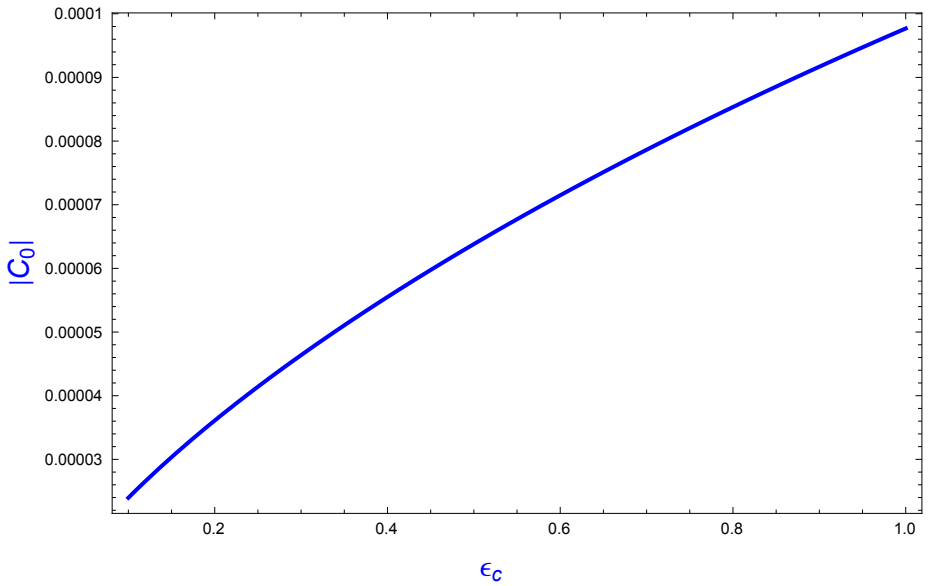

Figure 4.7: Absolute of coefficient of RCP transmitted field of dielectric cylinder with coating of dispersive MNG cylinder with respect to permittivity of chiral metamaterial: $f == 10.2$GHz, $\kappa = 0.01$, $a = 5$mm, $b = 10$mm.

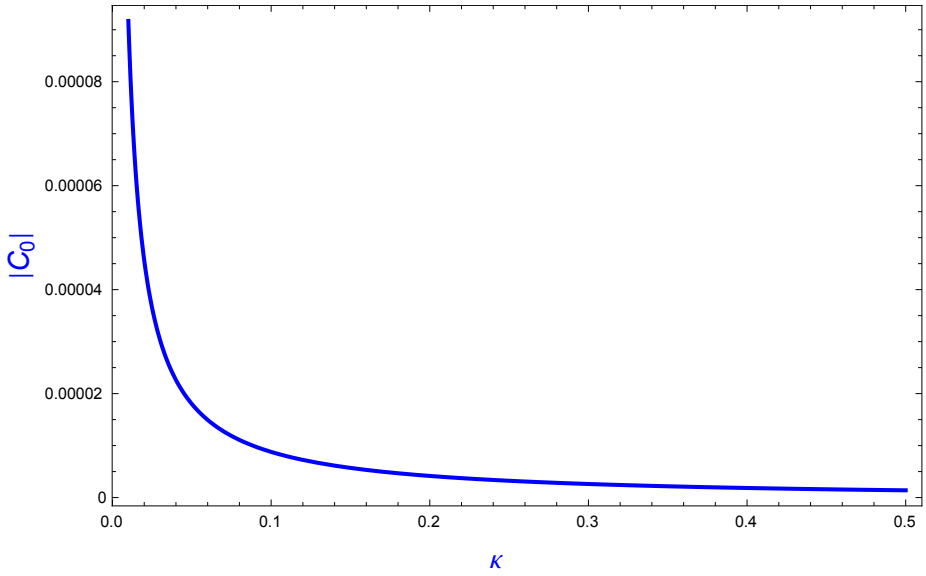

Figure 4.8: Absolute of coefficient of RCP transmitted field of dielectric cylinder with coating of dispersive MNG cylinder with respect to the chirality of chiral metamaterial: $f = 10.2$GHz, $\epsilon_c = 0.9$, $a = 5$mm, $b = 10$mm.

For Fig. 4.5 frequency range is selected for which coating layer is dispersive MNG, and behavior of coefficient of RCP transmitted field in chiral metamaterial is observed. In Fig. 4.6 effect of permittivity of chiral metamaterial is seen for a fixed frequency. The frequency is selected for which permittivity is positive while permeability of metamaterial becomes negative at this frequency. It can be seen that with increasing permittivity of host chiral metamaterial coefficient of RCP transmitted field in chiral metamaterial increases. Fig. 4.7 shows the effect of chirality of host chiral metamaterial on coefficient of RCP transmitted from dielectric cylinder coated with dispersive DPS metamaterial, placed in chiral metamaterial. The coefficient of RCP transmitted field in chiral metamaterial decreases with chirality of host chiral metamaterial.

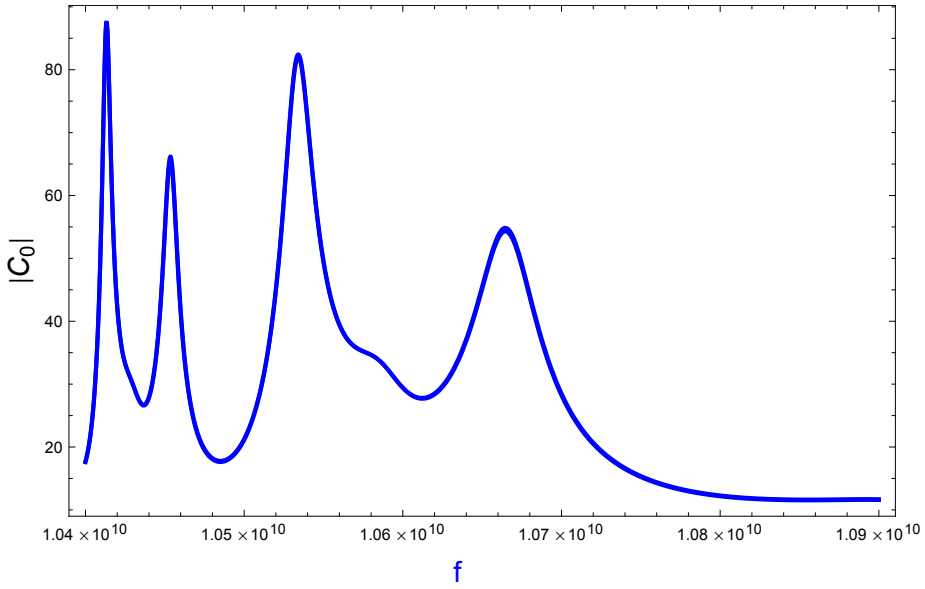

Figure 4.9: coefficient of RCP transmitted field of dielectric cylinder with coating of dispersive DNG cylinder: $\epsilon_c = 0.9$, $\kappa = 0.01$, $a = 5$mm, $b = 10$mm.

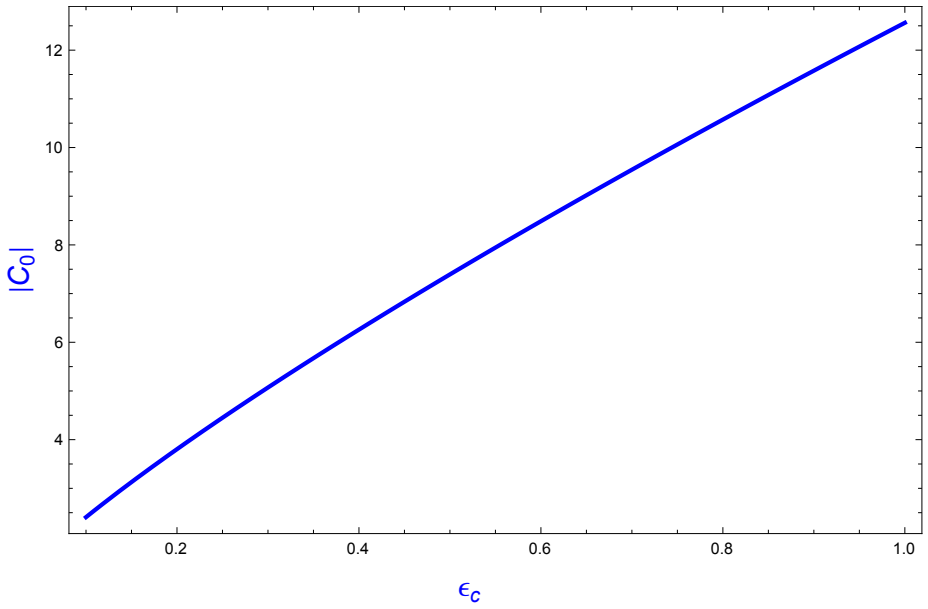

Figure 4.10: coefficient of RCP transmitted field of dielectric cylinder with coating of dispersive DNG cylinder with respect to permittivity of chiral metamaterial: $f = 10.9$GHz, $\kappa = 0.01$, $a = 5$mm, $b = 10$mm.

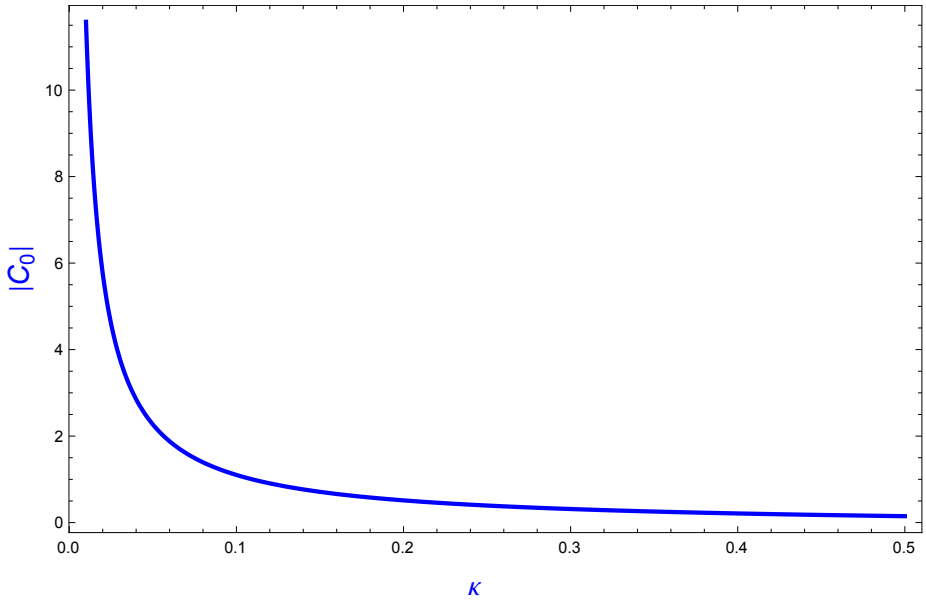

Figure 4.11: coefficient of RCP transmitted field of dielectric cylinder with coating of dispersive DNG cylinder with respect to the chirality of chiral metamaterial: $f = 10.9$GHz, $\epsilon_c = 0.9$, $a = 5$mm, $b = 10$mm.

For Fig. 4.8 frequency range is selected for which coating layer is dispersive DNG, and behavior of coefficient of RCP transmitted field in chiral metamaterial is observed, and it is also observed that resonance contributions appears in this case as that of coated DPS cylinder. In Fig. 4.9 effect of permittivity of chiral metamaterial is seen and in Fig. 4.10 effect of chirality of host chiral metamaterial on field transmitted from dielectric cylinder coated with dispersive DNG metamaterial is observed, and noted that t coefficient of RCP transmitted field increases with increasing the permittivity of the host chiral medium and decreases with increasing the chirality of the host medium.

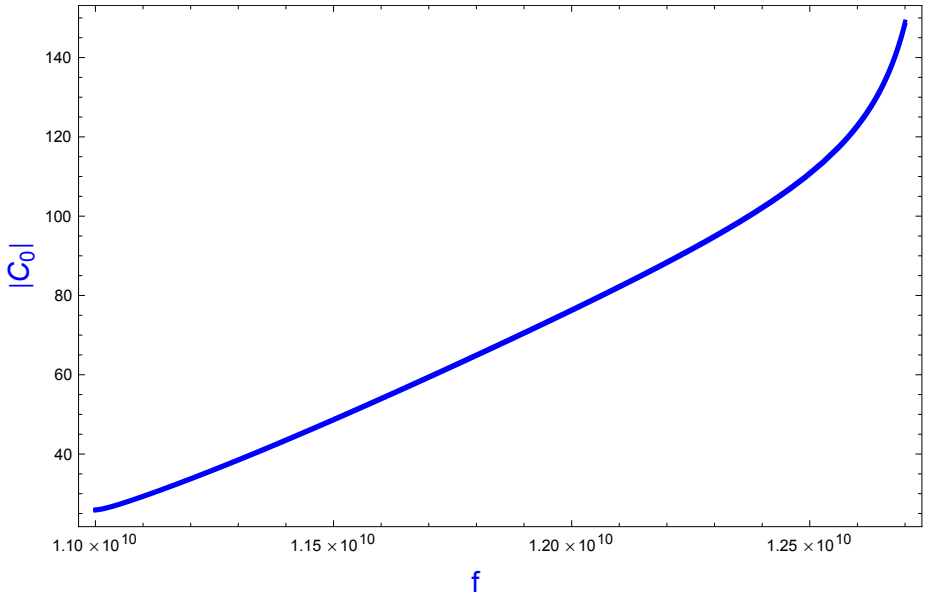

Figure 4.12: Absolute of coefficient of RCP transmitted field of dielectric cylinder with coating of dispersive ENG cylinder: $\epsilon_c = 0.9$, $\kappa = 0.01$, $a = 5$mm, $b = 10$mm.

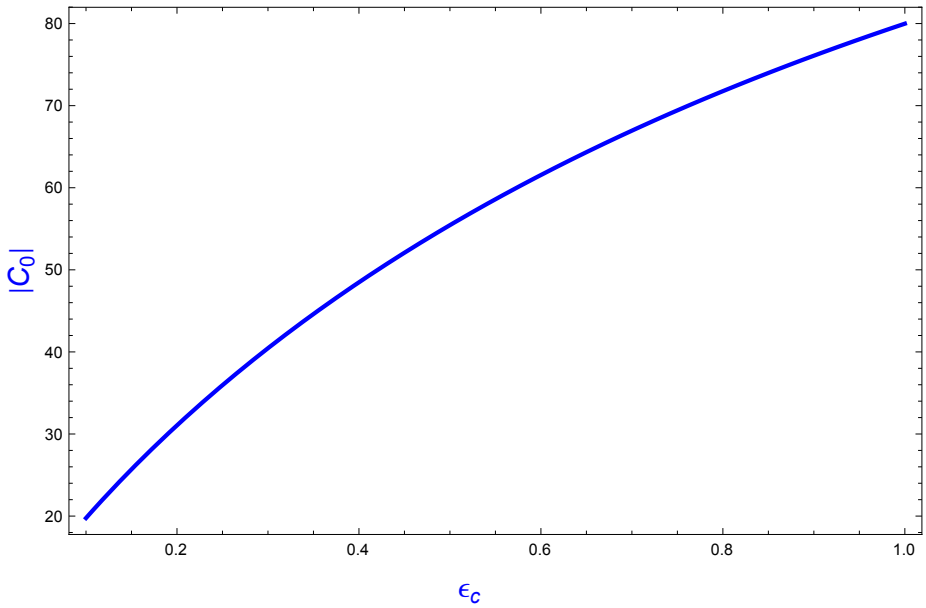

Figure 4.13: Absolute of coefficient of RCP transmitted field of dielectric cylinder with coating of dispersive ENG cylinder with respect to permittivity of chiral metamaterial: $f == 12$GHz, $\kappa = 0.01$, $a = 5$mm, $b = 10$mm.

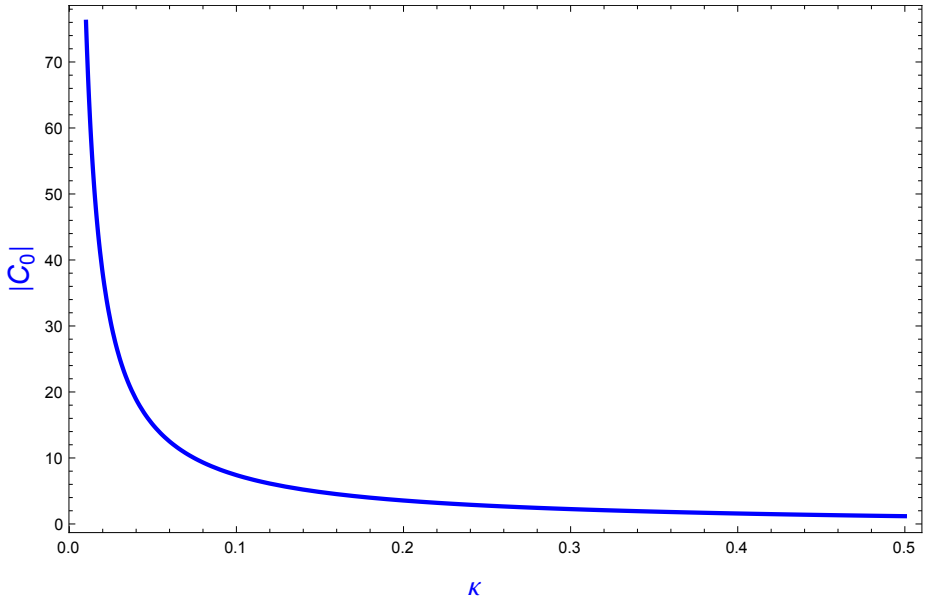

Figure 4.14: Absolute of coefficient of RCP transmitted field of dielectric cylinder with coating of dispersive ENG cylinder with respect to the chirality of chiral metamaterial: $f = 12$GHz, $\epsilon_c = 0.9$, $a = 5$mm, $b = 10$mm.

In Fig. 4.11 dielectric cylinder with dispersive ENG coating layer is considered , and behavior of coefficient of RCP transmitted field in chiral metamaterial is observed. In Fig. 4.12 effect of permittivity of chiral metamaterial is observed for dielectric coated with dispersive ENG cylinder. It can be seen that with increasing permittivity of host chiral metamaterial coefficient of RCP transmitted field in chiral metamaterial increases. Fig. 4.13 shows the effect of chirality of host chiral metamaterial on field transmitted from dielectric cylinder coated with dispersive ENG metamaterial, placed in chiral metamaterial. The coefficient of RCP transmitted field in chiral metamaterial decreases with chirality of host chiral metamaterial.

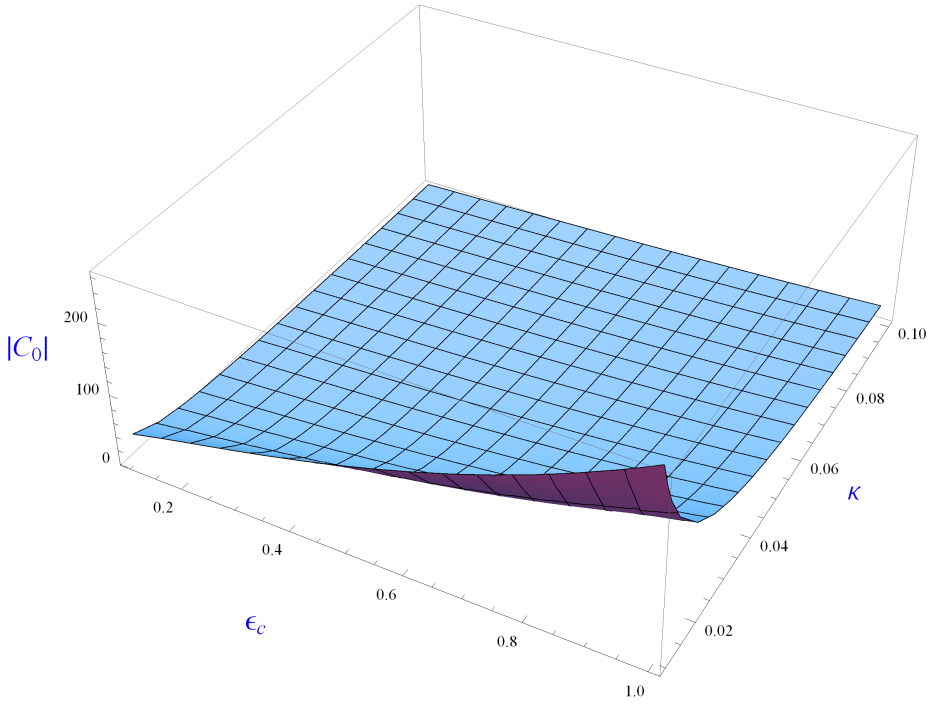

Figure 4.15: Absolute value of Absolute of coefficient of RCP transmitted field of dispersive DPS coating cylinder with respect to permittivity and chirality of the host medium: $a = 5$mm, $b = 10$mm and $f = 1$GHz.

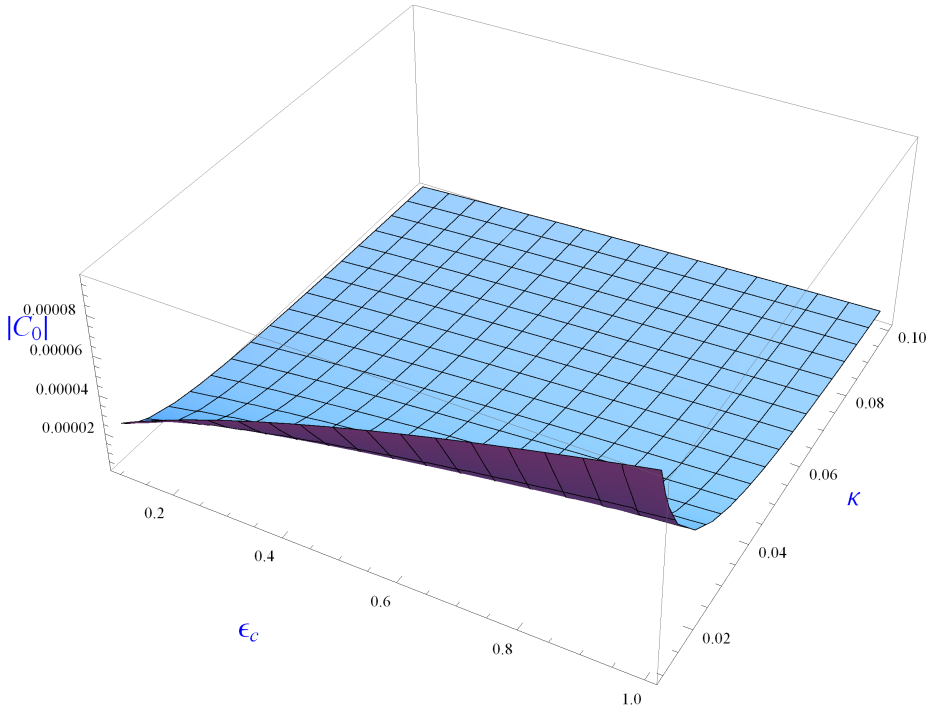

Figure 4.16: Absolute of coefficient of RCP transmitted field of dispersive MNG coating cylinder with respect to permittivity and chirality of the host medium: $a = 5$mm, $b = 10$mm and $f = 10.2$GHz.

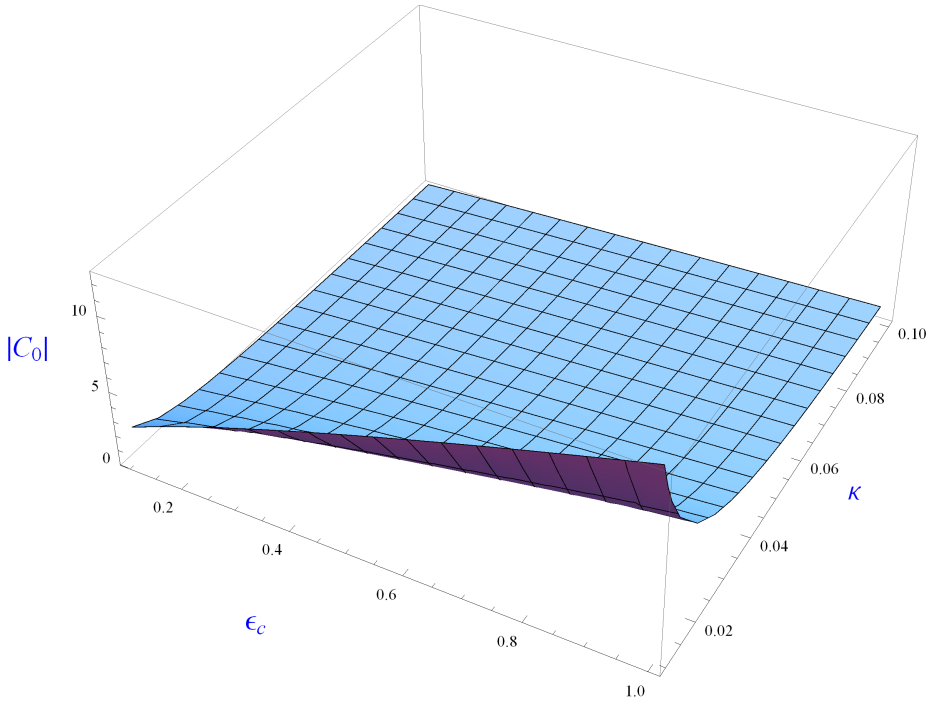

Figure 4.17: Absolute of coefficient of RCP transmitted field of dispersive DNG coating cylinder with respect to permittivity and chirality of the host medium: $a = 5$mm, $b = 10$mm and $f = 10.9$GHz.

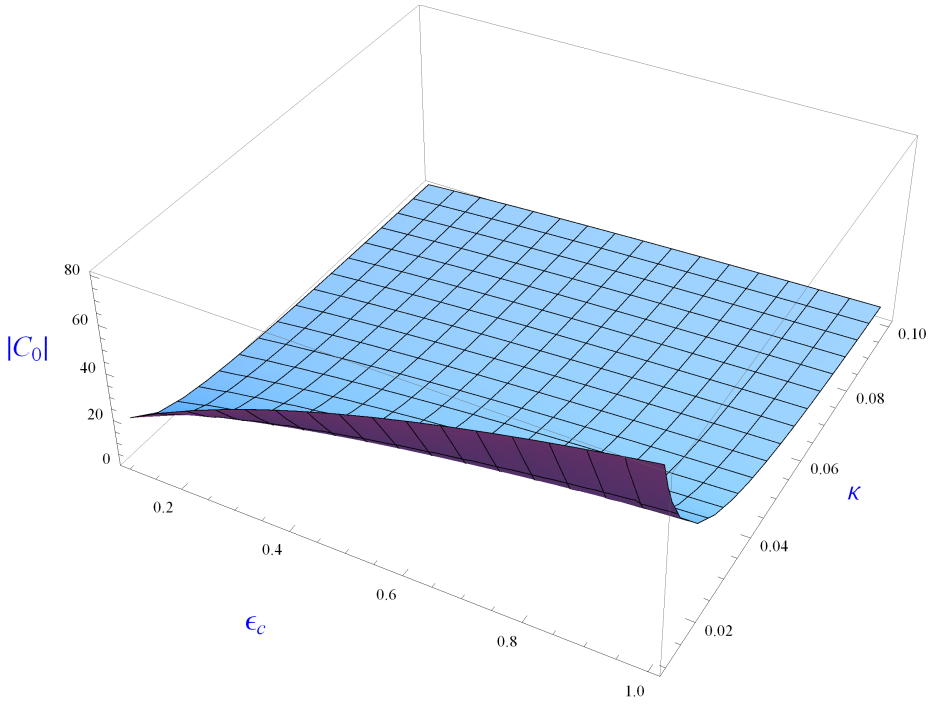

Figure 4.18: Absolute of coefficient of RCP transmitted field of dispersive ENG coating cylinder with respect to permittivity and chirality of the host medium: $a = 5$mm, $b = 10$mm and $f = 12$GHz.

In Fig. 3.14-Fig. 3.17 combine effect of permittivity and chirality of the host chiral medium is observed and it is noticed that for DPS, MNG, DNG and ENG cylinders coefficient of RCP/LCP transmitted field decreases with chirality and increases with relative permittivity of the chiral medium, it is also noted that coefficients of RCP and LCP transmitted field are same for all cases.

4.3 Summary

In this chapter a dielectric cylinder coated with dispersive dielectric magnetic metamaterial is considered to be placed in an unbounded chiral metamaterial. An infinite electric line source as a source of excitation is placed at the center of the dielectric cylinder. For DPS and DNG coating layers resonance appears. It is noticed that coefficient of RCP transmitted field decreases with increasing the chirality of chiral metamaterial and increases with increasing the relative

permittivity of the chiral metamaterial for DPS, MNG, DNG and ENG coating layers. Resonance appears for DPS and DNG coating layers and transmitted field is very weak for MNG coating layer.

Chapter 5

Conclusion

This chapter contains the conclusions of the work presented in this thesis.
The behavior of coefficients of RCP and LCP transmitted field from a non-dispersive dielectric placed in unbounded chiral metamaterial is investigated. It is also observed that with increasing the permittivity of chiral medium coefficient of RCP transmitted field decreases and increases with increasing the permittivity of non-dispersive dielectric slab. And transmission from slab can be increased with setting the value of chirality of chiral metamaterial as transmission increases with chirality. It is also noticed that transmission can be minimized with increasing the width of slab because it is observed that field effect is week away from the source.
It is noted that for dispersive dielectric magnetic medium type of medium changes for certain frequency range and medium may behave either as DPS, MNG, DNG or ENG medium. For one dimensional problem of dispersive slab it is observed that the behavior of coefficients of RCP and LCP transmitted field from a dispersive dielectric magnetic slab placed in unbounded chiral metamaterial is same. It is also observed that with increasing the permittivity of chiral medium coefficient of RCP transmitted field decreases and increases with increasing the permittivity of dispersive slab. It is also noticed that at $f = 10.3$GHz and at $f = 11$GHz transmission coefficient is unity while reflection is zero. So it is concluded that at 10.3GHz and 11GHz there is complete transmission. It is concluded that when dispersive slab is placed in chiral nihility metamaterial coefficient of RCP and LCP transmitted field become weak

as compared to those in host chiral metamaterial. For dispersive dielectric DPS slab and dispersive ENG slab coefficient of RCP transmitted field decreases with frequency while for dispersive DNG and dispersive MNG slab behavior is opposite.

For two dimensional problem when a dispersive dielectric magnetic cylinder is considered to be placed in unbounded chiral metamaterial. It is observed that coefficient of transmitted field through a dispersive DNG cylinder is strong as compared to DPS, MNG and ENG cylinders. And when a dispersive MNG cylinder is placed in unbounded chiral metamaterial coefficient of RCP and LCP transmitted field are weak and same. The behavior of coefficient of transmitted field through a DPS, MNG, DNG or ENG cylinder of very small radius placed in unbounded chiral nihility metamaterial is somewhat similar to that of a source placed in unbounded chiral nihility metamaterial. When radius of cylinder containing a line source at its origin is very small then it can be concluded that the line source is not radiating or line source is unable to radiate.

By using the coating layer of dispersive dielectric magnetic medium on the dielectric cylinder, effects of different parameters on coefficient of transmitted field are also analyzed. It is concluded that coefficient of RCP/LCP transmitted field from dielectric cylinder coated with dispersive ENG and MNG cylinder is weak as compared to dispersive DPS and dispersive DNG coating layers. It is noticed that coefficient of transmitted field is very strong when dielectric cylinder is coated with dispersive DPS metamaterial and placed in unbounded dielectric medium.

For the case of dispersive slab transmission coefficient becomes unity at certain frequency, so that can be used as a transparent medium. It is noticed that when a dispersive cylinder of very small radius is placed in chiral nihility then transmission is approximately equal to zero, so it is concluded that we can hide a source by coating that source with chiral nihility metamaterial. And it is also investigated that for the case of dispersive cylinder placed in an unbounded chiral metamaterial resonances appear for DNG and MNG cylinders, and for coated cylinder resonance aiso appears for dispersive DPS cylinder. For MNG cylinder it can be used as a bandpass filter.

Bibliography

[1] J. C. Bose. On the rotation of plane of polarisation of electric waves by a twisted structure. *Proceedings of the Royal Society of London*, 63(389-400): 146–152, 1898.

[2] V. G. Veselago. The electrodynamics of substances with simultaneously negative values of img align= absmiddle alt= ? eps/img and μ. *Physics-Uspekhi*, 10(4):509–514, 1968.

[3] D.R. Smith, W.J. Padilla, D.C. Vier., S.C. Nemat-Nasser, and S. Schultz. Composite medium with simultaneously negative permeability and permittivity.

[4] D. R. Smith and N. Kroll. Negative refractive index in left-handed materials. *Physical Review Letters*, 85(14):2933, 2000.

[5] J. B. Pendry. Negative refraction makes a perfect lens. *Physical review letters*, 85(18):3966, 2000.

[6] R.A. Shelby, D.R. Smith, S.C. Nemat-Nasser, and S. Schultz. Microwave transmission through a two-dimensional, isotropic, left-handed metamaterial. *Applied Physics Letters*, 78(4):489–491, 2001.

[7] I. V. Lindell, S.A. Tretyakov, K.I. Nikoskinen, and S. Ilvonen. Bw media-media with negative parameters, capable of supporting backward waves. *Microwave and Optical Technology Letters*, 31(2):129–133, 2001.

[8] R. W. Ziolkowski and E. Heyman. Wave propagation in media having negative permittivity and permeability. *Physical review E*, 64(5):056625, 2001.

[9] M. W. McCall, A. Lakhtakia, and W. S. Weiglhofer. The negative index of refraction demystified. *European Journal of Physics*, 23(3):353, 2002.

[10] N. Garcia and M. Nieto-Vesperinas. Left-handed materials do not make a perfect lens. *Physical review letters*, 88(20):207403, 2002.

[11] R. A. Shelby, D. R. Smith, and S. Schultz. Experimental verification of a negative index of refraction. *science*, 292(5514):77–79, 2001.

[12] C. Caloz, C-C Chang, and T. Itoh. Full-wave verification of the fundamental properties of left-handed materials in waveguide configurations. *Journal of Applied Physics*, 90(11):5483–5486, 2001.

[13] A. K. Iyer and G. V. Eleftheriades. Negative refractive index metamaterials supporting 2-d waves. In *Microwave Symposium Digest, 2002 IEEE MTT-S International*, volume 2, pages 1067–1070. IEEE, 2002.

[14] C. Caloz and T. Itoh. Transmission line approach of left-handed (lh) materials and microstrip implementation of an artificial lh transmission line. *Antennas and Propagation, IEEE Transactions on*, 52(5):1159–1166, 2004.

[15] I. V. Lindell, A. H. Sihvola, and J. Kurkijärvi. Karl f. lindman: The last hertzian, and a harbinger of electromagnetic chirality. *IEEE antennas & propagation magazine*, 34(3):24–30, 1992.

[16] D.L. Jaggard, A.R. Mickelson, and C.H. Papas. On electromagnetic waves in chiral media. *Applied physics*, 18(2):211–216, 1979.

[17] N. Engheta and D.L. Jaggard. Electromagnetic chirality and its applications. *Antennas and Propagation Society Newsletter, IEEE*, 30(5):6–12, 1988.

[18] N. Engheta and S. Bassiri. One-and two-dimensional dyadic green's functions in chiral media. *Antennas and Propagation, IEEE Transactions on*, 37 (4):512–515, 1989.

[19] D. L. Jaggard, X. Sun, and N. Engheta. Canonical sources and duality in chiral media (antenna arrays). *Antennas and Propagation, IEEE Transactions on*, 36(7):1007–1013, 1988.

[20] S. F. Mahmoud. Characteristics of a chiral-coated slotted cylindrical antenna. *Antennas and Propagation, IEEE Transactions on*, 44(6):814–821, 1996.

[21] I. V. Lindell, A. H. Sihvola, A. J. Viitanen, and S. A. Tretyakov. Geometrical optics in inhomogeneous chiral media with application to polarization correction of inhomogeneous microwave lens antennas. *Journal of Electromagnetic Waves and Applications*, 4(6):533–548, 1990.

[22] A. Lakhtakia, M. W. McCall, and W. S. Weiglhofer. Negative phase-velocity mediums. *Introduction to complex mediums for optics and electromagnetics*, pages 347–63, 2003.

[23] A. Lakhtakia. An electromagnetic trinity from negative permittivity and negative permeability. *International Journal of Infrared and Millimeter Waves*, 23(6):813–818, 2002.

[24] S. Ahmed and Q.A. Naqvi. Directive em radiation of a line source in the presence of a coated nihility cylinder. *Journal of Electromagnetic waves and Applications*, 23(5-6):761–771, 2009.

[25] Q.A Naqvi. Fractional dual interface in chiral nihility medium. *Progress In Electromagnetics Research Letters*, 8:135–142, 2009.

[26] Q. Cheng, T. J. Cui, and C. Zhang. Waves in planar waveguide containing chiral nihility metamaterial. *Optics Communications*, 276(2):317–321, 2007.

[27] S. Tretyakov, I. Nefedov, A. Sihvola, S. Maslovski, and C. Simovski. Waves and energy in chiral nihility. *Journal of electromagnetic waves and applications*, 17(5):695–706, 2003.

[28] A. Lakhtakia. On perfect lenses and nihility. *International Journal of Infrared and Millimeter Waves*, 23(3):339–343, 2002.

[29] A. Lakhtakia and J. A. Sherwin. Orthorhombic materials and perfect lenses. *International Journal of Infrared and Millimeter Waves*, 24(1):19–23, 2003.

[30] A. Lakhtakia and J. B. Geddes III. Scattering by a nihility cylinder. *AEUE-International Journal of Electronics and Communications*, 61(1):62–65, 2007.

[31] A. Lakhtakia and T. G. Mackay. Fresnel coefficients for a permittivity-permeability phase space encompassing vacuum, anti-vacuum, and nihility. *Microwave and optical technology letters*, 48(2):265–270, 2006.

[32] R. W. Ziolkowski. Propagation in and scattering from a matched metamaterial having a zero index of refraction. *Physical Review E*, 70(4):046608, 2004.

[33] C.-W. Qiu, N. Burokur, S. Zouhdi, and L.-W. Li. Chiral nihility effects on energy flow in chiral materials. *JOSA A*, 25(1):55–63, 2008.

[34] V. R. Tuz and C.-W. Qiu. Semi-infinite chiral nihility photonics: Parametric dependence, wave tunneling and rejection. *Progress In Electromagnetics Research*, 103:139–152, 2010.

[35] X. Cheng, H. Chen, Xian-Min Zhang, B. Zhang, and B.-I. Wu. Cloaking a perfectly conducting sphere with rotationally uniaxial nihility media in monostatic radar system. *Progress In Electromagnetics Research*, 100:285–298, 2010.

[36] S. Ahmed and Q.A. Naqvi. Electromagnetic scattering from a chiral-coated nihility cylinder. *Progress In Electromagnetics Research Letters*, 18: 41–50, 2010.

[37] Q.A. Naqvi. Planar slab of chiral nihility metamaterial backed by fractional dual/pemc interface. *Progress In Electromagnetics Research*, 85:381–391, 2008.

[38] S.R. Qamar, A. Naqvi, A.A. Syed, and Q.A. Naqvi. Radiation characteristics of elementary sources located in unbounded chiral nihility metamaterial. *Journal of Electromagnetic Waves and Applications*, 25(5-6):713–722, 2011.

[39] S. A. Darmanyan, M. Neviere, and A.A. Zakhidov. Surface modes at the interface of conventional and left-handed media. *Optics Communications*, 225(4):233–240, 2003.

[40] N. C. Panoiu and Osgood R. M.Jr. Numerical investigation of negative refractive index metamaterials at infrared and optical frequencies. *Optics communications*, 223(4):331–337, 2003.

[41] C. Sabah and S. Uckun. Multilayer system of lorentz/drude type metamaterials with dielectric slabs and its application to electromagnetic filters. *Progress In Electromagnetics Research*, 91:349–364, 2009.

[42] S. Enoch, G. Tayeb, P. Sabouroux, N. Guérin, and P. Vincent. A metamaterial for directive emission. *Physical Review Letters*, 89(21):213902, 2002.

[43] J. B. Pendry, A. J. Holden, DJ. Robbins, and W.J. Stewart. Magnetism from conductors and enhanced nonlinear phenomena. *Microwave Theory and Techniques, IEEE Transactions on*, 47(11):2075–2084, 1999.

[44] N. Engheta and R. W. Ziolkowski. A positive future for double-negative metamaterials. *Microwave Theory and Techniques, IEEE Transactions on*, 53 (4):1535–1556, 2005.

[45] J. Sun, W. Sun, T. Jiang, and Y. Feng. Directive electromagnetic radiation of a line source scattered by a conducting cylinder coated with left-handed metamaterial. *Microwave and optical technology letters*, 47(3):274–279, 2005.